SANDIA REPORT

SAND96-0098 • UC-721
Unlimited Release
Printed May 1996

Estimates of the Solubilities of Waste Element Radionuclides in Waste Isolation Pilot Plant Brines: A Report by the Expert Panel on the Source Term

David E. Hobart, Carol J. Bruton, Frank J. Millero, I-Ming Chou,
Kathleen M. Trauth, D. Richard Anderson

Prepared by
Sandia National Laboratories
Albuquerque, New Mexico 87185 and Livermore, California 94550
for the United States Department of Energy
under Contract DE-AC04-94AL85000

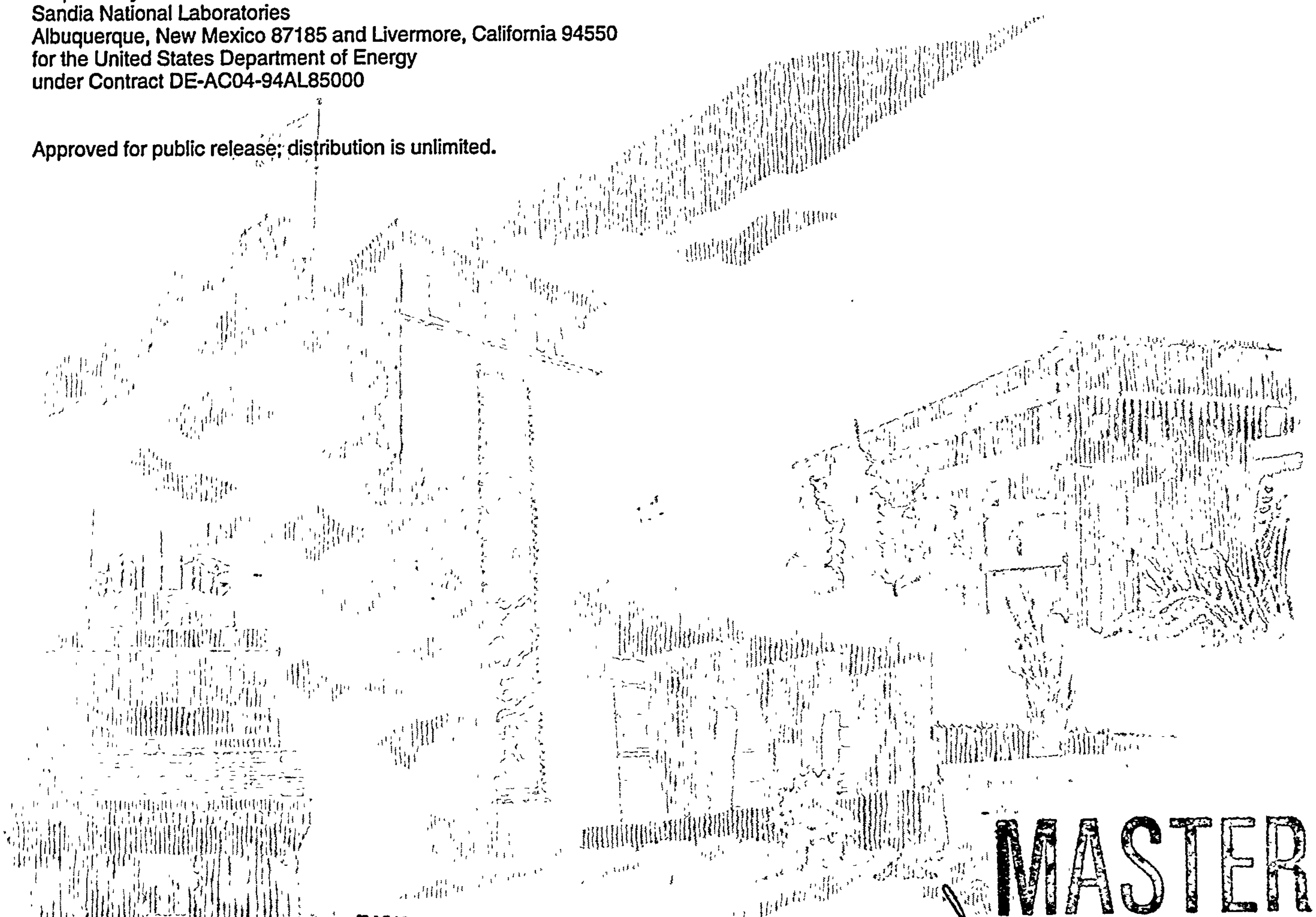

SF2900Q(8-81)

Issued by Sandia National Laboratories, operated for the United States Department of Energy by Sandia Corporation.

Printed in the United States of America. This report has been reproduced directly from the best available copy.

Available to DOE and DOE contractors from
Office of Scientific and Technical Information
PO Box 62
Oak Ridge, TN 37831

Prices available from (615) 576-8401, FTS 626-8401

Available to the public from
National Technical Information Service
US Department of Commerce
5285 Port Royal Rd
Springfield, VA 22161

NTIS price codes
Printed copy: A06
Microfiche copy: A01

SAND96-0098
Unlimited Release
Printed May 1996

Distribution
Category UC-721

ESTIMATES OF THE SOLUBILITIES OF WASTE ELEMENT RADIONUCLIDES IN WASTE ISOLATION PILOT PLANT BRINES: A REPORT BY THE EXPERT PANEL ON THE SOURCE TERM

David E. Hobart*, Carol J. Bruton§, Frank J. Millero†, I-Ming Chou‡,
Kathleen M. Trauth**, and D. Richard Anderson**

Sandia National Laboratories
Albuquerque, NM 87185 and
Livermore, CA 94550.

ABSTRACT

The Waste Isolation Pilot Plant (WIPP) is a research and development facility mined in Southeastern New Mexico bedded salts for demonstrating the safe disposal of transuranic waste. Sandia National Laboratories' (SNLs') evaluation of the long-term performance of the WIPP includes estimation of the cumulative releases of radionuclide elements (radium, thorium, uranium, neptunium, plutonium, americium, and curium) to the accessible environment. Nonradioactive lead is added to this list of elements considered because of the large quantity expected in WIPP wastes. Estimation of cumulative releases is dependent upon reliable assessment of the solubilities of these elements. Because sufficient WIPP-specific data on radionuclide solubility in high-ionic-strength brine solutions was scarce, SNL staff assembled an expert panel and utilized an elicitation process to develop solubility probability distributions. To estimate the solubilities of these elements in WIPP brines, the Panel used the following approach. 1) Existing thermodynamic data for radionuclide aqueous species were used to identify the most likely aqueous species in solution under potential ranges of WIPP conditions through the construction of aqueous speciation diagrams. 2) Existing thermodynamic data for radionuclide-bearing solid phases and expert judgment were used to identify potential solubility-limiting solid phases given potential ranges of WIPP conditions, being careful to select two solids: one limiting radionuclide concentrations to low values (the 0.1 fractile), and the other to high values (the 0.9 fractile). 3) Thermodynamic data for radionuclide aqueous species and radionuclide-bearing solid phases selected above for each radionuclide were used to calculate the activities of the radionuclide aqueous species in equilibrium with each solid. 4) Activity coefficients of the radionuclide-bearing aqueous species were estimated using Pitzer's equations for aqueous species that were considered by panel members to be chemically similar to the radionuclide-

* Glenn T. Seaborg Institute for Transactinium Science, Livermore, CA 94551.
§ Earth Sciences Department, Lawrence Livermore National Laboratory, Livermore, CA 94550
† Rosenstiel School of Marine and Atmospheric Science, University of Miami, Miami, FL 33149-1098.
‡ United States Geological Survey, Reston, VA 22092.
** Sandia National Laboratories, Albuquerque, NM 87185 and Livermore, CA 94550.

bearing aqueous species. These activity coefficients were then used to calculate the concentration of each radionuclide at the 0.1 and 0.9 fractiles. 5) The 0.5 fractile was chosen to represent experimental data (Nitsche [1991] in Yucca Mountain, Nevada well J-13 water for neptunium, plutonium, and americium, for example) with activity coefficient corrections as described above. 6) Because of information available outside of the GEMBOCHS database, the probability distributions for lead and radium were developed as discussed in separate sections of the text. 7) Expert judgment was used to develop the 0.0, 0.25, 0.75, and 1.0 fractiles by considering the sensitivity of solubility to the potential variability in the composition of brine and gas, and the extent of waste contaminants, and extending the probability distributions accordingly. The results were used in the 1991 and 1992 performance assessment calculations.

Research sponsored by Sandia National Laboratories, Albuquerque, NM 87185 and Livermore, CA 94550 for the U.S. Department of Energy under contract DE-AC04-94AL85000 and by the Office of Basic Energy Sciences, Division of Chemical Sciences, U.S. Department of Energy under contract W-7405-eng-36 with the University of California.

ACKNOWLEDGMENTS

The authors wish to extend their appreciation to Prof. Stephen C. Hora (University of Hawaii at Hilo). Gratitude is also extended to Mr. Phillip Palmer, Los Alamos National Laboratory, for valuable assistance. The authors also appreciate the review comments developed by Dr. Laurence Brush and Dr. Ruth Weiner of Sandia National Laboratories. Dr. Weiner also assisted by suggesting some explanatory text. Thanks also go to technical editors Faith Puffer and Lee Bowman Tye, and to word processors Theresa Allen, Jackie Ripple, Debbie Rivard, and Leona Tartaglia at Tech Reps, Inc. This work was sponsored by Sandia National Laboratories, Albuquerque, NM 87185 and Livermore, CA 94550 for the United States Department of Energy under contract DE-AC04-76DP00789 and by the Office of Basic Energy Sciences, Division of Chemical Sciences, U.S. D.O.E. under contract W-7405-eng-36 with the University of California.

PREFACE

This report describes the development of probability distributions used in the 1991 and 1992 preliminary performance assessments. Many of the assumptions made for this work: brine volume, redox conditions, important radionuclides, etc., have been refined since 1991, and some have changed considerably. The reader should keep in mind that this report relies on the conceptual model of the WIPP as it was in 1991, which is not necessarily the model in 1995 or that used in the application for certification with 40 CFR Part 191.

CONTENTS

Figures

Tables

INTRODUCTION

Background

The Waste Isolation Pilot Plant (WIPP) was authorized by Congress in 1979 as a research and development facility to demonstrate the safe management, storage, and eventual disposal of transuranic waste generated by the defense programs (U.S. Department of Energy, 1979). Located in the 2,000-ft thick Salado Formation of marine bedded salt in southeastern New Mexico, approximately 24 miles east of Carlsbad (Figure 1), WIPP is a mined geologic repository for radioactive waste disposal. The bedded salts consist of thick halite (NaCl) and interbeds of minerals such as clays (sheet silicates) and anhydrites ($CaSO_4$) of the late Permian period (about 255 million years ago) that do not support flowing water (Figure 2) (Bertram-Howery et al., 1990). Deep salt formations have a number of characteristics that are desirable in a host rock for nuclear waste disposal. Salt formations have a very low water content and low permeability, reducing the potential for groundwater radionuclide migration. Salts are self-sealing, and, in addition, salt is easily mined (OECD/CEC, 1984). A major mechanism that would permit migration of radionuclides from the repository to the accessible environment is a disruptive event that introduces significant quantities of water.

Before operating, the WIPP must comply with the U. S. Environmental Protection Agency's *Environmental Standards for the Management and Disposal of Spent Nuclear Fuel, High-Level and Transuranic Radioactive Wastes* (U.S. Environmental Protection Agency, 1985, 1993). Important criteria in 40 CFR 191 in determining the suitability of the WIPP for permanent disposal of radioactive waste include standards (Subpart B, Section 191.13), which place limits on the probability that cumulative radionuclide releases to the accessible environment over the next 10,000 years will exceed prescribed quantities. Subpart B, Section 191.15 requires that the radiation dose received by any member of the public in the accessible environment be limited for 10,000 years after disposal, and Subpart C contains groundwater protection requirements that limit the radionuclide concentrations in underground sources of drinking water for 10,000 years.

Sandia National Laboratories (SNL) is currently evaluating the long-term performance of the WIPP. Performance assessment is an analysis that: "(1) identifies the processes and events that might affect the disposal system; (2) examines the effects of these processes and events on the performance of the disposal system; and (3) estimates the cumulative releases of radionuclides, considering the associated uncertainties, caused by all significant processes and events." (U.S. EPA, 1985, p. 38086) These estimates are incorporated into an overall probability distribution of a release. The performance of a computer modeled disposal system is analyzed probabilistically through the use of a Monte Carlo technique described elsewhere (Helton et al., 1991, p. III-1 to III-53). Sensitivity analysis performed by SNL involves determining the contribution of individual input variables to the uncertainty in model predictions (Helton et al., 1991, p. II-1).

The most significant disruptive event considered by SNL is one of *future human intrusion*. Even though passive institutional controls (e.g., permanent markers, records, and other controls, indicating the dangers of the waste and their location) will be used, salt formations are often associated with economic resources such as petroleum and natural gas. Thus, future drilling is a possibility. A typical example of a human intrusion scenario is depicted in Figure 3. This example consists of a single borehole that penetrates through a waste-filled room and into the underlying pressurized brine reservoir in the Castile Formation. Upwelling pressurized brine fills the

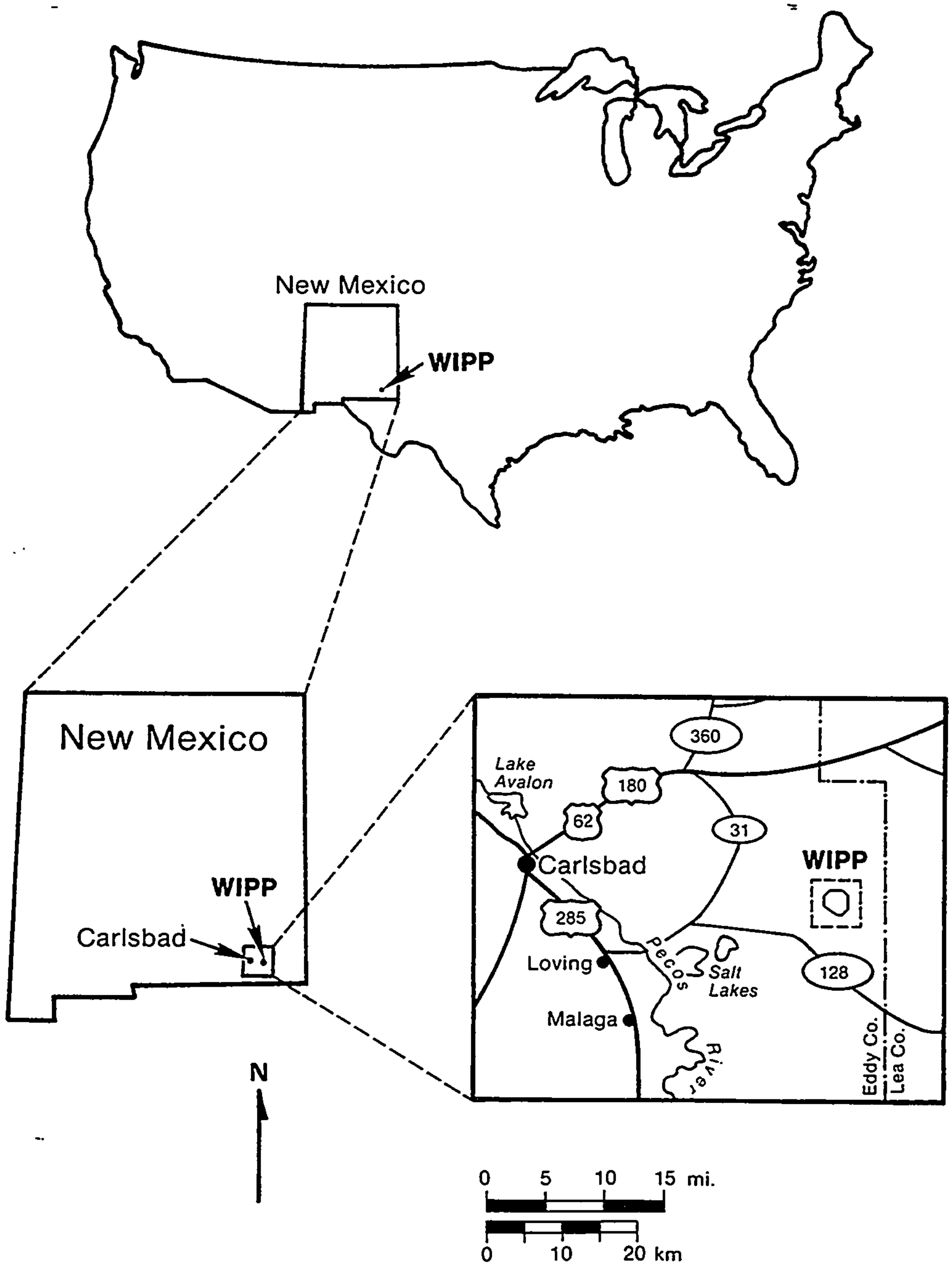

Figure 1. WIPP location map (after Bertram-Howery and Hunter, 1989).

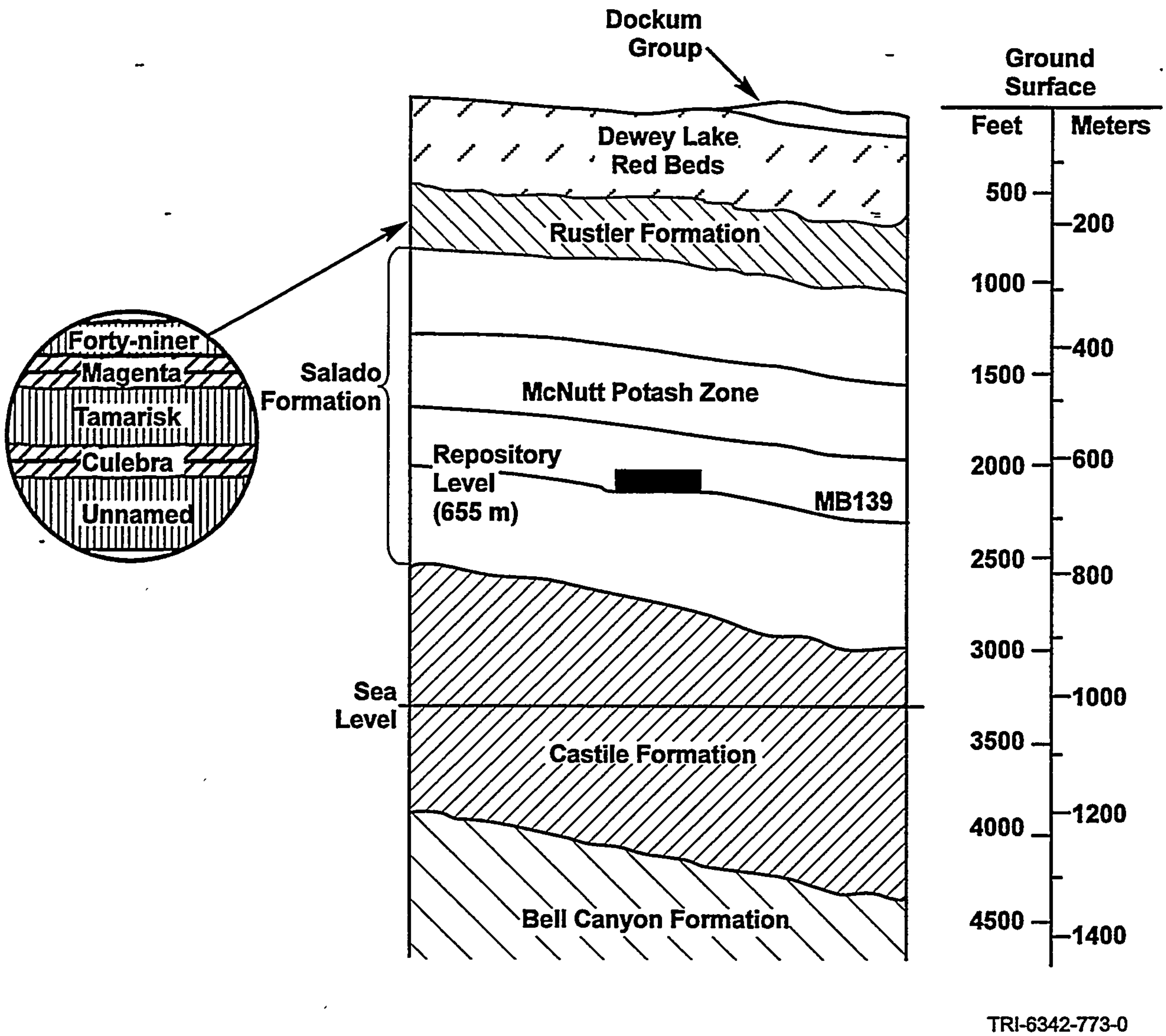

Figure 2. WIPP stratigraphy (modified from Rechard et al., 1990).

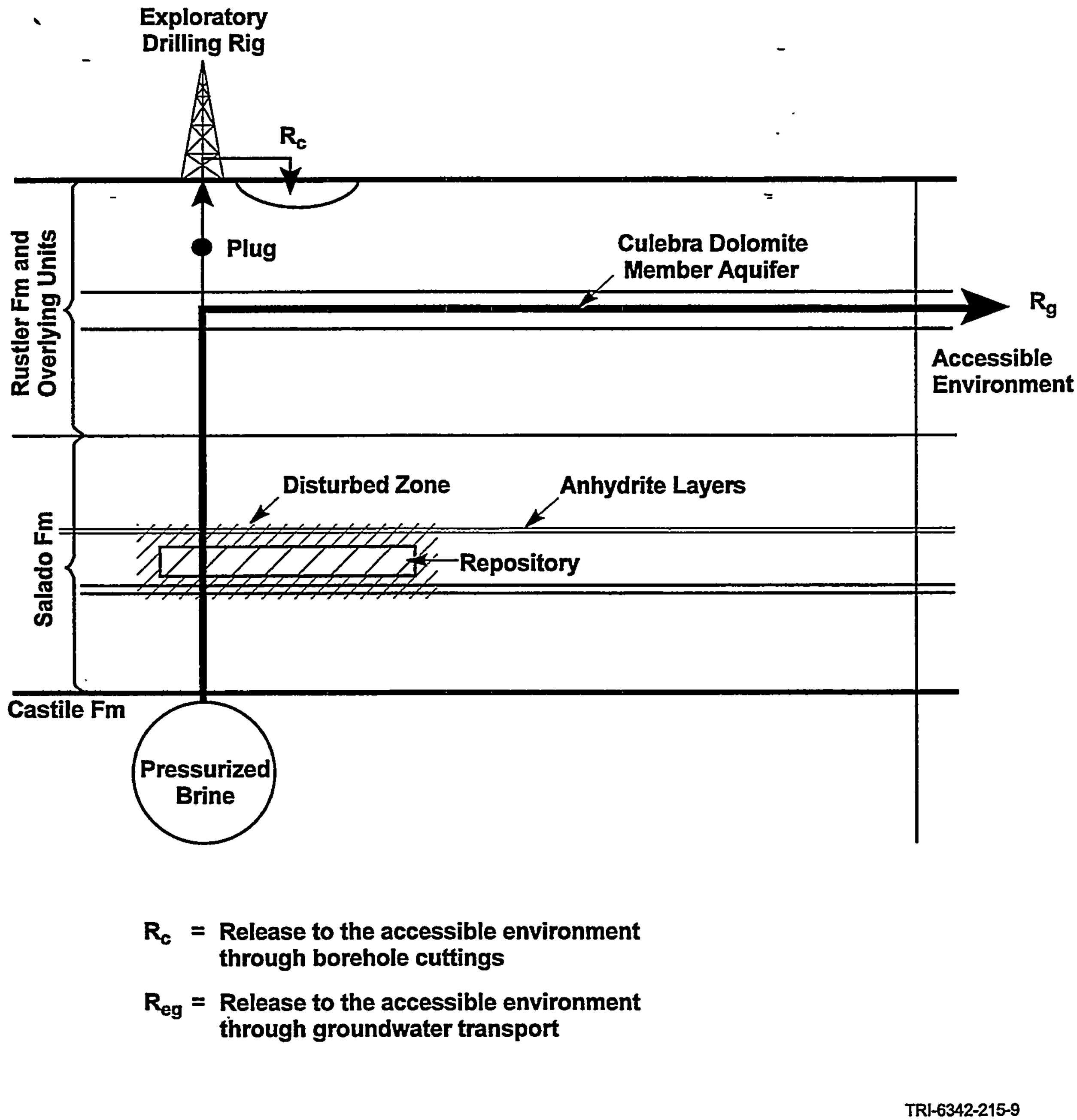

Figure 3. Conceptual model for future human intrusion into the WIPP repository (designated E-1) (Bertram-Howery et al., 1990).

repository and associated drifts, solubilizes the radionuclides contained in the waste, and migrates out into the overlying Culebra Dolomite aquifer and out to the accessible environment. In this situation, the high salt concentration in the brine is expected to increase the mobility of radionuclides through complexation with chloride, carbonate, sulfate, and other ligands present in the brine, as well a host of inorganic and organic ligands present as co-contaminants in the waste package.

The radionuclides of greatest concern in the WIPP inventory (and their daughter products) at the time of the expert judgment elicitation included radium, thorium, uranium, neptunium, plutonium, americium, and curium (see Table 1, which is a reprint of Lappin et al., 1990, Table 4-3). These are also among the radionuclides of significant environmental concern in most radioactive wastes (Kerrisk, 1985; Oversby, 1987; Hobart, 1990). Nonradioactive lead is included on the WIPP list of elements addressed because it is expected to be present in substantial quantities as shielding debris. Predictions of the solubility of the above radionuclides and lead in WIPP brines are needed for a source term as input for modeling the potential release of radionuclides into the environment.

The sensitivity analysis performed on the 1990 preliminary performance assessment indicated that the solubilities of radionuclides were important to the results: "Releases to the accessible environment due to groundwater transport were dominated by solubility limit and retardation..." (Helton et al., 1991, p. ii).

Problem Statement

In the conduct of the performance-assessment calculations, the estimation of the releases is probabilistic in nature, requiring system parameters to be described with probability distributions. Sufficient WIPP-specific radionuclide solubility data were not available (in the high ionic strengths encountered at WIPP) to perform a simple statistical test to develop the appropriate probability distributions for the preliminary performance assessment being conducted. The problem was how to develop the necessary distributions. The WIPP Performance Assessment Division chose to use an expert judgment panel as a means to develop the necessary probability distributions, relying on the knowledge and expertise of the panel members to evaluate available data. The expert judgment panel for solubilities was called the Source Term Expert Panel, or simply the Panel, in this report.

The expert judgment process was constrained by several factors that would, of course, affect the results. First, the experts were to rely on existing data, although various experimental programs were under way. The preliminary performance assessments were conducted to refine the process for evaluating a proposed repository and to identify those parameters that most impact the results. The performance assessment calculations were conducted while experimental programs were ongoing, and judgment had to be applied with incomplete information. In addition, the GEMBOCHS thermodynamic database used in this effort is in a state of continuous development.

Second, the information was to be developed rapidly in order to be available for the 1991 preliminary performance assessment calculations. The decision to use an expert panel was made in January 1991. The WIPP Performance Assessment Division had committed to performing calculations and providing reviewed documentation to its Department of Energy (DOE) customer by December of 1991. Scheduling an expert panel to provide information by the predetermined date for the start of calculations in April 1991 meant that with the

Table 1. Mass Inventory of Radionuclide Species and Stable Lead in the Repository (reprinted from Lappin et al., 1990, Table 4-3)

Decay Chain or Waste Species	Radio-nuclide	Half Life (years)	Ci/g	Initial Inventory* (g)	Inventory at 175 Years† (g)
$^{240}Pu \rightarrow ^{236}U$	^{240}Pu	6.54×10^3	2.28×10^{-1}	5.27×10^5	5.17×10^5
	^{236}U	2.34×10^7	6.47×10^{-5}	0	9.52×10^3
^{239}Pu	^{239}Pu	2.41×10^4	6.21×10^{-2}	7.88×10^6	7.84×10^6
$^{238}Pu \rightarrow ^{234}U$	^{238}Pu	8.77×10^1	1.71×10^1	3.06×10^5	0^{**}
$\rightarrow ^{230}Th \rightarrow ^{226}Ra$	^{234}U	2.44×10^5	6.26×10^{-3}	0	3.01×10^5
$\rightarrow ^{210}Pb$	^{230}Th	7.70×10^4	2.02×10^{-2}	0	$0^{‡}$
	^{226}Ra	1.60×10^3	9.89×10^{-1}	0	$0^{§}$
	^{210}Pb	2.23×10^1	7.64×10^1	0	$0^{§}$
^{241}Pu	^{241}Pu	1.44×10^1	1.03×10^2	4.56×10^4	0^{**}
$\downarrow$	^{241}Am	4.32×10^2	3.43×10^0	2.25×10^5	2.06×10^5
$^{241}Am \rightarrow ^{237}Np$	^{237}Np	2.14×10^6	7.05×10^{-4}	1.53×10^4	7.93×10^4
$\rightarrow ^{233}U \rightarrow ^{229}Th$	^{233}U	1.59×10^5	9.65×10^{-3}	9.82×10^5	9.81×10^5
	^{229}Th	7.43×10^3	2.10×10^{-1}	0	$0^{‡}$
Stable Pb	-	-	-	1.33×10^9	1.33×10^9

* Initial inventory at the time of decommissioning (in Ci) is from U.S. DOE[a] (1990, Table B.2.13), except stable Pb, from Lappin et al. (1989, Table E-5). The inventory of stable Pb is not scaled up, because stable Pb is not depleted in any of the cases.

† Transport calculations start 175 years after institutional control begins, i.e., after 100 years of institutional control and an effective plug life of 75 years.

** Because ^{238}Pu and ^{241}Pu have short half-lives and large retardation factors, their migration from the source is minimal. Therefore, the conservative approach taken here converts all ^{238}Pu and ^{241}Pu to daughter products at simulation beginning.

‡ Because of large retardation factors relative to their parents, ^{230}Th and ^{229}Th migration is controlled by their parents. In addition, both radionuclides have very little mass in place at 175 years. Therefore they are not considered to be present at 175 years.

§ These nuclides are not present in quantities large enough at 175 years to warrant source inclusion.

preliminary activities (nominations, selection, contracting, etc.), the Panel would have just over one month to develop the necessary information with the concomitant limitation in the technical resources that could be utilized.

Third, there was great uncertainty about the conditions expected in the repository, i.e., the Panel was not able to assume that actions would be taken (e.g., the use of specially designed backfill) to fix the conditions (i.e., with respect to Eh, pH, etc.) in the repository after closure.

This report is intended to document the events that took place in 1991 in developing input parameters for the 1991 (and subsequently 1992) performance assessment calculations. Any subsequent data collection or analyses regarding solubilities are not pertinent to this effort, and are not discussed here. Further information on the conduct of the Panel can be found in Trauth et al. (1992).

Expert Judgment Concepts

A few concepts regarding expert judgment are presented here. Bonano et al. (1990) present a thorough discussion of the elicitation and use of expert judgment for a repository program. Hora and Iman (1989) present a succinct discussion of the procedure for expert judgment elicitation.

Expert judgment is the best professional opinion of experts in a particular field. It is used to synthesize what is known (existing data) to provide the required information for a particular application. Expert judgment is not a substitute for measured data, but examines whatever data exist (however abundant or sparse, under whatever experimental conditions they were collected) to provide the required information. Measured data from appropriate, practical experiments performed in a timely manner are always preferred. The extent to which directly applicable data exist, and the degree to which a phenomenon is understood, dictate the extent to which judgment must be used to provide the required information. Consideration of alternate data sources for inclusion in the current application is a problem-directed process. The appropriate use of expert judgment must be evaluated on a case-by-case basis, and is driven by the individual circumstances.

Expert judgment is an integral part of science. The use of professional judgment is a normal part of the conduct of science. The development of a conceptual model to describe a natural phenomenon requires judgment to examine the current state of knowledge and to produce a coherent model of the behavior of a natural system. Judgment is required in developing mathematical and computational models to represent conceptual models. Before data are ever collected from an experiment, judgment is used in developing the hypothesis to be evaluated and in establishing the experimental conditions. Experimental data require interpretation for appropriate use in computational models.

As used in this report, data and information are different. Data may be collected through measurements or observations, under experimental or natural conditions. Information may be defined as data interpreted and used for a specific application. It is important to realize that the use of expert judgment does not constitute creating data. It should also be realized that even when data are available, expert judgment may be necessary to develop information for the application required (e.g., to consider the impact of large physical distances/areas and long time periods).

Source Term Expert Panel

A brief discussion of the conduct of the Panel as it relates to the context in which the effort was conducted is presented below.

Issue Statement

The Panel was asked to develop probability distributions for "the equilibrium dissolved mass concentration of the i^{th} radionuclide in WIPP brines that contact WIPP wastes" and "the equilibrium suspended mass concentration of the i^{th} radionuclide (suspended in the form of colloids or particulates) in WIPP brines that contact WIPP wastes" (Trauth et al., 1992, p. B-10). The eight elements of concern in performance assessments were given as americium, curium, neptunium, plutonium, thorium, and uranium, radium, and lead.

Probability distributions characterize where a fixed, but unknown, quantity might fall. This fixed quantity is the concentration of a specific radionuclide in repository brine that might be forced up an intruding borehole. The existence of a sufficient amount of brine to transport radionuclides was assumed by the performance assessment calculations.

The issue statement prescribed the fields that must be covered by the experts—both actinide, transition, and alkali earth metals chemistry, and high ionic strength chemistry.

Panel Selection

Nominees for Panel members were sought from the SNL principal investigator for the source term, from a member of the external Performance Assessment Peer Review Panel, from a member of the National Academy of Sciences WIPP Panel, and from a University of New Mexico consultant. The pool of nominees was further increased with additional names provided by the individuals contacted originally. Nominees were evaluated by two individuals familiar with performance assessment (Dr. G. Ross Heath, University of Washington, and Chair of the Performance Assessment Peer Review Panel) and decision analysis—the discipline encompassing expert judgment (Dr. Detlof von Winterfeldt, University of Southern California) based on established criteria (see Trauth, et al., 1992), and selected four members for the Panel (the first four authors of this report).

Task Assignment

The Panel met in Albuquerque, New Mexico, March 7-8, 1991 and again April 8-9, 1991. During the first meeting, the Panel members were given an introduction to the WIPP Project and the performance assessment effort. A considerable amount of time was spent in providing them with information regarding performance assessment modeling, waste form/backfill/closure characteristics, disposal room chemistry, and the SNL experimental program on radionuclide chemistry. In addition, the Panel members received training in the use of expert judgment and the development of probability distributions. During the first meeting, the panelists were also presented with the issue statement describing the human intrusion scenarios, information on the computer program that models the brine inflow to and outflow from the rooms and drifts, and the statement of the problem, as well as published papers and reports identified from a literature search. These papers and reports focus on radionuclide solubility in high ionic strength solutions in salt formations, and include the United States repository program as well as experiments conducted in Germany, Canada, Finland, Sweden, and by the Commission of the European Communities, Joint Research Center at Ispra, Italy. Other topics include speciation, colloids, the leaching of radionuclides from vitrified high level waste, and the impact of backfill materials.

Panel Deliberations

During the second meeting, the panelists presented their concept for how to develop the required probability distributions. The distributions were developed in real-time during the meeting. Modifications were made to two of the radium distributions directly after the meeting and the values distributed to the Panel. Separate probability distributions were developed if particular conditions would affect the results (i.e., the presence or absence of carbonate or sulfate ions) or for different radionuclide oxidation states (III, IV, V, VI).

The probability distributions for radionuclide solubilities (and nonradioactive lead) developed by the Panel are provided in Tables 2 and 3 (for actinides, and for lead and radium, respectively). The values represent a theoretically derived concentration for the repository as a whole, and are based on the assumption that the concentration is a fixed value. The development of the probability distributions did not take into account inventory limits, nor did it consider waste dissolution rates. The concentrations are presented in terms of a cumulative probability distribution. Thus, the values under the column heading 0.0 within the category of "Cumulative Probabilities of Concentrations (M)" indicate the concentration below which there is a 0% probability of occurrence. In the second column of that group, there is a 10% probability that the fixed concentration is below that value. In the fourth column, the values represent concentrations, where there is a 50% probability of the fixed concentration being above that value and a 50% probability of the fixed concentration being below that value. In the extreme right-hand column, the values indicate that there is a 100% probability that the fixed concentration is below that value.

Although the issue statement requested the development of probability distributions for suspended species, the Panel did not feel that they could properly address colloids. There were not sufficient thermodynamic data available on colloids to treat them in a fashion similar to dissolved species.

Table 2. Radionuclide Source-Term Expert Panel Assessment of Concentrations (Actinides)

Element	Solution Species	Solid Species Maximum and Minimum	Cumulative Probabilities of Concentrations (M)						
			0.0	0.10	0.25	0.50	0.75	0.90	1.00
Th(IV)	$Th(OH)_4^0$	$Th(OH)_4$ ThO_2	5.5×10^{-16}	5.5×10^{-15}	1.0×10^{-12}	1.0×10^{-10}	1.0×10^{-8}	2.2×10^{-7}	2.2×10^{-6}
U(VI)	$UO_2(CO_3)_2^{2-}$	$UO_3 \bullet 2H_2O$ UO_2	1.0×10^{-7}	1.0×10^{-6}	3.0×10^{-5}	2.0×10^{-3}	1.0×10^{-2}	0.1	1.0
U(IV)	$U(OH)_4^0$	UO_2 (amorphous) U_3O_8	1.0×10^{-15}	1.0×10^{-8}	1.0×10^{-7}	1.0×10^{-6}	5.0×10^{-6}	1.0×10^{-5}	1.0×10^{-4}
Np(V)	$(NpO_2CO_3)^-$	$NpO_2(OH)$ (amorphous) $NaNpO_2CO_3 \bullet 3.5H_2O$	3.0×10^{-11}	3.0×10^{-10}	3.0×10^{-8}	6.0×10^{-7}	1.0×10^{-5}	1.2×10^{-3}	1.2×10^{-2}
Np(IV)	$(Np(OH)_5)^-$	$Np(OH)_4$ NpO_2	3.0×10^{-16}	3.0×10^{-15}	6.0×10^{-11}	6.0×10^{-9}	6.0×10^{-7}	2.0×10^{-6}	2.0×10^{-5}
Pu(V)	$(PuO_2)^+$	$Pu(OH)_4$ PuO_2	2.5×10^{-17}	2.5×10^{-16}	4.0×10^{-13}	6.0×10^{-10}	2.0×10^{-7}	5.5×10^{-5}	5.5×10^{-4}
Pu(IV)	$(Pu(OH)_5)^-$	$Pu(OH)_4$ PuO_2	2.0×10^{-16}	2.0×10^{-15}	6.0×10^{-12}	6.0×10^{-10}	6.0×10^{-8}	4.0×10^{-7}	4.0×10^{-6}
Am(III)	$(AmCl_2)^+$	$Am(OH)_3$ (amorphous) $AmOHCO_3$	5.0×10^{-14}	5.0×10^{-11}	2.0×10^{-10}	1.0×10^{-9}	1.2×10^{-6}	1.4×10^{-3}	1.4
Cm(III)	Cm^{3+}	*	5.0×10^{-14}	5.0×10^{-11}	2.0×10^{-10}	1.0×10^{-9}	1.2×10^{-6}	1.4×10^{-3}	1.4

* The probability distribution for Cm (III) was made exactly that of Am (III), as discussed in the section on curium.

Table 3. Radionuclide Source-Term Expert Panel Assessment of Concentrations (Lead and Radium)

Element and Solution Species	Solid Species	Condition	Cumulative Probabilities of Concentrations (M)						
			0.0	0.10	0.25	0.50	0.75	0.90	1.00
Pb(II) $PbCl_4^{2-}$	$PbCO_3$	Carbonate Present	1.0×10^{-9}	1.0×10^{-5}	1.0×10^{-4}	8.0×10^{-3}	4.4×10^{-2}	6.2×10^{-2}	8.0×10^{-2}
	$PbCl_2$	Carbonate Absent	0.01	0.10	1.0	1.64	2.5	6.0	10.0
Ra(II) Ra^{2+}	$RaSO_4$ and $(Ra/Ca)SO_4$	Sulfate Present	1.0×10^{-11}	1.0×10^{-10}	1.0×10^{-9}	1.0×10^{-8}	1.0×10^{-7}	2.0×10^{-7}	1.0×10^{-6}
	$RaCO_3$ and $(Ra/Ca)CO_3$	Carbonate Present	1.6×10^{-9}	1.6×10^{-8}	1.6×10^{-7}	1.6×10^{-6}	1.6×10^{-5}	1.6×10^{-1}	1.0
	$RaCl_2 \bullet 2H_2O$	Carbonate and Sulfate Absent	2.0	4.0	8.6	11.0	14.5	17.2	18.0

PROCEDURE

The Source Term Expert Panel was tasked with assigning concentrations for Pb, Ra, Th, U, Np, Pu, Am, and Cm to the 0.0, 0.1, 0.25, 0.5, 0.75, 0.9, and 1.0 fractiles of the probability distribution in WIPP brines. Trauth et al. (1993) describe the probability approach to performance assessment taken by SNL. The ideal way to assign such values is to use directly applicable experimentally determined values. However, few WIPP-specific experimental radionuclide solubility studies were available at the time the Panel was convened. In addition, the large ranges in the chemical conditions that could exist in the post-emplacement WIPP environment make it virtually impossible to explore all conditions experimentally. In such cases, one usually turns to geochemical models based on available experimental data to predict radionuclide concentrations under other conditions.

Solubility data did exist for radionuclides in dilute waters at the time the Panel was convened. However, these data must be extended to high ionic strengths which are out of the range of Debye-Hückel theory for calculating activity coefficients. The Pitzer and Harvie-Moller-Weare equations have been used successfully to describe activity coefficients in high ionic strength saline solutions. Once again, however, the constants required by these equations for the radionuclides of interest were not available. As stated in step 4), below, analogs chemically similar to the radionuclides of interest were used in the equations.

In order to make the best use of all available data in the time available, the Panel decided to use the following approach to obtain the 0.0, 0.1, 0.25, 0.5, 0.75, 0.9, and 1.0 fractiles.

1) Existing thermodynamic data for radionuclide aqueous species and expert judgment were used to identify the most likely aqueous species in solution (under potential ranges of WIPP conditions) through the construction of speciation (Eh-pH) diagrams. These data were obtained from the GEMBOCHS database version data1.com.R9, developed at Lawrence Livermore National Laboratory for use with the EQ3/6 computer code (Wolery, 1979[1]). The database included the then recently compiled uranium database of the Nuclear Energy Agency (NEA), and the latest sources of data for most of the radionuclides.

2) Existing thermodynamic data for radionuclide-bearing solid phases (again from the GEMBOCHS database version data1.com.R9) and expert judgment were used to identify potential solubility-limiting solid phases (given potential ranges of WIPP conditions), being careful to select two solids, one yielding radionuclide concentrations at low values (a sparingly soluble solid), and the other at high values (a highly soluble solid). Various radionuclide-bearing solid phase(s) were suppressed when calculating the Eh-pH diagrams described in 1) in order to aid in identification of solids that provide upper and lower limits to radionuclide activities in solution. In some cases, such as with uranium, educated judgment was used to select solids serving as upper and lower solubility-limiting phases.

3) Thermodynamic data for radionuclide aqueous species and radionuclide-bearing solid phases selected above for each radionuclide were used to calculate the activities (effective concentrations) of the dominant radionuclide aqueous species in equilibrium with each solid.

---

[1] The EQ3/6 software package overview can now be found in Wolery, 1992.

4) Activity coefficients of the radionuclide-bearing aqueous species, under high ionic strength brine conditions, were estimated by the use of specific-ion interaction (SIT) and Pitzer's equations (Pitzer, 1974, 1979; Pitzer and Kim, 1974; Pitzer and Mayorga, 1973, 1974) for aqueous species that were considered by Panel members to be chemically similar to the radionuclide-bearing aqueous species. These activity coefficients were then used to calculate the concentrations of each radionuclide at the 0.1 and 0.9 fractiles.

5) The 0.5 fractile was chosen to represent experimental data (Nitsche, 1991 in Yucca Mountain, Nevada, well J-13 water for neptunium, plutonium, and americium, for example) with activity coefficient corrections to WIPP Brine A as described above.

6) Because of information available from sources outside of the GEMBOCHS database, the probability distributions for lead and radium were developed as discussed in the text (section entitled "Development of Lead and Radium Probability Distributions").

7) Expert judgment was used to develop the 0.0, 0.25, 0.75, and 1.0 fractiles by considering the sensitivity of solubility to the potential variability in the composition of brine and gas, and the extent of waste contaminants, and extending the probability distributions accordingly. Large variability in pH, Eh, ionic strength of the brine, or ligands present or absent would be expected to introduce significant variations in solubility, so distributions were extended orders of magnitude in some cases.

Using this approach, the fractile concentrations given in Tables 2 and 3 for each element were obtained. In all cases, it is important to maintain the link between the concentrations and the fractiles of the probability distribution. The range in concentrations should not be reported; rather, each fractile concentration must be linked with the probability that the concentration will occur. The requirement imposed by the probability approach is that the 0.0 and 1.0 fractiles represent the absolute minimum and maximum concentrations that may occur, and should be considered as pushing the variable to extremes. This requirement ensures that the concentrations range over many orders of magnitude. However, as emphasized by the elicitor, the range of values between 0.0 and 0.1 and between 0.9 to 1.0 will have less impact on the performance assessment (PA) results than the values between the 0.1 and 0.9 fractiles owing to their lower probability of occurrence.

The implementation of the procedure discussed in the next section is meant for both the individual interested in the treatment of solubilities for performance assessment modeling and the individual interested in the implementation of the expert judgment process. A more general discussion of the actual steps taken in developing the probability distributions is provided in this report. Additional references and material are found in the appendices.

IMPLEMENTATION OF THE PROCEDURE

Background

Assumptions

A number of assumptions were made in order to implement the procedure. The pH of the repository environment was expected to be near 7 for the purposes of selecting the dominant aqueous species in step 1). A pH of 7.6 (the pH_{Free} of Brine A; discussed in the "Brine Composition" section) was used for calculating activities of radionuclide aqueous species in equilibrium with the solids in step 3). A somewhat oxidizing environment, related to the human intrusion scenario, was also assumed for the purpose of selecting the dominant aqueous species. The consideration of different oxidation states for the actinides incorporates the impact of differing Eh potentials. A temperature of 25°C was selected because it is close to that expected in the rooms and because extensive thermodynamic data are readily available at this temperature. The representative aqueous solution for solubilities was selected to be WIPP Brine A. WIPP Brine A was selected because it is an intergranular brine expected to accumulate in WIPP disposal rooms and because WIPP Brine A is well characterized (Molecke, 1983). Naturally occurring ligands in Brine A were considered and incorporated into the procedure, with the exception of fluoride and phosphate (these ligands are noted to be of inconsequential concentration). Organic ligands from the WIPP waste itself were not included in the speciation calculations, because they were assumed to occur in insignificant concentrations as compared to the "native" inorganic ligands in the brine (Choppin, 1988). Effects of surface complexing, sorption, and colloid formation were not considered. In addition, the activity of water was assumed to be 1 for the calculations used to develop the 0.1 and 0.9 fractiles, even though it has been calculated as 0.78 in WIPP Brine A.

Calculation of Solubility-Limited Radionuclide Concentrations

The concept of a solid limiting the solution concentration of a radionuclide is central to the calculation of the metal concentrations defining the 0.1, 0.5, and 0.9 fractiles. The equilibrium between a given solid and an aqueous (or solution) species is expressed by a mass action expression with an associated thermodynamic equilibrium constant K.[2] For example, equilibrium between solid $PbCl_2$ and the aqueous species Pb^{2+} and Cl^- is expressed by the mass action expression

$$PbCl_2(\text{solid}) = Pb^{2+} + 2Cl^- \tag{1}$$

for which the thermodynamic equilibrium constant K is defined

$$K = \left(a_{Pb^{2+}}\ a_{Cl^-}\right) / \left(a_{PbCl_2(\text{solid})}\right) \tag{2}$$

where a_i refers to the activity of the i^{th} species. Activity can be considered an effective concentration. The activity of an aqueous species is related to its concentration in solution by the activity coefficient γ according to

[2] K is later referred to as Ksp.

$$a_{Pb^{2+}} = \gamma_{Pb^{2+}} m_{Pb^{2+}} \quad (3)$$

where m refers to molality (moles per kilogram H_2O). The activity coefficients of aqueous species may be close to unity in dilute waters, such as many groundwaters. For high ionic strength brine solutions however, the activity of an aqueous species may be many times its "analytical concentrations." Therefore, serious discrepancies may be encountered if calculations are made using analytical concentrations instead of activities.

Activity coefficients may be determined experimentally or calculated by mathematical modeling. In dilute solutions, the Debye-Hückel Equation (Appendix A) has been useful. However, the Debye-Hückel expression is not accurate for predicting activity coefficients at high ionic strengths. The estimation of activity coefficients in high ionic strength media can be made through the use of ionic interaction models which are discussed briefly in Appendix B.

We have assumed that the activity of all solids is unity in this report, which is valid if the solid is pure and contains no solid solution. Thus equation (2) reduces to

$$K = a_{Pb^{2+}}\, a_{Cl^-} \quad (4)$$

The thermodynamic equilibrium constant K is calculated using thermodynamic data for each species in the mass action expression such as (1). Thermodynamic databases such as GEMBOCHS, which is used for many calculations in this report, contain tabulations of these equilibrium constants. We can use readily available aqueous speciation computer codes to calculate the activity of species such as chloride in a given solution, such as was done for WIPP Brine A in this report.

We can use equations such as (4) and (3) to calculate the concentrations of Pb^{2+} with $PbCl_2$ in given solution. In more general terms, this is how we use equilibrium with a solid to define the accompanying metal concentration in solution. However, we must take explicit account of the fact that metals speciate in solution to form a variety of aqueous species, also called aqueous complexes.

In general, radionuclide or metal ions do not exist in solution as simple hydrated ions (e.g., Pb^{2+}) particularly under near-neutral pH conditions. For example, in chloride solutions, Pb(II) may combine with chloride to form $PbCl_3^-$, $PbCl_4^{2-}$, etc. Radionuclide and metal concentrations in solution may be significantly increased by the formation of these aqueous complexes.

In view of the importance of aqueous speciations to the calculation of metal concentrations in solution, we calculated the identity of the predominant metal-bearing aqueous species under different Eh and pH conditions at 25°C. The resulting aqueous speciation or Eh-pH diagrams, shown for example in Figures 4 and 5 for thorium and uranium, illustrate graphically the identity of the aqueous species that is calculated to quantitatively dominate (that is, possess the largest activity or effective concentration) the collection of metal-bearing aqueous species that form at given values of Eh and pH. Each diagram was calculated for the composition of WIPP Brine A (Table 4).

The dominant aqueous species under oxidizing conditions and a pH of 7.6 (see above) was identified using these speciation or Eh-pH diagrams. Mass action expressions were written between the dominant metal-bearing

Table 4. The Composition of Selected Brines from the WIPP Site*

Ion	G-Seep	SB-3	Brine A	Brine B
From Brush (1990, Table 2.2)				
Na^+	4.11	3.87	1.77	4.97
Mg^{2+}	0.63	1.00	1.44	<0.005
Ca^{2+}	0.0077	0.009	0.02	0.02
K^+	0.35	0.51	0.77	<0.005
B^{3+}	0.144	0.127	0.020	0.020
Cl^-	5.10	6.01	5.35	4.93
Br^-	0.017	0.014	0.01	0.01
SO_4^{2-}	0.303	0.170	0.04	0.04
pH_{NBS}	6.1	6.0	6.5	6.5
Calculated by Panel				
$B(OH)_4^-$	0.015	0.033	0.015	0.0004
$B(OH)_3$	0.129	0.094	0.005	0.020
pH_{Free}	7.10	7.16	7.56	7.22
pH_{Total}	6.65	6.85	7.49	7.09
Activity of water, a_{H_2O}	0.785	0.744	0.783	0.806
Density†	1.209	1.219	1.188	1.170
Ionic Strength, I**	6.68	7.58	7.02	5.12
Equivalent modality, E‡	5.738	6.397	5.455	5.025

* From the tabulation of Brush (1990, Table 2.2). The values of Na^+ have been adjusted to achieve charge balance. Composition is expressed as moles per liter, M.

† Estimated using Young's rule (Millero, 1979).

** Ionic strength, $I = \frac{1}{2} \Sigma z_i^2 c_i$, where z is the ionic charge and c is concentration

‡ Equivalent modality, $E = \frac{1}{2} \Sigma zc$.

aqueous species and the solubility-limiting solid. These mass action expressions were then used to define the metal concentrations in solution.

It is recognized that some error is introduced by not fully accounting for the formation of the full range of metal-bearing aqueous complexes, and focusing instead on the most dominant species. However, such calculations would be time-consuming and highly dependent on changes in solution composition, and would in general introduce less than a 50% deviation in the calculated concentrations.

Brine Composition

The compositions of the WIPP intergranular brines have been considered by Brush (1990). These intergranular brines are those expected to accumulate in WIPP disposal rooms after filling and sealing. Horita et al. (1991) have studied WIPP intragranular brines. These brines are present as fluid inclusions, and are not expected to accumulate in the repository to any significant extent. The brines are largely Na-K-Mg-Ca-Cl-SO_4 brines that have been formed from seawater. Brush (1990) has suggested that four possible brines need to be considered. The compositions of these brines are given in Table 4. The G Seep brine was collected from the WIPP underground workings. The SB-3 (standard brine) brine was defined by Brush and Anderson (1989), while Brines WIPP-A and WIPP-B are standard brines thought to be in equilibrium with the minerals overlying the site (WIPP-A) and entering from below the site (WIPP-B). WIPP-A brine was selected for the present study because its composition is representative of those brines found in the Salado Formation (such as SB-3), and also because halite solubility and density data for this brine have been obtained at temperatures between 20 and 100°C (Chou et al., 1982).

The differences in the brines can be examined by using the Pitzer equations (Pitzer, 1979) and the resultant effect on the activity coefficients of the major components of the brines can be determined. At present, the Pitzer equations at 25°C can be used to determine the activity coefficients of species (ions) in brines composed of H-Na-K-Mg-Ca-Cl-SO_4-Br-OH-HCO_3-CO_3-CO_2-$B(OH)_3$-$B(OH)_4$ to high ionic strengths (Harvie and Weare, 1980; Harvie, Møller, and Weare, 1984; Felmy and Weare, 1986; Møller, 1988). Researchers (including Frank J. Millero) have calculated activity coefficients in these brines using Pitzer programs (Pitzer, 1974, 1979; Pitzer and Kim, 1974; Pitzer and Mayorga, 1973, 1974). Activity coefficients in WIPP brines are given in Table 5. It should be pointed out that single ion activity coefficients must be adjusted to a common scale before they can be compared for different media. These activity coefficients can be used to estimate the stoichiometric pK* of carbonic acid, boric acid, hydrogen sulfide, and water in the brines. These values calculated for WIPP brines are given in Table 6.

To use these stoichiometric pK*s to estimate the anions of acids that can complex metals in the brines, it is necessary to know the total hydrogen ion concentration [H^+] in the brines. The pH reported by Brush is National Bureau of Standards (NBS) based rather than being a measurement of total [H^+]. It is possible to estimate the values from the values of pH measured using NBS (now National Institute of Standards and Technology [NIST]) buffers by calibration of the electrode system in brines of similar composition. A WIPP Brine A solution was prepared for this effort and used to calculate pH_{Free} and pH_{Total} as discussed in Appendix C, and reported in Table 4.

The initial compositions of the brines of the WIPP sites are such that reasonable estimates of activity coefficients for anions (from Cl^- and SO_4^{2-} salts) and for cations (from Na^+ and Mg^{2+} salts) can be made. This allows one to estimate the activity coefficients of free ions in the ionic brines. The effect of the major and minor anions on trace cations can be estimated using an ion-pairing model (subsequently documented in Millero, 1992). To use this model, it is first necessary to consider the ligands besides Cl^- and SO_4^{2-} that can form complexes with the nuclides of interest.

Table 5. Activity Coefficients of Solutes (γ) in the WIPP Brines Calculated Using Pitzer's Equations*

Ion	G-Seep	SB-3	Brine A	Brine B
H^+	1.04	1.86	2.27	2.29
Li^+	2.14	2.63	2.97	2.07
Na^+	0.80	0.86	0.74	0.86
K^+	0.41	0.39	0.36	0.50
Rb^+	0.51	0.51	0.47	0.53
Cs^+	0.31	0.30	0.39	0.29
NH_4^+	0.52	0.53	0.50	0.57
$TRISH^+$	0.47	0.47	0.45	0.52
Mg^{2+}	0.94	1.30	0.70	1.09
Ca^{2+}	0.55	0.72	0.40	0.70
Sr^{2+}	0.48	0.62	0.38	0.56
Ba^{2+}	0.19	0.20	0.15	0.25
Mn^{2+}	0.42	0.49	0.36	0.50
Fe^{2+}	0.63	0.83	0.51	0.84
Co^{2+}	0.69	0.92	0.58	0.94
Ni^{2+}	0.81	1.14	0.67	1.08
Cu^{2+}	0.21	0.22	0.17	0.31
Zn^{2+}	0.06	0.04	0.05	0.11
UO_2^{2+}	0.92	1.23	0.82	1.38
F^-	0.40	0.38	0.35	0.46
Cl^-	1.16	1.48	1.62	0.88
Br^-	1.61	2.18	2.35	1.10
I^-	2.25	3.19	3.27	1.49
OH^-	0.004	0.36	0.0020	0.28
HCO_3^-	0.41	0.42	0.461	0.43
$B(OH)_4^-$	0.052	0.018	0.0064	0.26
HSO_4^-	1.10	1.52	1.99	0.71
HS^-	0.76	0.70	0.63	0.88
HSO_3^-	1.40	1.79	2.19	1.01
ClO_4^-	1.16	1.68	2.328	0.68
NO_3^-	0.55	0.69	1.006	0.38
$H_2PO_4^-$	0.60	0.90	1.938	0.31
$Acet^-$	1.04	0.95	0.589	1.45
SO_4^{2-}	0.02	0.025	0.0324	0.0210
CO_3^{2-}	0.003	0.0016	0.00157	0.016
SO_3^{2-}	0.09	0.11	0.128	0.094
HPO_4^{2-}	0.005	0.0032	0.00275	0.0098
PO_4^{3-}	1.1E(−5)	5.3E(−6)	2.1E(−6)	8.3E(−5)
TRIS	1.145	1.093	0.948	1.257
NH_3	1.650	1.765	1.692	1.468

* These activity coefficients have been corrected to include the impact of the liquid junction potential. This corrected activity coefficient is described in Appendix C and is referred to as *f*.

Table 5. Activity Coefficients of Solutes (γ) in the WIPP Brines Calculated Using Pitzer's Equations (continued)

Ion	G-Seep	SB-3	Brine A	Brine B
$B(OH)_3$	2.348	2.784	2.501	1.808
H_2S	1.970	2.044	2.001	1.794
SO_2	1.459	1.536	1.488	1.337
CO_2^-	1.043	3.372	2.697	2.619

Table 6. Calculated pK*s for the Ionization of Acid in the WIPP Brines

Acid	G-Seep	SB-3	Brine A	Brine B
H_2O	11.68	11.55	11.75	13.90
H_2S	6.59	6.79	6.84	7.03
H_2CO_3	5.50	5.72	5.95	5.94
H_3BO_3	7.60	7.31	7.00	8.76
H_2SO_3	1.86	2.20	2.38	2.10
H_3PO_4	1.94	2.38	2.79	2.00
NH_4	9.72	9.99	10.09	9.97
HSO_4	0.33	0.48	0.55	0.81
HCO_3	8.80	8.88	8.69	9.44
HSO_3	6.00	6.24	6.29	6.50
H_2PO_4	5.13	5.02	4.71	6.06
HPO_4	9.71	9.83	9.59	10.63

Ligands Present in the Brines

After the WIPP is closed and the shafts are sealed, the various components of the waste can contribute a number of anions or ligands that can affect the speciation and concentrations of radionuclides in the brine. From an examination of the behavior of metals in natural waters like seawater, it can be determined that OH^-, CO_3^{2-}, Cl^-, and SO_4^{2-} are the naturally occurring inorganic ligands expected to significantly influence the activity of metals in the brines. Of these, the concentrations of OH^- and CO_3^{2-} will probably change with time. The summary of Brush (1990) offers a good starting point for the amounts of the various ligands one might expect in the brine after waste emplacement. The intermediate values selected by Brush are given in Table 7. Most of the waste-introduced organic ligands are in the micro-molar level, and are assumed not to compete with the expected concentration of carbonate ion (Choppin, 1988 [reproduced in Appendix D]). Additional information on brine ligands is found in Appendix E.

The effect of major inorganic ligands on the solubility of the key elements in the brines was considered in the calculation of the 0.1, 0.5, and 0.9 fractiles as described in this report.

Table 7. Estimates of the Concentrations of Ligands in the WIPP Brines*

Ligand	Concentration
chloride†	5.0 - 6.0 M
sulfate†	0.04 - 0.3 M
ascorbate	10 mM
NO_3^-	400 mM
carbonate	1 M
acetate	7 mM
citrate	700 µM
EDTA	1 µM
α-hydroxyisobutyrate	400 nM
lactate	200 µM
oxalate	9 mM
oxine	100 µM
1,10-phenanthroline	400 nM
TTA	20 µM

* Brush (1990, Table 7.3)
† Brush (1990, Table 2.2)

Development of Actinide Probability Distributions

The speciation diagrams that were used to select an aqueous species and the Eh-pH diagram(s) that were used to select solubility-limiting solid phases are provided in the text. These diagrams for WIPP Brine A were created specifically for this effort. The pH range of 3 to 12 should encompass most brine pH conditions. The determination of the dominant aqueous (i.e., dissolved) species in a particular solvent, represented by a speciation diagram, is independent of the total amount of radionuclide initially introduced into solution. The only exception to this statement is when a radionuclide forms an oligomer, a species containing two or more atoms of the same radionuclide. Calculations suggest that oligomers don't form under the range of radionuclide concentrations in WIPP Brine A, and therefore, radionuclide activities are not given for the aqueous speciation diagrams.

By use of the aqueous speciation diagram, a dominant aqueous species is selected for subsequent calculations. Other less significant species containing that radionuclide exist, but are not considered in order to simplify the calculations. Aqueous species occupy domains that on the diagrams are separated by lines. Lines separating dominant aqueous species indicate conditions at which activities are equal.

A determination of the dominant solid phases, however, is heavily dependent on the activity of the radionuclide. Therefore, activities are given for the solid phase Eh-pH diagrams. In some cases, several Eh-pH diagrams for solid phases were examined to select the solid species for consideration:

> "To supplement the Eh-pH diagram showing aqueous speciation, Eh-pH diagrams considering both solid and aqueous species were constructed. The location and movement of the boundaries between solid and aqueous species in response to variations in the activity of the radionuclide illustrate the ability of solids to sequester radionuclides under varying Eh and pH conditions. The

diagrams also show how the identities and compositions of solubility-limiting solids vary with Eh and pH." (Chu and Bernard, 1991, Appendix D)

The thermodynamic data used to develop the previously discussed diagrams were obtained from the GEMBOCHS database version data1.com.R9, developed at Lawrence Livermore National Laboratory for use with the EQ3/6 computer code (Wolery, 1979). The database included the then recently compiled uranium database of the NEA, and the latest sources for most of the radionuclides. Curium was not calculated, since thermodynamic data for this species were not available in this database. This usage of speciation diagrams to identify pertinent species and the use of the GEMBOCHS thermodynamic database to assess radionuclide solubilities and determine the impact of changing Eh and pH conditions has been performed previously by one of the Panel members (Carol J. Bruton) (Appendix D from Chu and Bernard, 1991).

The mass-action equations used to calculate solution activities for equilibrium conditions between the aqueous and solid species are found in Appendix F. The terms within these mass-action equations show that the calculated solution activities are a function not only of the species in equilibrium, but may be a function of the pH, the oxygen fugacity, or other solution parameters, such as the activities of sodium, chloride, or carbonate. The manner in which variations in the environmental conditions could impact the calculated activities was one of the considerations in developing the 0.0 and 1.0 fractiles.

It is very common to report concentrations and perform activity calculations in terms of the molality (moles per kilogram of solution) of the solution. The concentrations reported in Tables 2 and 3 are in terms of molarity (moles per liter of solution). In the case of WIPP Brine A, the difference in concentrations calculated in terms of molality and molarity is approximately 20%. Because of the assumptions being made and the nature of the calculations, the resultant estimated concentration ranges span orders of magnitude, so a difference of 20% will not have a great impact. Concentrations were thus labeled as molarity for the performance assessment calculations. It should also be noted that because of the order of magnitude calculations being performed, the values in Tables 2 and 3 were often rounded off.

Experimental solubility data for some elements in high ionic strength media did exist at the time of the Panel meetings. Care must be taken in the direct use of individual experimental data because of qualifying criteria:

1) that sufficient time was allowed for the experiments to reach equilibrium or steady state;

2) that the aqueous species and the solubility limiting compounds were correctly identified;

3) that accurate phase separation was performed; and

4) that accurate concentration measurements were made.

Because of the availability of the experimental results of Nitsche and coworkers (Nitsche, 1991) on neptunium, plutonium, and americium solubilities in low ionic strength water (from Yucca Mountain well J-13), the Panel chose to specifically use them to develop the probability distributions. Corrections of these data to higher ionic strength values were made using Pitzer's equations and specific ion interaction theory (SIT) formalism in order to estimate 0.5 fractile solubilities of these elements in Brine A. Pitzer equations are shown in Appendix G.

In its deliberations and calculations, the Panel considered what species would be formed on dissolution, but not what species would be present in the waste and would be stable on dissolution.

The following discussion provides additional details on how the probability distributions in Tables 2 and 3 were developed.

Thorium

The dominant aqueous species for thorium above a pH of 5 and the full range of Eh is $Th(OH)_4(aq)$ as shown in Figure 4. The solids chosen for the thorium system are ThO_2(thorianite) and $Th(OH)_4$ based upon the analogous reasoning presented below for plutonium. The equilibrium equation between $Th(OH)_4(aq)$ and ThO_2, a sparingly soluble solid, was chosen to represent the 0.1 fractile with a calculated value of 5.5×10^{-15} M. The equilibrium equation between $Th(OH)_4(aq)$ and $Th(OH)_4$, a quite soluble solid, was chosen to represent the 0.9 fractile, with a calculated value of 2.2×10^{-7} M.

Other Fractiles

The 0.5 fractile for Th(IV) was estimated using an equilibrium constant, K, of 52.3 for the reaction:

$$Th(OH)_4 \quad Th^{4+} + 4OH^- \tag{6}$$

for a calculated value of 1.0×10^{-10} M. The other fractiles were estimated by providing for the likelihood that carbonate and chloride concentrations and other conditions will be variable.

Uranium

Figure 5 shows that the U(IV) species $U(OH)_4(aq)$ dominates at Eh values less than about 0. The $U(OH)_4(aq)$ species was selected in contrast to the use of the aqueous species $Np(OH)_5^-$ and $Pu(OH)_5^-$ for other radionuclides. Thermodynamic data for $U(OH)_5^-$ did not exist in the database used in these calculations and was thus not available for consideration. At more oxidizing Eh potentials and pH values between 5.5 and 11, the U(VI) species $UO_2CO_3(aq)$, $UO_2(CO_3)_2^{2-}$ and $UO_2(CO_3)_3^{4-}$ dominate. $UO_2(CO_3)_2^{2-}$ was chosen as the uranium species under more oxidizing conditions because it is dominant at pH 7.6, the value that was chosen as a reference point for these calculations.

The selection of uranium-bearing solids to represent the 0.1 and 0.9 fractiles for U(IV) and U(VI) proved problematic because of the wide variety of solids that contain uranium in different, including mixed, oxidation states. For example, thermodynamic properties for the solids UO_2, U_3O_8, U_3O_7, and U_4O_9 are available. The discussion below describes the approach for selecting U(IV) and U(VI) solubility limiting solids.

Uranium(IV)

Eh-pH diagrams were constructed to identify the solid that controls uranium solubility at a minimum in the $U(OH)_4(aq)$ stability field. As shown in Figure 6, U_3O_8 appeared as the most stable solid in the stability field of $U(OH)_4(aq)$ and was thus chosen as the solid for the 0.1 fractile.

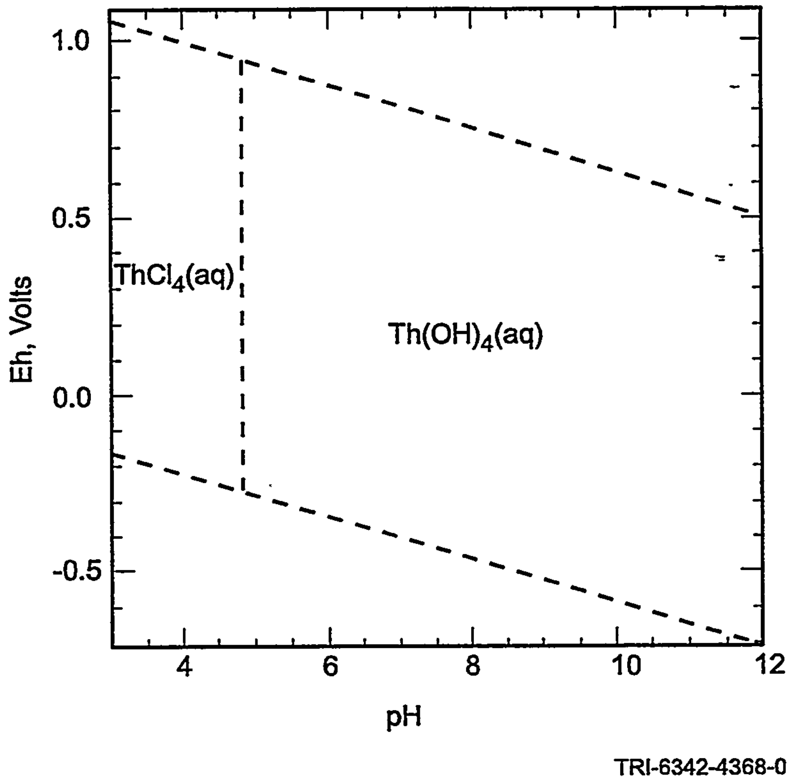

Figure 4. Calculated aqueous speciation diagram for thorium in WIPP Brine A.

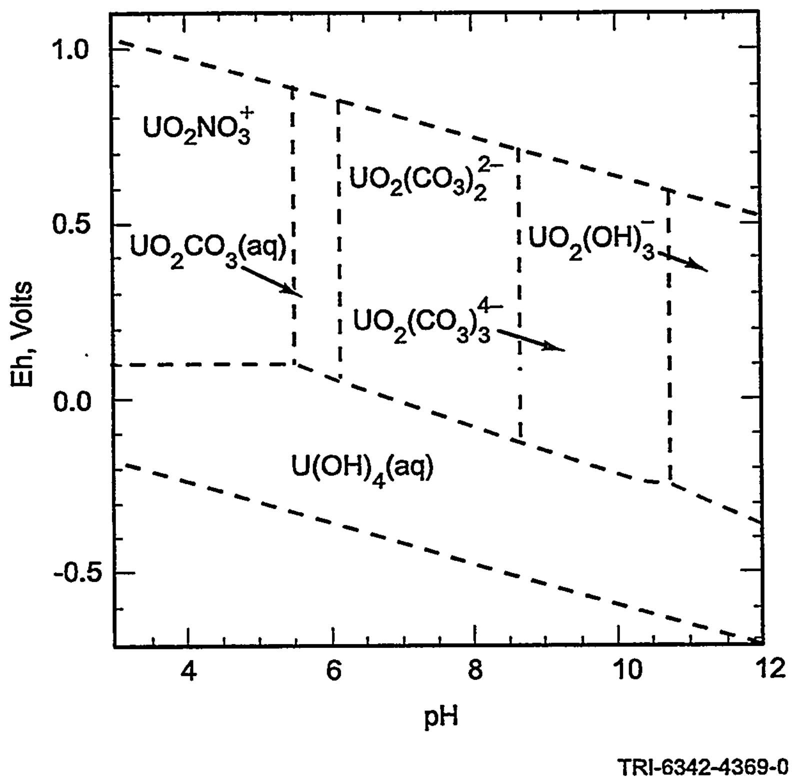

Figure 5. Calculated aqueous speciation diagram for uranium in WIPP Brine A.

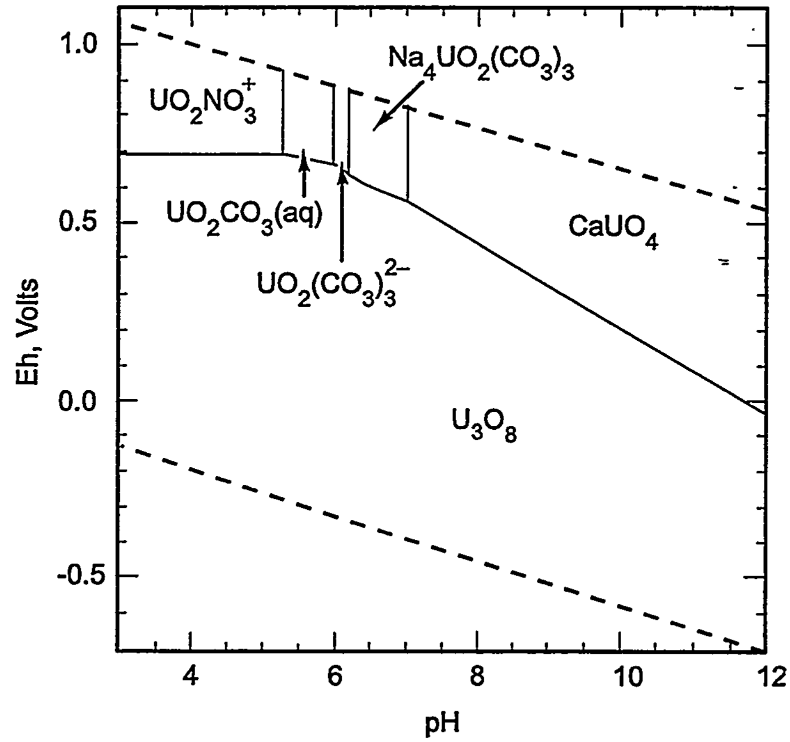

Figure 6. Calculated Eh-pH diagram for uranium in WIPP Brine A (assuming that the activity of the dominant uranium-bearing aqueous species equals 1×10^{-6}.

The reaction between U_3O_8 and $U(OH)_4(aq)$ involves a change in oxidation state, and can be written as a function of the oxygen fugacity (or partial pressure of oxygen). Therefore, we must estimate the expected partial pressure of oxygen in order to calculate the concentration of uranium corresponding to the 0.1 fractile. We considered an oxygen partial pressure of 1×10^{-56} bars that corresponds to a pH of 7.6 and an Eh of -0.05 V along the upper border of the $U(OH)_4(aq)$ stability field shown in Figure 5. This would have resulted in a calculated concentration of 2×10^{-7} M. Since the intent was to develop a "minimum" value, an oxygen partial pressure of 1×10^{-52} bars was used which spread the distribution a bit more. The equilibrium equation between $U(OH)_4(aq)$ and the solid U_3O_8 represented the 0.1 fractile, with a calculated value of 1.0×10^{-8} M.

In the choice of UO_2(amorphous) for the 0.9 fractile, we considered that amorphous phases are well known to precipitate readily from solution, especially at low temperatures. For this reason, they tend to control element concentrations in solution at comparatively high values. Thus, UO_2(amorphous) was considered as an upper limit to uranium solubility in the stability field of $U(OH)_4(aq)$. The equilibrium between these two species results in a calculated concentration of 1.4×10^{-5} M. An added advantage to choosing this species is that its reaction with $U(OH)_4(aq)$ is independent of pH and other solution variables. Note that the values for U(IV) at the 0.25, 0.5, 0.75, 0.9, and 1.0 fractiles are lower values than published in earlier material on this subject. An error in the value of an activity coefficient was subsequently discovered. In the previous drafts, the activity coefficient for the uranyl carbonate species was inadvertently used.

Uranium(VI)

The solid-defining the 0.1 fractile was problematic. Figure 6 shows that the solids $Na_4UO_2(CO_3)_3$ and $CaUO_4$ are calculated to be most stable under oxidizing conditions. However, Panel members did not have sufficient confidence in the thermodynamic data for these solids to select them to calculate fractile concentrations. The panel members used expert judgment to select UO_2(uraninite) as the solid defining the 0.1 fractile. As was the case with U(IV), equilibrium between $UO(CO_3)_2^{2-}$ and UO_2(uraninite) required specification of the fugacity of oxygen. An oxygen fugacity equal to 1×10^{-55} bars, that corresponds to the lower limit of the stability field of $UO_2(CO_3)_2^{2-}$ (see Figure 5), was selected. A choice of a higher oxygen fugacity would have produced increased uranium concentrations in solution, whereas a lower limit was desired. The equilibrium calculations thus result in a value for the 0.1 fractile of 1.0×10^{-6} M.

$UO_3 \cdot 2H_2O$ (schoepite) was selected as the solubility controlling phase for the 0.9 fractile because mass actions expressions between $UO_2(CO_3)_2^{2-}$ and schoepite yielded the largest concentrations of uranium in solution relative to other uranium oxides. Equilibrium between $UO_2(CO_3)_2^{2-}$ and schoepite, used to define the 0.9 fractile, required definition of the activity of HCO_3^- in Brine A, which was calculated to be $1 \times 10^{-2.34}$. The 0.9 fractile was thus calculated to be 0.1 M.

Other Fractiles

For U(IV), the interior fractiles were assigned based purely on the 0.1 and 0.9 fractiles without further data input. The 0.0 and 1.0 fractiles were estimated by providing for the likelihood that carbonate and chloride concentration, and other conditions will be variable in the brine.

For U(VI), the 0.5 fractile was estimated using a solubility product for UO_2CO_3 taken from the literature in the manner described for neptunium, plutonium, and americium. The remainder of the fractiles were estimated by providing for the likelihood that carbonate and chloride concentration, and other conditions, will be variable in the brine.

Neptunium

Figure 7 shows the aqueous speciation of Np in WIPP Brine A. Over the relevant Eh and pH range, neptunium species exist in the Np(IV) and Np(V) valence states. $NpO_2CO_3^-$ and $Np(OH)_5^-$ were chosen to represent the dominant species at Eh values greater than and less than about 0.2 V, respectively.

Although $NpO_2Cl(aq)$ appears in the aqueous speciation diagram to be the dominant aqueous species at the selected Eh and pH range, the Panel decided to use $NpO_2CO_3^-$ instead. The Panel believed that, in the presence of carbonate ion at pH values greater than 7, carbonate complexation should dominate the solution species. The Panel felt that the thermodynamic data for NpO_2Cl and $NpO_2CO_3^-$ that placed the stability boundary at a very high pH value (about 8.8) was in question.

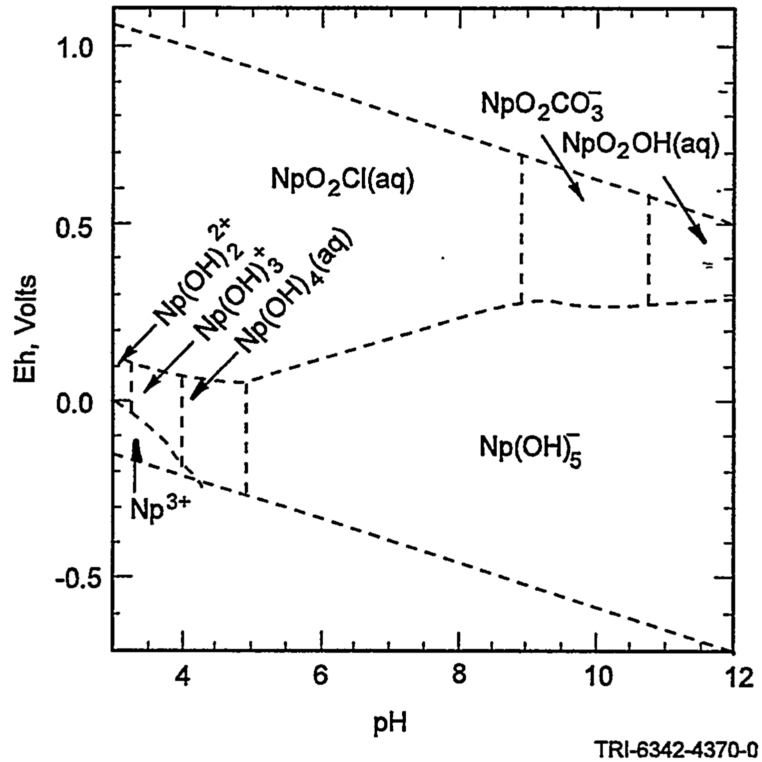

Figure 7. Calculated aqueous speciation diagram for neptunium in WIPP Brine A.

At the time that the Panel was convened, there was significant controversy in the scientific community regarding the validity of $Np(OH)_5^-$ and also $Pu(OH)_5^-$ as species. Since the convening of the Expert Panel, the NEA included thermodynamic data for $U(OH)_5^-$ in their critical compilation of data for uranium species, although it is considered minor relative to $U(OH)_4$ (aq) at pH values less than 12. Given a lack of time to adequately address the thermodynamic data in GEMBOCHS (version data1.com.R9), the Panel decided to accept on a provisional basis the GEMBOCHS data for $Np(OH)_5^-$ and $Pu(OH)_5^-$.

Neptunium(IV)

Equilibrium calculations from the GEMBOCHS database, expressed in an Eh-pH diagram, indicate that NpO_2 is the most sparingly soluble neptunium-bearing solid. Figure 8 illustrates the Eh-pH region over which NpO_2 is stable. Suppression of NpO_2 in the construction of this diagram yields Figure 9, at an activity of 10^{-6}. Note that at Eh values less than about 0.2, $Np(OH)_4$ replaces NpO_2 as the solubility-limiting phase. Therefore, NpO_2 and $Np(OH)_4$ were selected as the solubility limiting solids. The selection of NpO_2 and $Np(OH)_4$ solids as solubility-limiting phases is analogous to the selection of PuO_2 and $Pu(OH)_4$ discussed in greater detail in the plutonium section. Solubility limits are a function of the crystalline/amorphous nature of the solid phase, and aging has an effect. Strickert et al. (1984) discuss the effect of aging on the solubility of neptunium.

The neptunium concentration resulting from the equilibrium between the sparingly soluble NpO_2 and the aqueous $Np(OH)_5^-$ in WIPP Brine A was selected to represent the 0.1 fractile, with a calculated value of 3.0×10^{-15} M. The neptunium concentration resulting from the equilibrium between $Np(OH)_4$ and $Np(OH)_5^-$ was

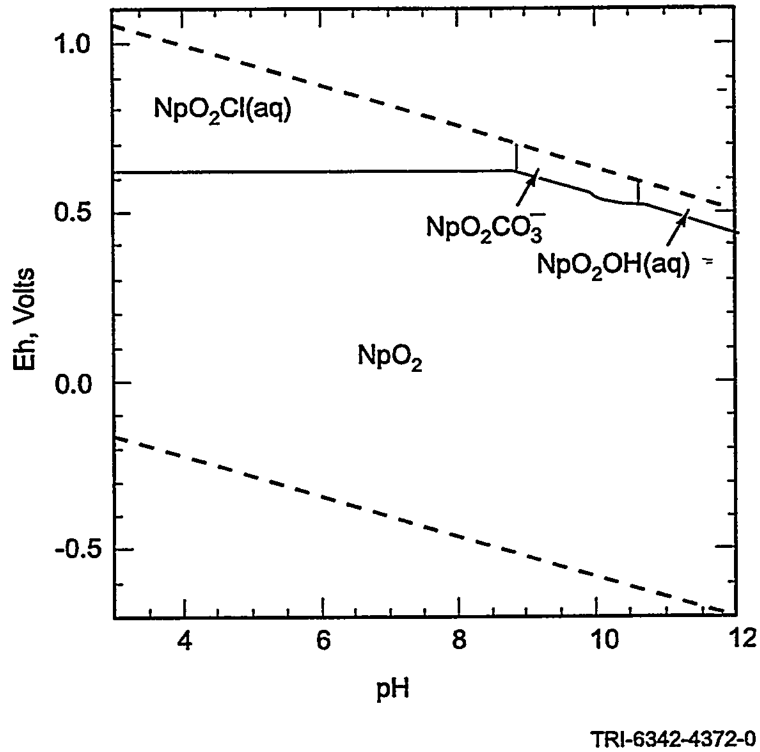

Figure 8. Calculated Eh-pH diagram for neptunium in WIPP Brine A (assuming that the activity of the dominant neptunium-bearing aqueous species equals 1×10^{-8}).

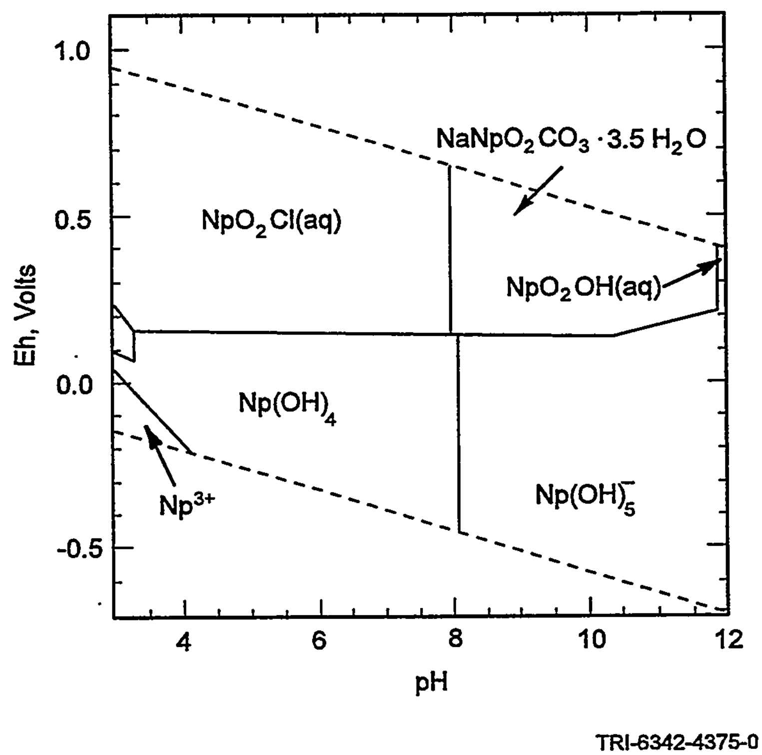

Figure 9. Calculated Eh-pH diagram for neptunium in WIPP Brine A (assuming that the activity of the dominant neptunium bearing aqueous species equals 1×10^{-6}) with the solid NpO_2 suppressed.

selected to represent the 0.9 fractile, with a calculated value of 2.0×10^{-6} M, representing a highly soluble neptunium-bearing solid.

Neptunium(V)

Nitsche (1991) found that $NaNpO_2CO_3 \cdot 2.5H_2O$ exists and controls the solubility of neptunium in J-13 water, rather than NpO_2, which was selected as the sparingly soluble solid for Np(IV). NpO_2OH(amorphous) was selected as an upper limit to neptunium solubility under oxidizing conditions because it is a less stable, hydroxide-bearing phase. Therefore, the concentration of neptunium resulting from the equilibrium between $NaNpO_2CO_3 \cdot 2.5H_2O$ and $NpO_2CO_3^-$ was selected to represent the 0.1 fractile, with a calculated value of 3.0×10^{-10} M. The concentration of neptunium resulting from the equilibrium between NpO_2OH(amorphous) and $NpO_2CO_3^-$ was selected to represent the 0.9 fractile, with a value of 1.2×10^{-3} M.

Other Fractiles

A solubility product for neptunium is listed in Table 8 and was derived (along with the solubility product for plutonium and americium) from solubility data of Nitsche (1991). The solubility products at given ionic strengths were estimated by assuming that the solids $Np(OH)_4$, $Pu(OH)_4$, and $AmOHCO_3$ existed in equilibrium with the reported concentrations of neptunium, plutonium, and americium at pH values of 6, 7, and 8.5. The concentration of total carbonate was that of J-13 water (see, for example, Ogard and Kerrisk, 1984). The solubility products were then extrapolated to infinite dilution using the Pitzer equations. The resulting thermodynamic solubility constants are shown in Table 8. These thermodynamic solubility constants were then used in combination with the ion pairing model to estimate neptunium, plutonium, and americium concentrations for the 0.5 fractile in high ionic strength Brine A. The concentration calculated for neptunium was 6.0×10^{-9} M and was the value used for Np(IV). The 0.1 and 0.9 fractiles for Np(V) are greater than those for Np(IV), suggesting a higher solubility. Thus, the 0.5 fractile value for Np(V) was assessed as two orders of magnitude greater than the value for Np(IV), at a value of 6.0×10^{-7} M.

The 0.0, 0.25, 0.75, and 1.0 fractiles were estimated by providing for the impact of the variability of carbonate and chloride concentrations, and of other conditions.

Table 8: Estimated Solid Phases and Thermodynamic Solubility Products

Element	Solid Phase	pKsp (in pure water)
Americium	$Am(OH)CO_3$	24.39
Curium	$Cm(OH)CO_3$	24.39 (equated to Am)
Lead	$PbCO_3$	13.2
	$PbCl_2$	4.77
Neptunium	$Np(OH)_4$	32.32
Plutonium	$Pu(OH)_4$	51.73
Thorium	$Th(OH)_4$	52.3
Uranium	UO_2CO_3	8.74

Plutonium

The speciation diagram for aqueous (i.e., dissolved) species of plutonium in WIPP Brine A is shown in Figure 10. $Pu(OH)_5^-$ and PuO_2^+ are the dominant species in solution at a pH of 7 and Eh values greater than about 0.0 V, for Pu(IV) and Pu(V), respectively.

Plutonium(III)

Plutonium(III) may be formed under certain conditions (reducing potential and low pH) within the repository. However, slightly oxidizing potential conditions at near neutral pH in the upper aquifer could oxidize Pu(III) (i.e., to higher oxidation states). In addition, alpha-radiolysis of brine solutions may create oxidizing conditions sufficient to oxidize Pu(III). When oxidized, Pu(III) forms Pu(IV), which subsequently and rapidly forms a colloidal species (hydrolyzed plutonium dioxide). Thus, there is a thermodynamic driving force making Pu(III) unstable under these slightly oxidizing potentials and near neutral pHs. As indicated earlier, colloid behavior could not be addressed by the Panel with the limited thermodynamic data available at the time of the meetings. Because the Panel was charged with developing probability distributions for solubilities associated with fluid potentially moving up a borehole, (i.e., human intrusion) and into the upper aquifer, conditions in an upper aquifer were assumed.

In retrospect, the Panel has undertaken a series of calculations to assess the impact of selecting Pu(III) as an aqueous species for calculating concentrations. Plutonium(III) is the dominant aqueous species under reducing conditions and low pH. At higher pH values, i.e., pH greater that 7.6 (see Figure 11), its stability range is quite narrow. If Pu(III) was the dominant solution species in equilibrium with PuO_2 and $Pu(OH)_4$, the calculated concentrations for the 0.1 and 0.9 fractiles would be 3.5×10^{-15} M and 4.8×10^{-7} M, respectively, which are consistent with the values calculated for Pu(IV) and Pu(V). These calculations were made assuming an oxygen fugacity of 1×10^{-78} bars, corresponding to an Eh of about –0.4 V and a pH of 7.6.

Plutonium(IV)

In natural systems, freshly precipitated solids tend to be amorphous and hydrous, and age into more crystalline forms. Experimental evidence has shown that an amorphous hydrous phase approximated in composition by $Pu(OH)_4$ is the first solid species to precipitate out of a supersaturated plutonium solution. Over time, $Pu(OH)_4$ would tend to convert to PuO_2. The solubility and aging of plutonium oxides is discussed in Rai and Ryan (1982). $Pu(OH)_4$ is unstable in comparison with PuO_2, and equilibrium with $Pu(OH)_5^-$ would result in a solution with relatively higher plutonium concentrations. Equilibrium with PuO_2 results in substantially lower Pu concentrations in solution. PuO_2 and $Pu(OH)_4$ were thus selected as the solid species resulting in the 0.1 and 0.9 fractiles, respectively.

Equations representing equilibrium between the aqueous species ($Pu(OH)_5^-$) and each of the selected solid species were developed in order to solve for the activity of plutonium in solution for each of the two cases. These equations are found in Appendix F. The calculated concentration of plutonium when aqueous plutonium as $Pu(OH)_5^-$ is in equilibrium with PuO_2 was assessed as the 0.1 fractile with a calculated value of 2.0×10^{-15} M for the distribution. The calculated concentration of plutonium when aqueous plutonium as $Pu(OH)_5^-$ is in

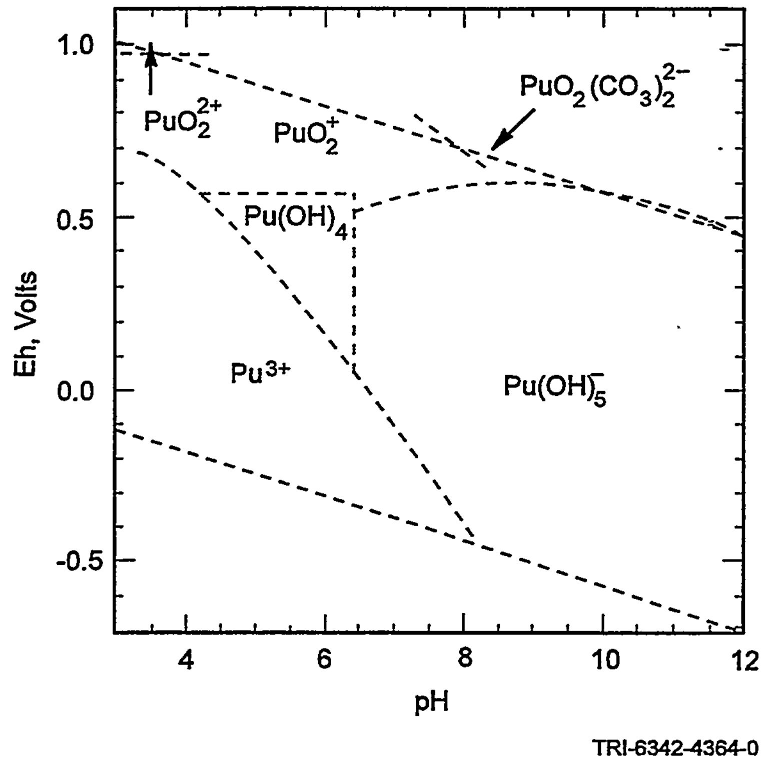

Figure 10. Calculated aqueous speciation diagram for plutonium in WIPP Brine A.

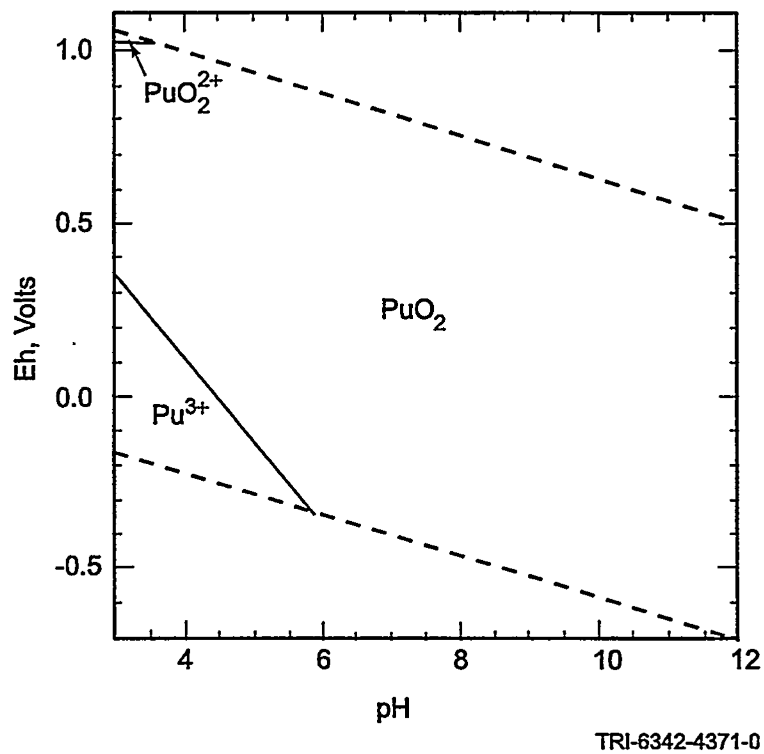

Figure 11. Calculated Eh-pH diagram for plutonium in WIPP Brine A (assuming that the activity of the dominant plutonium-bearing aqueous species equals 1×10^{-8}).

equilibrium with $Pu(OH)_4$ was assessed as the 0.9 fractile with a calculated value of 4.0×10^{-7} M for the probability distribution for Pu(IV).

Note that the consequences of the formation of colloidal Pu(IV) have not been addressed in this report. No accounting for the formation of these species is included in the GEMBOCHS database, and there is no future expectation that they could be accounted for because of the inability to treat them mathematically.

Plutonium(V)

As with Pu(IV), PuO_2 and $Pu(OH)_4$ were the solids of interest. A series of activity diagrams were constructed to help to identify the solubility-limiting solid phases. As previously mentioned, PuO_2 was the most stable solubility-limiting phase (Figure 11). $Pu(OH)_4$ was the next most stable phase, as evidenced when PuO_2 was suppressed (Figure 12). The Pu(VI) species, $PuO_2(OH)_2$, was calculated to occur at extremely high oxidation potential, but such conditions are not expected to be reached. No Pu(V) solids were calculated to be stable at plutonium activities as high as 1×10^{-6}, so equilibrium calculations were made with Pu(IV) solids. A pH of 7.6 and an oxygen fugacity of 1×10^{-11} bars were assumed in order to calculate the plutonium concentrations. The plutonium concentration calculated for the equilibrium between the PuO_2^+ aqueous species and the PuO_2 solid species was assessed as the 0.10 fractile, with a calculated value of 2.5×10^{-16} M. The plutonium concentration calculated for the equilibrium between the PuO_2^+ aqueous species and the $Pu(OH)_4$ solid species was assessed as the 0.90 fractile, with a calculated value of 5.5×10^{-5} M. The most probable solubility limiting solid in equilibrium with aquo Pu(V), analogous to the Np(V) case, is sodium Pu(V) carbonate ($NaPuO_2CO_3 \cdot xH_2O$). However, at the time the Panel was convened, this solid was not included in the GEMBOCHS database, and the above solids were chosen.

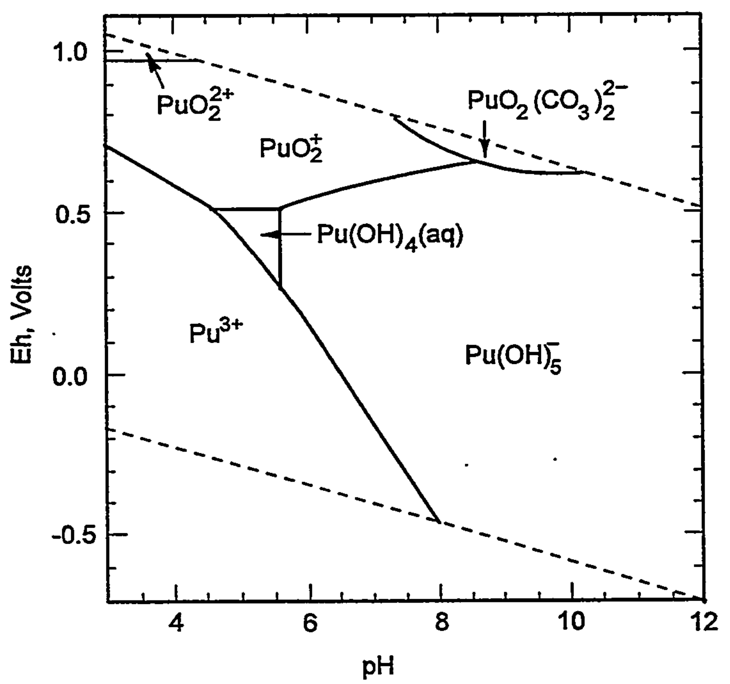

Figure 12. Calculated Eh-pH diagram for plutonium in WIPP Brine A (assuming that the activity of the dominant plutonium-bearing aqueous species equals 1×10^{-8}) with the solid PuO_2 suppressed.

Other Fractiles

The development of the 0.5 fractile for plutonium was the same process as that reported for neptunium. The 0.1 and 0.9 fractiles for Pu(IV) and Pu(V) are closer to each other than was the case for the oxidation states of neptunium, so the calculated plutonium 0.5 fractile (6.0×10^{-10} M) was used for both oxidation states.

As was the case with neptunium, the development of the 0.0, 0.25, 0.75, and 1.0 fractiles was based on a consideration of the impact of the variability of carbonate and chloride concentrations, and of other conditions.

Americium

Figure 13 shows the aqueous speciation of Am in WIPP Brine A. $AmCl_2^+$ is the dominant aqueous species in solution at pH values less than about 7.5 and over a wide range of Eh conditions. $AmCl_2^+$ was thus chosen as the solution species in terms of which the dissolution reaction for the solubility-limiting solid phases was expressed.

There are three Am-bearing solid phases in the GEMBOCHS data1.com.R9 database—$AmOHCO_3$, $Am(OH)_3$, and $Am(OH)_3$(amorphous). Dissolution reactions of these phases written in terms of $AmCl_2^+$ (Appendix F) show that equilibrium with $AmOHCO_3$ yielded the smallest Am activities in solution, whereas $Am(OH)_3$(amorphous) yielded the highest. $Am(OH)_3$ yielded an intermediate value, and was thus not used. The concentration of Am in equilibrium with the sparingly soluble $AmOHCO_3$ in WIPP Brine A was therefore selected to represent the 0.1 fractile, with a calculated value of 5.0×10^{-11} M. Equilibrium with $Am(OH)_3$(amorphous) was selected as the 0.9 fractile, with a calculated value of 1.4×10^{-3} M, representing a highly soluble Am-bearing solid.

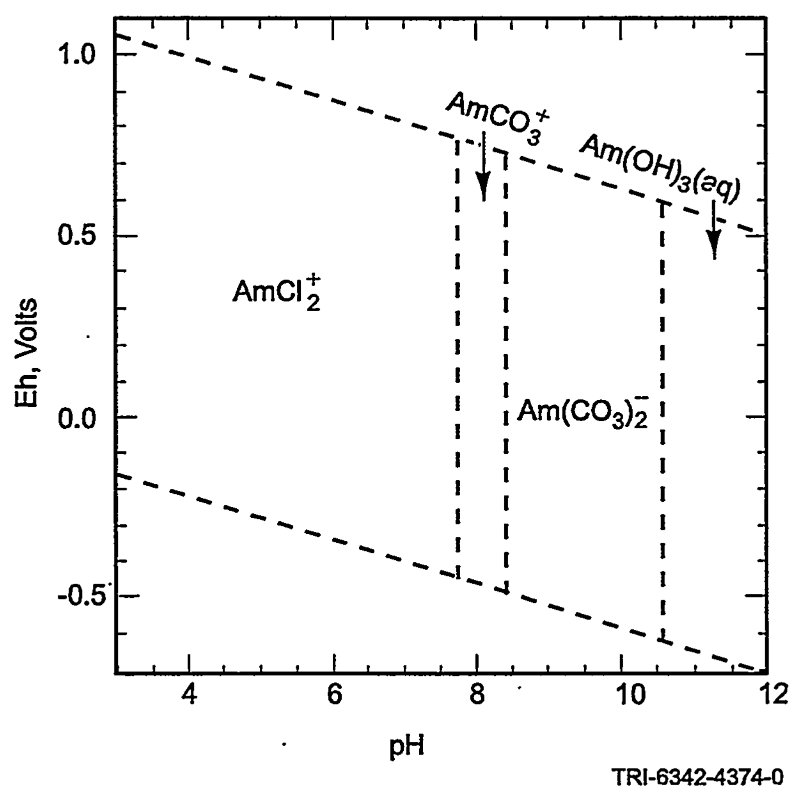

Figure 13. Calculated aqueous speciation diagram for americium in WIPP Brine A.

Examination of the aqueous speciation diagram in Figure 13 reveals that, under high pH conditions at WIPP, the dominant aqueous species of Am might be $AmCO_3^+$ or $Am(CO_3)_2^-$ instead of $AmCl_2^+$. Selection of either $AmCl_2^+$ or $AmCO_3^+$ as the solution species was made arbitrarily, since the transition line on the speciation diagram is quite close to the brine Eh-pH range assumed.

Other Fractiles

The development of the 0.5 fractile for americium was the same process as that reported for neptunium. The process resulted in a 0.5 fractile value of 1.0×10^{-9} M.

As was the case with neptunium, the development of the 0.0, 0.25, 0.75, and 1.0 fractiles was based on a consideration of the impact of the variability of carbonate and chloride concentrations, and of other conditions.

Curium

The "oxidation state analogy" is often invoked for predicting the chemical behavior of elements in an extended series (e.g., the 5 *f* actinide elements) for which no data exist. This method is based on the assumption that neighboring elements in the same oxidation states have similar chemical behavior by virtue of their similar charge-to-density ratios (electrostatic interactions). This method is more or less accurate depending on which region of the actinides is being evaluated. At the lighter end of the actinide series, for example, there is great variety in the oxidation states, their relative redox stabilities, and their hydrolysis behavior. Consequently, for example, predicting the solubility of PuO_2, based on that of ThO_2 is not particularly valid, especially when it is noted that Pu(IV) forms colloids and Th(IV) does not. Better estimates are expected on the heavier end of the actinide series, because the overall effect of the actinide contraction serves to moderate oxidation state variability, with enhanced stability of the trivalent state. Thus, estimation of Cm(III) solubilities, based on solubility data for Am(III) solubilities, is expected to be quite accurate. In general, the method is reasonably applicable, but should be used realizing its limitations and in conjunction with other information.

Development of Lead and Radium Probability Distributions

Equilibrium between the solubility limiting compound and the dissolved species controls the concentration of radionuclides in solution. The solubility limiting compound is a combination of the radionuclide species (cations) and the ligands (anions) present in solution. The nature of the various ligands in solution are critical factors in determining solubilities. In chloride brines, for example, in the absence of carbonate, highly soluble $PbCl_2$ controls the solubility of Pb(II) in solution. When carbonate is introduced into this chloride brine, less soluble $PbCO_3$ becomes the solubility limiting compound. Although high values of lead solubility result from chloride brines containing no other anions, it is unlikely that this situation would exist because of the prevalence of carbonate, sulfate, etc. in solution or present as rock forming minerals in the environment.

The case for radium solubility in brines is similar to that for lead. Although quite high concentrations of radium in solution were deemed theoretically possible when chloride was the only anion present in the brine, this situation is unlikely because of the prevalence of carbonate, sulfate, etc. in solution or as rock forming compounds in the environment. Because limited quantities of radium are expected to be present in and to dissolve from the waste, the solubility controlling solids for radium would most likely be mixed radium-calcium salts containing sulfate or carbonate ions. Even if chloride were the dominant solution ligand, insufficient quantities of radium exist in the waste inventory to form very high concentrations.

The concentrations of ligands in solution are also important factors in determining solubility. For example, in dilute chloride solutions, aquo Pb^{2+} is expected to be the dominant solution species. With increasing chloride concentration, lead chloro complexes form (e.g., $PbCl_4^{2-}$), and these become the dominant solution species in equilibrium with the solubility limiting compound. The solubility of radionuclides generally increases with increasing ligand concentration. This also holds true for the actinides, where the solubility of Am(III), for example, increases with higher concentrations of carbonate ions in solution.

Lead

The following discussion for lead illustrates the procedure that was used to develop the 0.5 fractile, unless otherwise noted.

Lead(II) is the only stable oxidation state expected in brines, and the dominant aqueous species is $PbCl_4^{2-}$. The solubility limiting solids expected for lead in brines are those containing chloride, sulfate, and carbonate ions. Dissolution of these solids is described in the following reactions:

$$PbCO_3(s) \quad Pb^{2+} + CO_3^{2-} \tag{7}$$

$$PbSO_4(s) \quad Pb^{2+} + SO_4^{2-} \tag{8}$$

$$PbCl_2(s) \quad Pb^{2+} + 2Cl^- \tag{9}$$

The generalized stoichiometric solubility product for the above reactions is given by

$$Ksp* = [Pb^{2+}]_T[X]_T{}^n = \frac{Ksp}{\gamma_T(Pb)\gamma_T(X)^n}, \tag{10}$$

where the subscript T refers to the total concentration, Ksp is the thermodynamic solubility product, and γ is the activity coefficient. The desired lead concentration can be determined from

$$[Pb]_T = \frac{Ksp*}{[X]_T{}^n} = \frac{Ksp}{\{\gamma_T(Pb)\gamma_T(X)[X]_T{}^n\}}, \tag{11}$$

where "*" refers to stoichiometric Ksp (that is, based on molalities rather than activities).

The values of $\gamma_T(X)$ can be obtained by using Pitzer's equations for the brine (Table 5). The stoichiometric or total activity coefficient of lead can be determined by using the ion pairing model (subsequently documented in Millero and Hawke, 1992). When these calculations are made for various ionic media, one finds that for lead in Yucca Mountain J-13 well water and in seawater, the carbonate ion controls the solubility, while in the WIPP brines the chloride ion controls the solubility. This is due to the relatively high concentration of Mg^{2+} in these waters and the formation of strong magnesium-carbonate complexes which scavenge excess carbonate ions. The formation of chloride complexes controls the fraction of free lead in the brines.

When using the ion pairing model to estimate the activity (a_{Pb}) or total activity coefficient (γ_T), one assumes that they are related by

$$a_{Pb} = [Pb]_T \gamma_T(Pb) = [Pb]_F \gamma_F(Pb), \tag{12}$$

where the subscript F refers to the free or uncomplexed ion. An estimate of the values of the activity coefficient for free ions can be calculated at a given ionic strength using the values tabulated in Table 5, which include the interactions with Cl^- and SO_4^{2-} or the values given in Table 9 that include the interaction of the metals with Cl^-. It is also possible to use estimates of γ from ClO_4^- salts and account for the interactions with Cl^- and SO_4^{2-} using the ion pairing model. The desired total activity coefficient for lead in the brine can be determined from

$$\gamma_T(Pb) = \left(\frac{[Pb]_F}{[Pb]_T}\right)\gamma_F(Pb)\,. \tag{13}$$

The fraction of free lead in the solution can be calculated from the summation of a lead containing species expressed in terms of individual complexation constants:

$$\begin{aligned}[Pb]_F / [Pb]_T = 1/\{1 + \beta_{PbCl}[Cl] + \beta_{PbCl_2}[Cl]^2 + \\ \beta_{PbCl_3}[Cl]^3 + \beta_{PbSO_4}[SO_4] + \beta_{Pb(SO_4)_2}[SO_4]^2 + \\ \beta_{PbHCO_3}[HCO_3] + \beta_{PbCO_3}[CO_3] + \beta_{Pb(CO_3)_2}[CO_3]^2 + \\ \beta_{PbOH}/[H] + \beta_{Pb(OH)_2}/[H]^2\}\end{aligned} \tag{14}$$

where β_i are the stability constants for the formation of the ion pair at the ionic strength of the brine. Some of the terms in this equation can be neglected if the free ion activity coefficients include the interaction with Cl^- or SO_4^{2-}. Although values are known for the stability constants in water, the values at higher ionic strength are not readily available. Recently the limited data available have been used to estimate the ionic strength dependence of the stability constants for the formation of divalent and trivalent ion pairs (subsequently documented in Millero and Hawke, 1992, and in Millero, 1992). These results have been used to estimate the stability constants in the brines (given in Tables 10 and 11). With these constants, it is easy to estimate the fraction of free metal in a given solution, and changes in this fraction can be related to changes in the solubility of a given metal.

As mentioned previously, the lead chloro complex, $PbCl_4^{2-}$, was selected as the dominant aqueous species and the solubility limiting cases selected were $PbCl_2$ (very soluble) for the case of a pure chloride brine and $PbCO_3$ (much less soluble) for the case of carbonate introduced into a chloride brine. The 0.5 fractiles for lead were established using the solubility products for $PbCO_3$ (pK_{sp} of 13.2) and $PbCl_2$ (pK_{sp} of 4.77) in carbonate-present and carbonate-free systems, respectively. These experimental K_{sp} measurements were extrapolated to zero ionic strength (infinite dilution) using Pitzer's equations. The thermodynamic values of the equilibrium constant were

Table 9. Calculated Free Activity Coefficients of the Trace Ionic Metals in WIPP Brines A and B*

Ion	NaCl Media†		$NaClO_4$ Media**	
	Brine A	Brine B	Brine A	Brine B
H^+	33.066	10.359	234.22	32.31
Na^+	2.019	1.319	2.019	1.319
K^+	0.633	0.593		
Mg^{2+}	6.149	1.796	923.62	61.33
Ca^{2+}	2.293	0.908	169.66	19.39
Sr^{2+}	1.294	0.610	64.87	9.98
Ba^{2+}	0.323	0.253	8.25	2.624
Mn^{2+}	1.063	0.616	1440.9	85.93
Fe^{2+}	2.147	0.919	1249.2	73.14
Co^{2+}	2.581	1.104	1249.2	73.14
Ni^{2+}	3.489	1.264	1195.1	68.96
Cu^{2+}	0.261	0.256	722.6	50.79
Zn^{2+}	0.014	0.050	963.1	57.97
Cd^{2+}			210.5	18.78
Pb^{2+}	15.25	3.443	14.54	3.263
UO^{2+}	3.455	1.722	15.392	438.62
Al^{3+}	1.089	0.266		
Sc^{3+}	0.395	0.137		
Y^{3+}	0.224	0.088		
La^{3+}	0.124	0.060	70.39	4.977
Ce^{3+}	0.130	0.062	66.21	4.703
Pr^{3+}	0.118	0.056	62.26	4.444
Nd^{3+}	0.130	0.060	63.26	4.473
Sm^{3+}	0.161	0.072	69.64	4.840
Eu^{3+}	0.179	0.077	79.02	5.307
Cr^{3+}	0.486	0.166		
Ga^{3+}	9.606	1.495		
F^-	0.106	0.164	SAME AS IN NaCl	
Cl^-	0.634	0.593		
OH^-	1.311	0.915		
NO_3^-	0.061	0.111		
HCO_3^-	0.107	0.157		
$B(OH)_4^-$	0.116	0.108		
CO_3^{2-}	0.0145	0.0043		
SO_4^{2-}	0.0008	0.0026		

* All the values are adjusted by assuming $\gamma_K = \gamma_{Cl}$

† See, for example, Millero and Hawke (1992, Table 3) for the Pitzer parameters for calculating activity coefficients.

** See, for example, Millero and Hawke (1992, Table 4) for the Pitzer parameters for calculating activity coefficients.

Table 10. Stability Constants, K, for the Formation of Divalent Metal Ion Pairs*

Ion Pair	log K			
	Ionic Strength of 0.7	Ionic Strength of 5.0	Ionic Strength of 6.0	Ionic Strength of 7.0
$MnSO_4$	0.85	0.87	1.08	1.34
$MnHCO_3$	0.55	–0.004	–0.01	0.014
$MnCO_3$	2.84	3.28	3.58	3.92
MnCl	–0.29	0.39	0.67	0.99
MnOH	3.17	5.41	6.07	6.78
$Mn(OH)_2$	5.07	7.10	7.79	8.53
$FeSO_4$	0.75	0.75	0.96	1.22
$FeHCO_3$	0.69	0.11	0.11	0.14
$FeCO_3$	4.11	4.29	4.55	4.84
$Fe(CO_3)_2$	5.70	3.74	3.47	3.23
FeCl	–0.46	0.20	0.49	0.81
FeOH	4.22	6.43	7.09	7.81
$Fe(OH)_2$	6.63	8.63	9.32	10.07
$CoSO_4$	1.61	1.61	1.82	2.08
$CoHCO_3$	0.63	0.06	0.05	0.08
$CoCO_3$	3.16	3.34	3.59	3.89
CoCl	–0.41	0.25	0.53	0.85
CoOH	4.07	6.28	6.95	7.66
$Co(OH)_2$	8.42	10.43	11.12	11.86
$NiSO_4$	0.83	0.81	1.02	1.29
$Ni(SO_4)_2$	1.84	2.41	2.77	3.17
$NiHCO_3$	0.83	0.13	0.08	0.07
$NiCO_3$	4.07	4.45	4.76	5.11
NiCl	–0.49	0.15	0.44	0.76
NiOH	3.85	6.04	6.71	7.42
$Ni(OH)_2$	8.22	10.20	10.89	11.64
$CuSO_4$	0.88	0.75	0.93	1.15
$CuHCO_3$	1.02	0.31	0.27	0.26
$CuCO_3$	5.40	5.70	5.97	6.28
$Cu(CO_3)_2$	8.73	5.45	4.85	4.29
CuCl	–0.22	0.31	0.56	0.84
CuOH	5.70	7.78	8.41	0.08
$Cu(OH)_2$	10.9	12.83	13.48	14.18

* Stability constants developed from the infinite dilution values subsequently published in Millero and Hawke (1992, Table 10), converted for the higher ionic strength solutions indicated.

Table 10. Stability Constants, K, for the Formation of Divalent Metal Ion Pairs (Continued)

Ion Pair	log K			
	Ionic Strength of 0.7	Ionic Strength of 5.0	Ionic Strength of 6.0	Ionic Strength of 7.0
$ZnSO_4$	0.81	0.81	1.02	1.27
$Zn(SO_4)_2$	2.18	2.77	3.11	3.51
$ZnHCO_3$	0.87	0.29	0.28	0.30
$ZnCO_3$	3.31	3.71	4.02	4.36
$Zn(CO_3)_2$	6.13	6.88	7.23	7.61
ZnCl	−0.34	0.31	0.59	0.91
ZnOH	4.66	6.87	7.53	8.24
$Zn(OH)_2$	10.2	12.22	12.91	13.65
$CdSO_4$	0.91	0.41	0.53	0.70
$CdHCO_3$	0.35	−0.22	−0.23	−0.26
$CdCO_3$	2.96	2.88	3.09	3.34
CdCl	0.97	1.13	1.31	1.54
$CdCl_2$	1.02	2.22	2.70	3.22
$CdCl_3$	1.07	4.62	5.63	6.69
CdOH	3.55	5.27	5.84	6.45
$Cd(OH)_2$	6.79	8.30	8.89	9.54
$PbSO_4$	1.08	−0.02	−0.10	−0.16
$Pb(SO_4)_2$	2.94	2.43	2.49	2.57
$PbHCO_3$	1.06	−0.62	−0.92	−1.20
$PbCO_3$	5.48	4.79	4.80	4.84
$Pb(CO_3)_2$	9.05	8.71	8.76	8.84
PbCl	0.75	0.31	0.30	0.30
$PbCl_2$	1.04	1.63	1.91	2.21
$PbCl_3$	1.29	4.23	5.05	5.89
PbOH	5.79	6.90	7.27	7.67
$Pb(OH)_2$	9.89	10.79	11.18	11.61

Table 11. Stability Constants, K, for the Formation of Lanthanide Metal Ion Pairs*

Ion Pair	log β			
	Ionic Strength of 0.7	Ionic Strength of 5.0	Ionic Strength of 6.0	Ionic Strength of 7.0
LaCl	0.31	−0.79	−1.10	−1.40
LaF	2.70	1.37	1.00	0.64
LaOH	4.35	3.31	3.03	2.75
$LaNO_3$	0.14	−1.26	−1.64	−2.02
LaH_2PO_4	2.30	1.10	0.74	0.38
$LaHCO_3$	1.56	0.23	−0.13	−0.49
$LaSO_4$	1.58	0.78	0.69	0.62
$LaCO_3$	5.29	4.65	4.60	4.57
$La(CO_3)_2$	9.17	10.10	10.52	10.98
$LaHPO_4$	3.27	2.46	2.40	2.39
$La(HPO_4)_2$	5.91	6.49	6.90	7.39
CeCl	0.32	−0.81	−1.12	−1.42
CeF	2.85	1.49	1.12	0.76
CeOH	5.22	4.15	3.87	3.59
$CeNO_3$	0.24	−1.19	−1.57	−1.94
CeH_2PO_4	1.91	0.33	−0.06	−0.44
$CeHCO_3$	1.48	0.12	−0.24	−0.60
$CeSO_4$	1.65	0.82	0.73	0.66
$CeCO_3$	5.41	4.74	4.69	4.66
$Ce(CO_3)_2$	9.35	10.25	10.67	11.13
$CeHPO_4$	3.37	2.53	2.47	2.46
$Ce(HPO_4)_2$	6.07	6.62	7.03	7.52
SmCl	0.32	−0.78	−1.09	−1.38
SmF	3.15	1.82	1.47	1.11
SmOH	5.43	4.40	4.12	3.85
$SmNO_3$	0.34	−1.06	−1.44	−1.81
SmH_2PO_4	1.72	0.16	−0.22	−0.60
$SmHCO_3$	1.29	−0.05	−0.40	−0.75
$SmSO_4$	1.65	0.84	0.76	0.70
$SmCO_3$	5.76	5.13	5.08	5.06
$Sm(CO_3)_2$	9.97	10.90	11.32	11.79
$SmHPO_4$	3.75	2.93	2.89	2.88
$Sm(HPO_4)_2$	6.70	7.27	7.69	8.19
ErCl	0.31	−0.65	−0.92	−1.19
ErF	3.57	2.39	2.06	1.74
ErOH	5.79	4.90	4.65	4.42
$ErNO_3$	−0.27	−1.53	−1.87	−2.21
ErH_2PO_4	1.75	0.34	−0.02	−0.36
$ErHCO_3$	1.32	0.13	−0.20	−0.51
$ErSO_4$	1.53	0.87	0.82	0.80

* Stability constants developed from the infinite dilution values subsequently published in Millero (1992, Table 5), converted for the higher ionic strength solutions indicated.

Table 11. Stability Constants, K, for the Formation of Lanthanide Metal Ion Pairs (Continued)

Ion Pair	log β			
	Ionic Strength of 0.7	Ionic Strength of 5.0	Ionic Strength of 6.0	Ionic Strength of 7.0
$ErCO_3$	6.11	5.62	5.60	5.62
$Er(CO_3)_2$	10.76	11.83	12.29	12.79
$ErHPO_4$	4.10	3.43	3.41	3.43
$Er(HPO_4)_2$	7.49	8.21	8.66	9.19

then used in combination with the ion pairing model to estimate lead concentrations in high ionic strength Brine A. A concentration of 8.0×10^{-3} M was calculated for the carbonate present case, while a concentration of 1.64 M was calculated for the carbonate absent case. The 0.0, 0.1, 0.25, 0.75, 0.9, and 1.0 fractiles were estimated by providing for the likelihood that carbonate concentrations will be variable in the carbonate-present system, and that chloride concentration may vary in the carbonate-absent system. Although high values of lead solubility are theoretically possible in a pure chloride brine, a pure chloride brine would not be expected because exposure to air or the repository formation would cause carbonate to form. Thus, lead in the concentrations shown in Table 3 for the carbonate-free system are not expected to exist at the WIPP, nor is there a great probability that chloride concentration will vary by the three orders of magnitude spanned by the 0.0 and 1.0 fractiles.

Radium

Langmuir and Riese (1985) suggested that concentrations of radium in natural waters and in waters associated with uranium mining and nuclear waste disposal are probably never high enough to reach saturation with pure radium solids such as $RaSO_4$ or $RaCO_3$. Maximum radium concentrations are limited instead by adsorption and/or solid solution formation. Riese (1982) found that adsorption of radium is inhibited by low pH and by high concentrations of calcium because of competition by H^+ and Ca^{2+} with Ra^{2+} for adsorption sites. These observations are consistent with the conclusion made by Hubbard et al. (1984) and Hubbard and Laul (1984) that radium is not adsorbed from present-day groundwater. Therefore, the solubility of radium in brines is most likely controlled by the formation of solid solutions in minerals such as anhydrite (calcium sulfate), barite (barium sulfate), anglesite (lead sulfate), celestite (strontium sulfate), calcite (calcium carbonate), witherite (barium carbonate), and cerussite (lead carbonate). Consequently, the activity coefficients of Ra^{2+}, Ca^{2+}, etc. in calcite- and/or anhydrite-saturated brines have to be estimated in order to evaluate the solubility of radium in brines.

There are many possibilities for brines to change their compositions after they enter the repository room. One scenario is that the brines may lose water through (a) evaporation, (b) radiolysis, and (c) reaction with Fe from waste containers, or some backfill materials, such as bentonite and $CuSO_4$. The computer program named PHRQPITZ developed by Plummer et al. (1988) was used to calculate the compositions and activity coefficients for brines derived from evaporation of WIPP-A. The amount of NaCl required to be added to WIPP-A to reach halite saturation have been determined experimentally (Chou et al., 1982); at 25°C, the total molality (m) of Na^+ for halite-saturated WIPP-A is 2.876, while PHRQPITZ predicts 2.966. PHRQPITZ results (printouts located in the SNL WIPP Records Center) are given for the case in which minerals, except dolomite and magnesite, were allowed to precipitate when saturation was reached, and for the case in which minerals other than halite were not allowed to precipitate when saturation was reached. These results (summarized in Table 12) indicate that at a given ionic

Table 12. Evaporation of Halite-Saturated WIPP-A Brine Using PHRQPITZ Program (Summary)

				molality						activity coefficient						
H_2O*	Ionic Strength	a_{H_2O} (activity)	pH	Na^+	Mg^{2+}	Ca^{2+}	Cl^-	CO_3^{2-}	SO_4^{2-}	Mg^{2+}	Ca^{2+}	Sr^{2+}	Ba^{2+}	SO_4^{2-}	CO_3^{2-}	Cl^-
0%†	7.792	0.750	6.5	2.034	1.598	0.022	6.012	1.2×10^{-4}	0.044	1.044	0.557	0.381	0.151	0.032	0.0057	1.835
0%**	8.722	0.700	6.38	2.964	1.598	0.022	6.942	6.9×10^{-5}	0.044	1.854	0.897	0.559	0.181	0.029	0.0061	2.028
10%‡	9.062	0.691	6.10	2.668	1.777	0.023	7.088	3.6×10^{-5}	0.049	1.916	0.890	0.583	0.182	0.031	0.0054	2.209
20%§	9.515	0.678	6.02	2.318	1.999	0.026	7.291	3.5×10^{-5}	0.057	2.029	0.895	0.622	0.185	0.033	0.0047	2.466
30%§	10.106	0.659	6.02	1.910	2.284	0.023	7.593	4.6×10^{-5}	0.057	2.253	0.924	0.691	0.191	0.035	0.0040	2.846
50%‖	9.633	0.681	6.19	2.606	1.770	0.010	7.300	6.6×10^{-5}	0.168	2.033	0.907	0.656	0.170	0.028	0.0065	0. 2.161
Supersaturation allowed except for halite (i.e., no minerals being precipitated except halite)																
10%	9.065	0.691	6.34	2.668	1.775	0.025	7.088	7.7×10^{-5}	0.049	1.914	0.892	0.583	0.182	0.031	0.0054	2.209
20%	9.516	0.678	6.29	2.319	1.997	0.028	7.292	8.6×10^{-5}	0.056	2.027	0.897	0.622	0.185	0.033	0.0047	2.465
30%	10.132	0.658	6.23	1.907	2.282	0.032	7.591	9.3×10^{-5}	0.064	2.248	0.924	0.691	0.190	0.035	0.0040	2.852
50%	12.421	0.577	5.98	0.908	3.195	0.044	8.864	7.7×10^{-5}	0.089	4.035	1.221	1.155	0.223	0.046	0.0025	4.741
70%	19.301	0.321	5.13	0.104	5.328	0.074	13.36	2.7×10^{-6}	0.148	55.28	4.981	9.646	0.387	0.087	0.0014	19.15

* Volume % of halite-saturated WIPP-A brine being removed as pure H_2O from the brine.
† WIPP-A brine; supersaturated with respect to aragonite, calcite, dolomite, and magnesite.
** Halite-saturated WIPP-A brine; supersaturated w.r.t. aragonite, calcite, dolomite, and magnesite.
‡ In equilibrium with halite and calcite.
§ In equilibrium with halite, calcite, and anhydrite.
‖ In equilibrium with halite, calcite, anhydrite, sylvite, syngenite, and polyhalite.
‡,§,‖ supersaturated with respect to dolomite and magnesite.

strength, I, the changes in activity coefficients from Ca^{2+} to Sr^{2+} and Ba^{2+} are quite systematic, which can be explained by the corresponding systematic changes in their ionic radii (see Table 13). Based on these systematic correlations, the activity coefficient of Ra^{2+} can be approximated by that of Ba^{2+} in the same solution.

Solubilities of radium in brines derived from evaporation of WIPP-A brine are estimated, assuming Ra^{2+}, $RaOH^{+}$, $RaCl^{+}$, $RaCO_3^0$, and $RaSO_4^0$ are the dominant species in solution. The possible complexation of radium by Br^-, F^-, PO_4^{3-}, and organic ligands is not considered in this study because they are most likely not important. The brine derived from the removal of 20% volume of halite-saturated WIPP-A brine as pure water is called WIPP-A-20 in this report. This brine is saturated with respect to halite, calcite, and anhydrite, and is supersaturated with respect to dolomite and magnesite (Table 12). Using the activity coefficient of Ba^{2+} for that of Ra^{2+}, and the activity coefficient information developed in Table 12 for SO_4^{2-}, CO_3^{2-}, and Cl^- for WIPP-A-20, together with the K_{sp} and $K_{(assoc)}$[3] data given in Table 14, solubilities of $RaSO_4$, $RaCO_3$, and $RaCl_2{\cdot}2H_2O$ in WIPP-A-20 were calculated. The results are given below:

(1) for the solid phase $RaSO_4$:

molality of Ra^{2+}, $m_{Ra^{2+}} = 1.6 \times 10^{-7}$

molality of $RaSO_4^0$, $m_{RaSO_4^0} = 0.31 \times 10^{-7}$

Total Ra in solution = 1.9×10^{-7} molal

(2) for the solid phase $RaCO_3$:

molality of Ra^{2+}, $m_{Ra^{2+}} = 0.162$

molality of $RaCO_3^0$, $m_{RaCO_3^0} = 1.59 \times 10^{-6}$

Total Ra in solution = 0.162 molal

(3) for the solid phase $RaCl_2{\cdot}2H_2O$:

$\text{Log } K_{sp} = -0.7647$ (from the EQ3/6 database)

molality of Ra^{2+} = 4.715 molal

molality of $RaCl^{+}$ = 12.43 molal

Total Ra in solution = 17.15 molal

The above three values calculated for total radium in the solution were assigned as the 0.9 fractiles for the three respective cases. In these calculations, the activity coefficients for $RaSO_4$, $RaCO_3$, and $RaCl^+$ were arbitrarily assumed to be unity. It is clear that radium sulfate is the least soluble, followed by the carbonate and the chloride solids. However, as mentioned earlier, the solubility of radium in brines is most likely controlled by the formation of solid solutions, such as radium incorporation in sulfate and carbonate minerals.

[3] K_{sp} and $K_{(assoc)}$ are equivalent to the thermodynamic equilibrium constants discussed earlier.

Table 13. Thermodynamic Data**

Cation M	Ionic* Radius (in Å)	Log Ksp MSO4	Log Ksp MCO3	Log Ksp M(NO3)2	D† MSO4	D† MCO3	D† M(NO3)2
Ca	1.12 (arag.)†	–4.36	–8.34 (aragonite)† –8.48 (calcite)**	-	(800)	(0.96) (aragonite) (0.82) (calcite)	
Sr	1.26	–6.64	–9.27	-	280	0.66	10
Ba	1.42	–9.97	–8.58	-	1.8	0.5	1.6
Ra	1.48	–10.26	–8.3	–2.24	1.0	1.0	1.0
Pb					11	0.067	

* In 8-fold coordination solids

† Distribution constant in Nernst-Berthelot or Henerson-Kraczek equation:

$$D = \left(\frac{N_{RaX}}{N_{MX}}\right) \Big/ \left(\frac{a_{Ra^{2+}}}{a_{M^{2+}}}\right),$$

where M = Ca, Sr, Ba, Ra, or Pb; X = SO_4^{2-}, CO_3^{2-}, or $2(NO_3^-)$, values in parentheses are estimates.

** Compiled from Langmuir and Riese (1985)

Table14. Formation Constants (log K (assoc) values) of Radium Complexes, Solubility Products (log Ksp values) of Radium Solids, and Enthalpies of Reaction (ΔH° at 25°C) based on the thermodynamic data in Table 15 (compiled by Langmuir & Riese, 1985, Table 2).

Reaction	log K (assoc) or log Ksp	ΔH° (kcal/mol)
1) $Ra^{2+} + OH^- = RaOH^+$	0.5	1.1
2) $Ra^{2+} + Cl^- = RaCl^+$	–0.10	0.50
3) $Ra^{2+} + CO_3^{2-} = RaCO_3^0$	2.5	1.7
4) $RaCO_3$(crystalline) = $Ra^{2+} + CO_3^{2-}$	–8.3	–2.8
5) $Ra^{2+} + SO_4^{2-} = RaSO_4$	2.75	1.3
6) $RaSO_4$(crystalline) = $Ra^{2+} + SO_4^{2-}$	–10.26	–9.4

Table 15. Thermochemical Data for Radium Solids and Aqueous Species, and for Auxiliary Aqueous Species at 25° C and 1 Bar (compiled by Langmuir & Riese, 1985, Table 1)

Solid or Aqueous Species	ΔH_f^o (kcal/mol)	ΔG_f^o (kcal/mol)	S^o (cal/mol deg)
Ra(crystalline)	0	0	17
Ra^{2+}	−126.1	−134.2	13
$RaOH^+$	−179.98	−172.30	16
$RaCl^+$	−165.54	−165.44	28
$RaCO_3^o$	−286.87	−263.78	16
$RaCO_3$(crystalline)	−290.73	−271.69	28
$RaSO_4^o$	−342.18	−315.90	34.5
$RaSO_4$(crystalline)	−352.88	−326.15	33
OH^-	−54.977	−37.604	−2.560
Cl^-	−39.933	−31.379	13.56
CO_3^{2-}	−161.84	−126.17	−13.6
SO_4^{2-}	−217.40	−177.95	4.50

Because WIPP-A-20 brine is saturated with respect to both calcite ($CaCO_3$) and anhydrite ($CaSO_4$), the effect of solid solution from these minerals on the solubility of radium in this brine can be evaluated from the Nernst-Berthelot (or Henderson-Kraczke) equation (see Langmuir and Riese, 1985):

$$\left(\frac{a_{Ra^{2+}}}{a_{M^{2+}}}\right)D = \left(\frac{N_{RaX}}{N_{MX}}\right) \qquad (15)$$

where D is an empirically determined distribution coefficient, N is the mole fraction in the solid solution, M refers to a cation, and X is SO_4^{2-} or CO_3^{2-}. The D values obtained by Goldschmidt (1940) were measured at N_{RaX} values between 10^{-5} and 10^{-11}. Langmuir and Riese (1985) pointed out that it seems unlikely that N_{RaX} will exceed 10^{-5} in natural water/rock systems. Therefore, N_{MX} in equation (15), above, is approximately equal to 1. Using the D values given in Table 13, and the concentration and activity coefficient data given in Table 12 for WIPP-A-20, the concentrations of Ra^{2+} in WIPP-A-20 can be calculated from equation (15). If Ra^{2+} concentration in WIPP-A-20 is controlled by the precipitation of anhydrite, log $m_{Ra^{2+}}$ is less than −8.8, assuming N_{RaSO_4} is less than 10^{-5}. This is two orders of magnitude less soluble than pure $RaSO_4$ in the same brine, where log $m_{Ra^{2+}}$ = −6.8. Similarly, if Ra concentration in WIPP-A-20 is controlled by the precipitation of calcite, log $m_{Ra^{2+}}$ is less than −5.8, assuming N_{RaCO_3} is less than 10^{-5}. This is five orders of magnitude less soluble than pure $RaCO_3$ in the same brine, where log $m_{Ra^{2+}}$ = −0.79.

Precipitation of Ba and Pb sulfates and carbonates will have a similar effect and their intensities will depend on the brine composition. For example, Langmuir and Melchior (1985) reported that the concentrations of radium in anhydrite, celestite, barite, calcite, and dolomite would be 0.022, 0.81, 14, 3.8×10^{-5}, and 1.9×10^{-5} ppm, respectively, assuming that these solid solutions are in equilibrium with a brine from Sawyer #l well, Wolfcamp, Zone 5, Palo Duro Basin, Texas. For this particular brine composition, barite is the most effective mineral for removing radium from the coexisting brine. However, it should be emphasized that even though it seems likely, control of radium concentrations by the solubility of trace radium in minerals cannot at this point be proven. Also, because WIPP-A brine does not contain any Ba^{2+} and Pb^{2+}, and has only trace amounts of Sr^{2+} (5 mg/L), the precipitation of radium from the brine as sulfate or carbonate solid solutions involving these cations is not possible.

Under reducing conditions, SO_4^{2-} will be converted to either HS^- or H_2S, and the solubility of radium in brines will be most likely controlled by coprecipitation in calcite. However, if $CaSO_4$ is added as a backfill material, then coprecipitation in anhydrite or gypsum may control radium solubility. Even though it has been speculated that N_{RaSO_4} in anhydrite and N_{RaCO_3} in calcite are not likely to exceed 10^{-5}, experimental verifications are required.

The solid solution model was used to estimate fractiles below 0.9. For the sulfate present case, the maximum radium solubility calculated considering the coprecipitation of radium and calcium with the sulfate, 1.0×10^{-9} M, was assigned as the 0.25 fractile. The 0.1 and 0.0 fractiles were estimated based upon the possibility that N_{RaX} is less than 10^{-5}. The 1.0 fractile was assigned to ensure that the concentration would not be exceeded.

The solid solution model was also used for the "carbonate present" case, where the maximum radium solubility calculated considering the coprecipitation of radium and calcium with the carbonate, 1.6×10^{-6} M, was assigned as the 0.5 fractile. The 0.25, 0.1, and 0.0 fractiles were estimated based upon the possibility that N_{RaX} is less than 10^{-5}. The 1.0 fractile was again assigned to ensure that the concentration would not be exceeded.

For the "carbonate and sulfate absent" case, the fractiles were assigned taking into account the impact of variations in the concentration of chloride. As was the case with lead, the theoretical solubility of radium in a pure chloride brine (i.e., sulfate and carbonate absent) is quite high. However, conditions at the WIPP are not expected to allow for a pure chloride brine because of the potential for contact with air or the repository formation minerals. In addition, the radium inventory is not sufficient to produce very high concentrations.

CONCLUSIONS

The expert judgment process was used to develop probability distributions for radionuclide solubilities for use in the 1991 (and subsequently 1992) preliminary performance assessment calculations. The Source Term Expert Panel used thermodynamic data, existing solubility data, and professional expertise to create a process for developing solubility probability distributions and to apply the process to the required elements.

The Panel did not provide probability distributions to describe the presence of radionuclide colloids. It is entirely appropriate for an expert panel to participate in modifying the issue statement if information is requested that cannot be provided under the current circumstances. There were not sufficient thermodynamic data available on colloids to be evaluated within the expert judgment process to develop the requested information.

The Panel developed the information within the required time constraints, and did so while incorporating the great uncertainty in room conditions (i.e., backfill not assumed to fix the conditions), and addressing the problem of limited WIPP-specific data.

The efforts of the Panel resulted in the development of very wide probability distribution. These wide distributions represent the impact of both great uncertainty in room conditions and the nature of probability distributions—i.e., that the 0.0 and 1.0 fractiles represent the very outer limits beyond which concentrations will not occur. The tails of the distributions (between the 0.0 and 0.10 fractiles, and between the 0.9 and 1.0 fractiles) are associated with much smaller probabilities than the main body of the distribution. Thus, in using and evaluating the probability distributions, the concentrations should never be unlinked from the probability of their occurrence.

If additional resources were applied to the effort, improvements in the process (e.g., selection of different solids) might have been possible. In addition, the ongoing development of the GEMBOCHS database could also improve the results.

Any subsequent use of these results in performance assessment calculations would need to be integrated with any data collected subsequent to the Panel deliberations.

REFERENCES

Bertram-Howery, S.G., and R.L. Hunter, eds. 1989. *Preliminary Plan for Disposal-System Characterization and Long-Term Performance Evaluation of the Waste Isolation Pilot Plant.* SAND89-0178. Albuquerque, NM: Sandia National Laboratories.

Bertram-Howery, S.G., M.G. Marietta, R.P. Rechard, P.N. Swift, D.R. Anderson, B.L. Baker, J.E. Bean, Jr., W. Beyler, K.F. Brinster, R.V. Guzowski, J.C. Helton, R.D. McCurley, D.K. Rudeen, J.D. Schreiber, and P. Vaughn. 1990. *Preliminary Comparison with 40 CFR Part 191, Subpart B for the Waste Isolation Pilot Plant, December 1990.* SAND90-2347. Albuquerque, NM: Sandia National Laboratories.

Bonano, E.J., S.C. Hora, R.L. Keeney, and D. von Winterfeldt. 1990. *Elicitation and Use of Expert Judgment in Performance Assessment for High-Level Radioactive Waste Repositories.* SAND89-1821; NUREG/CR-5411. Albuquerque, NM: Sandia National Laboratories.

Brönsted, J.N. 1922. "Studies on Solubility. IV. The Principal of the Specific Interaction of Ions," *The Journal of the Chemical Society.* Vol. 44, no. 5, 887-898.

Brush, L.H. 1990. *Test Plan for Laboratory and Modeling Studies of Repository and Radionuclide Chemistry for the Waste Isolation Pilot Program.* SAND90-0266. Albuquerque, NM: Sandia National Laboratories.

Brush, L.H., and D.R. Anderson. 1989. "Effects of Microbial Activity on Repository Chemistry, Radionuclide Speciation, and Solubilities in WIPP Brines," *Systems Analysis, Long-Term Radionuclide Transport, and Dose Assessments, Waste Isolation Pilot Plant (WIPP), Southeastern New Mexico; March 1989.* Eds. A.R. Lappin, R.L. Hunter, D.P. Garber, and P.B. Davies. SAND89-0462. Albuquerque, NM: Sandia National Laboratories. A-31 through A-50.

Choppin, G.R. 1988. "Estimation of Actinide Solubilities in WIPP." Unpublished report submitted to L.H. Brush, Sandia National Laboratories. Tallahassee, FL: Florida State University. (Reproduced in Appendix D.)

Chou, I-M., B. Buizinga, M.A. Clynne, and R.W. Potter. 1982. *The Densities of Halite-Saturated WIPP-A and NBT-6 Brines and Their NaCl Contents in Weight Percent, Molal, and Molar Units from 20° to 100°C.* U.S. Geological Survey Open-File Report 82-899. Denver, CO: U.S. Geological Survey.

Chu, M.S.Y., and E.A. Bernard. 1991. *Waste Inventory and Preliminary Source Term Model for the Greater Confinement Disposal Site at the Nevada Test Site.* SAND91-0170. Albuquerque, NM: Sandia National Laboratories.

Dickson, A.G., and M. Whitfield. 1981. "An Ion-Association Model for Estimating Acidity Constants (at 25°C and 1 atm Total Pressure) in Electrolyte Mixtures Related to Seawater (Ionic Strength <1 mol kg^{-1} H_2O)," *Marine Chemistry.* Vol. 10, no. 4, 315-333.

Felmy, A.R., and J.H. Weare. 1986. "The Prediction of Borate Mineral Equilibria in Natural Waters: Application to Searles Lake, California," *Geochimica et Cosmochimica Acta.* Vol. 50, no. 12, 2771-2783.

Garrels, R.M., and M.E. Thompson. 1962. "A Chemical Model for Sea Water at 25°C and One Atmosphere Total Pressure," *American Journal of Science*. Vol. 260, no. 1, 57-66.

Goldberg, E.D., and G.O.S. Arrhenius. 1958. "Chemistry of Pacific Pelagic Sediments," *Geochemica et Cosmochimica Acta*. Vol. 13, no. 2-3, 153-212.

Goldschmidt, B.- 1940. "Etude du Fractionnement par Cristallisation Mixte a L'aide des Radioelements," *Annales de Chimie (Paris)*. Ser. 11, Vol. 13, 88-174.

Grenthe, I., K. Spahiu, and T. Ericksen. 1992. "Analysis of the Solubility Equilibria of Yttrium Carbonate in Aqueous Perchlorate Media Using the Pitzer and Brønsted—Guggenheim—Scatchard Ion-Interaction Models," *Journal of the Chemical Society. Faraday Transactions*. Vol. 88, no. 9, 1267-1273.

Guggenheim, E.A. 1966. *Applications of Statistical Mechanics*. Oxford: Claredon Press

Harvie, C.E., and J.H. Weare. 1980. "The Prediction of Mineral Solubilities in Natural Waters: The Na-K-Mg-Ca-SO_4-Cl-H_2O System from Zero to High Concentration at 25°C," *Geochimica et Cosmochimica Acta*. Vol. 44, no. 7, 981-997.

Harvie, C.E., N. Møller, and J.H. Weare. 1984. "The Prediction of Mineral Solubilities in Natural Waters: The Na-K-Mg-Ca-H-Cl-SO_4-OH-HCO_3-CO_3-CO_2-H_2O System to High Ionic Strengths at 25°C," *Geochimica et Cosmochimica Acta*. Vol. 48, no. 4, 723-752.

Helton, J.C., J.W. Garner, R.D. McCurley, and D.K. Rudeen. 1991. *Sensitivity Analysis Techniques and Results for Performance Assessment of the Waste Isolation Pilot Plant*. SAND90-7103. Albuquerque, NM: Sandia National Laboratories.

Hobart, D.E. 1990. "Actinides in the Environment," *Proceedings of the Robert A. Welch Foundation Conference on Chemical Research XXXIV: Fifty Years with Transuranium Elements, Houston, TX, October 22-24, 1990*. Vol. 34, 378-436.

Hora, S.C., and R.L. Iman. 1989. "Expert Opinion in Risk Analysis: The NUREG-1150 Methodology," *Nuclear Science and Engineering*. Vol. 102, no. 4, 323-331.

Horita, J., T.J. Friedman, B. Lazar, and H.D. Holland. 1991. "The Composition of Permian Seawater," *Geochimica et Cosmochimica Acta*. Vol. 55, no. 2, 417-432.

Hubbard, N., and J.C. Laul. 1984. "Behavior of Natural Uranium, Thorium, and Radium Radionuclides In Brine," *Abstracts with Programs, Geological Society of America*. Vol. 16, no. 6, 545.

Hubbard, N., J.C. Laul, and R.W. Perkins. 1984. "The Use of Natural Radionuclides to Predict the Behavior of Radwaste Radionuclides in Far-Field Aquifers," *Scientific Basis for Nuclear Waste Management, Materials Research Society Symposia Proceedings, Boston, MA, November 14-17, 1983*. Ed. G.L. McVay. New York, NY: North-Holland. Vol. 26, 891-897.

Kerrisk, J.F. 1985. *An Assessment of the Important Radionuclides in Nuclear Waste.* LA-10414-MS. Los Alamos, NM: Los Alamos National Laboratory.

Langmuir, D., and D. Melchior. 1985. "The Geochemistry of Ca, Sr, Ba and Ra Sulfates in Some Deep Brines from the Palo Duro Basin, Texas," *Geochimica et Cosmochimica Acta.* Vol. 49, no. 11, 2423-2432.

Langmuir, D., and A. Riese. 1985. "The Thermodynamic Properties of Radium," *Geochimica et Cosmochimica Acta.* Vol. 49, no. 7, 1593-1601.

Lappin, A.R., R.L. Hunter, D.P. Garber, and P.B. Davies, eds. 1989. *Systems Analysis, Long-Term Radionuclide Transport, and Dose Assessments, Waste Isolation Pilot Plant (WIPP), Southeastern New Mexico; March 1989.* SAND89-0462. Albuquerque, NM: Sandia National Laboratories.

Lappin, A.R., R.L. Hunter, P.B. Davies, D.J. Borns, M. Reeves, J. Pickens, and H.J. Iuzzolino. 1990. *Systems Analysis, Long-Term Radionuclide Transport, and Dose Asssessments, Waste Isolation Pilot Plant (WIPP), Southeastern New Mexico; September 1989.* SAND89-1996. Albuquerque, NM: Sandia National Laboratories.

Millero, F.J. 1979. "Effects of Pressure and Temperature on Activity Coefficients," *Activity Coefficients in Electrolyte Solutions.* Ed. R.M. Pytkowicz. Boca Raton, FL: CRC Press. Vol. II, 63-151.

Millero, F.J. 1986. "The pH of Estuarine Waters," *Limnology and Oceanography.* Vol. 31, no. 4, 839-847.

Millero, F.J. 1990. "Marine Solution Chemistry and Ionic Interactions," *Marine Chemistry.* Vol. 30, no. 1-3, 205-229.

Millero, F.J. 1992. "Stability Constants for the Formation of Rare Earth Inorganic Complexes as a Function of Ionic Strength," *Geochimica et Cosmochimica Acta.* Vol. 56, no. 8, 3123-3132.

Millero, F.J., and R.H. Byrne. 1984. "Use of Pitzer's Equations to Determine the Media Effect on the Formation of Lead Chloro Complexes," *Geochimica et Cosmochimica Acta.* Vol. 48, no. 5, 1145-1150.

Millero, F.J., and D.J Hawke. 1992. "Ionic Interactions of Divalent Metals in Natural Waters," *Marine Chemistry.* Vol. 40, no. 1-2, 19-48.

Millero, F.J., and D.R. Schreiber. 1982. "Use of the Ion Pairing Model to Estimate Activity Coefficients of the Ionic Components of Natural Waters," *American Journal of Science.* Vol. 282, 1508-1540.

Millero, F.J., and V. Thurmond. 1983. "The Ionization of Carbonic Acid in Na-Mg-Cl solutions at 25°C," *Journal of Solution Chemistry.* Vol. 12, no. 6, 401-412.

Millero, F.J., P.J. Milne, and V.L. Thurmond. 1984. "The Solubility of Calcite, Strontianite and Witherite in NaCl Solutions at 25°C," *Geochimica et Cosmochimica Acta.* Vol. 48, no. 5, 1141-1143.

Millero, F.J., J.P. Hershey, and M. Fernandez. 1987. "The pK* of $TRISH_+$ in Na-K-Mg-Ca-Cl-SO_4 Brines - pH Scales," *Geochimica et Cosmochimica Acta.* Vol. 51, no. 3, 707-711.

Molecke, M.A. 1983. *A Comparison of Brines Relevent to Nuclear Waste Experimentation.* SAND83-0516. Albuquerque, NM: Sandia National Laboratories.

Møller, N. 1988. "The Prediction of Mineral Solubilities in Natural Waters: A Chemical Equilibrium Model for the Na-Ca-Cl-SO_4-H_2O System, to High Temperature and Concentration," *Geochimica et Cosmochimica Acta.* Vol. 52, no. 4, 821-837.

Mucci, A., and J.W. Morse. 1990. "Chemistry of Low-Temperature Abiotic Calcites: Experimental Studies on Coprecipitation, Stability and Fractionation," *Reviews in Aquatic Sciences.* Vol. 3, no. 2-3, 217-254.

Nitsche, H. 1991. "Basic Research for Assessment of Geologic Nuclear Waste Repositories: What Solubility and Speciation Studies of Transuranium Elements Can Tell Us," *Scientific Basis for Nuclear Waste Management XIV, Materials Research Society Symposium Proceedings, Boston, MA, November 26-29, 1990.* Eds. T.A. Abrajano, Jr. and L.H. Johnson. Pittsburgh, PA: Materials Research Society. Vol. 212, 517-529.

OECD/CEC (Organisation for Economic Co-Operation and Development and the Commission of European Communities). 1984. *Geological Disposal of Radioactive Waste. An Overview of the Current Status of Understanding and Development.* EUR 9130 EN. Paris, France: Organisation for Economic Co-Operation and Development.

Ogard, A.E. and J.F. Kerrisk. 1984. *Groundwater Chemistry Along Flow Paths Between a Proposed Repository Site and the Accessible Environment.* LA-10188-MS. Los Alamos, NM: Los Alamos National Laboratory.

Oversby, V.M. 1987. "Important Radionuclides in High Level Nuclear Waste Disposal: Determination Using a Comparison of the U.S. EPA and NRC Regulations," *Nuclear and Chemical Waste Management.* Vol. 7, no. 2, 149-161.

Pitzer, K.S. 1974. "Thermodynamics of Electrolytes. I. Theoretical Basis and General Equations," *Journal of Physical Chemistry.* Vol. 77, no. 2, 268-277.

Pitzer, K.S. 1979. "Theory: Ion Interaction Approach," *Activity Coefficients in Electrolyte Solutions.* Ed. R.M. Pytkowicz. Boca Raton, FL: CRC Press. Vol. I, 157-208.

Pitzer, K.S. 1991. Ion Interaction Approach: Theory and Data Correlation," *Activity Coefficients in Electrolyte Solutions.* Ed. K.S. Pitzer. 2nd ed. Boca Raton, FL: CRC Press. 76-101.

Pitzer, K.S., and J.J. Kim. 1974. "Thermodynamics of Electrolytes. IV. Activity and Osmotic Coefficients for Mixed Electrolytes," *Journal of the American Chemical Society.* Vol. 96, no. 18, 5701-5707.

Pitzer, K.S., and G. Mayorga. 1973. "Thermodynamics of Electrolytes. II. Activity and Osmotic Coefficients for Strong Electrolytes with One or Both Ions Univalent," *Journal of Physical Chemistry.* Vol. 77, no. 19, 2300-2308.

Pitzer, K.S., and G. Mayorga. 1974. "Thermodynamics of Electrolytes. III. Activity and Osmotic Coefficients for 2-2 Electrolytes," *Journal of Solution Chemistry.* Vol. 3, no. 7, 539-546.

Plummer, L.N., D.L. Parkhurst, G.W. Fleming, and S.A. Dunkle. 1988. *A Computer Program Incorporating Pitzer's Equations for Calculation of Geochemical Reactions In Brines*. U.S. Geological Survey Water-Resources Investigations Report 88-4153. Denver, CO: U.S. Geological Survey.

Rai, D., and J.L. Ryan. 1982. "Crystallinity and Solubility of Pu(IV) Oxide and Hydrous Oxide in Aged Aqueous Suspensions," *Radiochimica Acta*. Vol. 30, no. 4, 213-216.

Rechard, R.P., H. Iuzzolino, and J.S. Sandha. 1990. *Data Used in Preliminary Performance Assessment of the Waste Isolation Pilot Plant (1990)*. SAND89-2408. Albuquerque, NM: Sandia National Laboratories.

Riese, A.C. 1982. "Adsorption of Radium and Thorium onto Quartz and Kaolinite: A Comparison of Solution/Surface Equilibria Models." Ph.D. dissertation. Golden, CO: Colorado School of Mines.

Scatchard, G. 1936. "Concentrated Solutions of Strong Electrolytes," *Chemical Reviews*. Vol. 19, no. 3, 309-327.

Strickert, R.G., D. Rai, and R.W. Fulton. 1984. "Effect of Aging on the Solubility and Crystallinity of Np(IV) Hydrous Oxide," *Geochemical Behavior of Disposed Radioactive Waste*. Eds. G.S. Barney, J.D. Navratil, and W.W. Schulz. ACS Symposium Series 246. Washington, DC: American Chemical Society. 135-145.

Trauth, K.M., S.C. Hora, R.P. Rechard, and D.R. Anderson. 1992. *The Use of Expert Judgment to Quantify Uncertainty in Solubility and Sorption Parameters for Waste Isolation Pilot Plant Performance Assessment*. SAND92-0479. Albuquerque, NM: Sandia National Laboratories.

Trauth, K.M., S.C. Hora, and R.P. Rechard. 1993. *Expert Judgment as Input to Waste Isolation Pilot Plant Performance-Assessment Calculations. Probability Distributions of Significant System Parameters*. SAND91-0625. Albuquerque, NM: Sandia National Laboratories.

U.S. Department of Energy. 1979. "Department of Energy National Security and Military Applications of Nuclear Energy Authorization Act of 1980." Public Law 96-164.

U.S. Department of Energy. 1990. *Final Supplement Environmental Impact Statement, Waste Isolation Pilot Plant*. DOE/EIS-0026-FS. Washington, DC: U.S. Department of Energy, Office of Environmental Restoration and Waste Management. Vol. 2.

U.S. Environmental Protection Agency. 1985. "Environmental Standards for the Management and Disposal of Spent Nuclear Fuel, High-Level and Transuranic Radioactive Wastes; Final Rule," *Federal* Register. Vol. 50, no. 182, 38066-38089.

U.S. Environmental Protection Agency. 1993. "40 CFR Part 191: Environmental Radiation Protection Standards for the Management and Disposal of Spent Nuclear Fuel, High-Level and Transuranic Radioactive Wastes; Final Rule," *Federal Register*. Vol. 58, no. 242, 66398-66416.

Whitfield, M. 1975a. "An Improved Specific Interaction Model for Sea Water at 25°C and One Atmosphere Total Pressure," *Marine Chemistry*. Vol. 3, no. 3, 197-213.

Whitfield, M. 1975b. "The Extension of Chemical Models for Sea Water to Include Trace Components at 25°C and 1 Atm Pressure," *Geochimica et Cosmochimica Acta.* Vol. 39, no. 11, 1545-1557.

Wolery, T.J. 1979. *Calculation of Chemical Equilibrium Between Aqueous Solution and Minerals: The EQ 3/6 Software Package.* UCRL-52658. Livermore, CA: Lawrence Livermore National Laboratory.

Wolery, T.J. 1992. *EQ3/6, A Software Package for Geochemical Modeling of Aqueous Systems: Package Overview and Installation Guide (Version 7.0).* UCRL-MA-110662-Pt. 1. Livermore, CA: Lawrence Livermore National Laboratory.

APPENDIX A: DEBYE-HÜCKEL EQUATION FOR IONIC STRENGTH

APPENDIX A: DEBYE-HÜCKEL EQUATION FOR IONIC STRENGTH

The Debye-Hückel Equation for ionic strength, calculates activity coefficients, γ, as:

$$-\log \gamma_i = A\, z_i^2 \sqrt{I} \qquad \text{(A-1)}$$

where z is the charge of the ion of interest. A is given by

$$A = \frac{1}{2.303} \frac{e^2}{2\,DkT} \sqrt{\frac{8\pi e^2 N}{1000\,DkT}} \qquad \text{(A-2)}$$

where N is Avogadro's number, k is Boltzmann's constant, e is the charge of the electron, D is the dielectric constant of the solvent, and T is the absolute temperature. I is the ionic strength of the solution, expressed as:

$$I = \frac{1}{2} \sum z_i^2 [c_i] \qquad \text{(A-3)}$$

where brackets denote the analytical concentration of the i^{th} species.

APPENDIX B: ADDITIONAL INFORMATION ON IONIC INTERACTION MODELS

APPENDIX B: ADDITIONAL INFORMATION ON IONIC INTERACTION MODELS

Specific Ion-interaction Theory (as described by Grenthe et al., 1992)

"The Debye-Hückel term, which is dominant in the expression for the activity coefficients in dilute electrolyte solutions, accounts for electrostatic, non-specific long-range interactions. At higher concentrations short-range, non-electrostatic interactions have to be taken into account. This is usually done by adding ionic strength dependent terms to the Debye-Hückel expression. This method was first outlined by Brønsted (1922) and elaborated by Scatchard (1936) and Guggenheim (1966). The two basic assumptions in the specific ion-interaction theory are: (i) the activity coefficient γ_j of an ion j of charge z_j in a solution of ionic strength I_m is

$$\log \gamma_i = -z_j^2 D + \sum \varepsilon(j, k, I_m) m_k \qquad \text{(A1)}$$

where D is the Debye-Hückel term

$$D = \frac{A\sqrt{I_m}}{1 + Ba_j\sqrt{I_m}} \qquad \text{(A2)}$$

A and B are constants which are temperature dependent, and a_j is the effective diameter of the hydrated ions. The term Ba_j in the denominator of the Debye-Hückel term has been assigned the value 1.5, as proposed by Scatchard. The summation in eqn. (A1) extends over all ions k present in solution. Their molality is denoted m_k. The concentrations of the ions of the ionic medium are often much larger than those of the reacting species. Hence, the ionic medium ions will make the main contribution to the value of log γ_j for the reacting ions. This fact makes it possible to simplify the summation in eqn. (A1), so that only ion-interaction coefficients between the reacting ion species and the ionic medium ions are included." (Grenthe et al., 1992)

"The ion-interaction coefficients $\varepsilon(j, k, I_m)$ are zero for ions of the same charge sign and for uncharged species. The rationale behind this is that ε, which describes short-range interactions, must be small for ions that are kept apart by electrostatic repulsion." (Grenthe et al., 1992)

Research has been ongoing in developing means to estimate activity coefficients in high ionic strength media:

"The effect of composition on the activity of electrolytes can be estimated by using ionic interaction models. These models can be divided into two major types: (1) specific interaction and (2) ion pairing models. The specific interaction model yields reliable estimates of activity coefficients for the major ionic components of natural waters over a wide range of temperatures and ionic strengths. The ion pairing model yields estimates for the major and many minor components in dilute solutions. The combination of the two models yields a consistent model that can be used for all components of natural waters." (Millero, 1990)

"The most popular method used to account for the ionic interactions in natural waters is the ion pairing model. Since the suggested use of this model by Goldberg and Arrhenius (1958), it has been used by a number of workers to determine the speciation of ions in natural water. ... The use of the model to estimate activity coefficients was pioneered by Garrels and Thompson (1962) and extended by Dickson and Whitfield (1981) and Millero and Schreiber (1982). These latter studies allow one to estimate reliable activity coefficients for a number of major and minor ions to 1 m. ... The ion pairing model can at present be used to estimate the activity coefficients of the major and minor components...of natural waters at 25°C and below 1m. ... Extensions to higher ionic strength and other temperatures is complicated by the requirement for experimental data for the large number of ion pairs--50 in the case of seawater. The Pitzer model for the same components requires stability constants for only six ion pairs. Stability constants at temperatures other than 25°C are not readily available. Reliable extensions to higher ionic strength are difficult due to our lack of knowledge of the activity coefficients of the ion pairs of various charge type." (Millero and Hawke, 1992)

"The specific interaction model as formulated by Pitzer has made a large impact on our ability to estimate the activity of ionic and non-ionic solutes in natural waters. ... Weare and co-workers and others have extended the model. The present model can be used to make reliable estimates of the activity coefficients of the major components of natural waters over a wide range of temperatures to high ionic strengths." (Millero and Hawke, 1992)

"As first suggested by Whitfield (1975a, b) the combination of the two models can strengthen our ability to make reliable estimates of activity coefficients and to determine the speciation of metals in natural waters over a wide range of conditions. In recent years we have attempted to continue the joining of these two models. From this work it is clear that the Pitzer and ion pairing approaches are complementary for some of the strong cation-anion interactions. For example, the Pitzer model allows the prediction of mineral solubilities and geochemical precipitation sequences, while the ion pairing model allows the prediction of chemically reactive species in solution. Both approaches are mathematical methods that can be used to estimate activity coefficients." (Millero and Hawke, 1992)

APPENDIX C: CORRECTING pH_{NBS} VALUES TO DETERMINE $(H^+)_{Free}$ AND $(H^+)_{Total}$

APPENDIX C: CORRECTING pH_{NBS} VALUES TO DETERMINE $(H^+)_{Free}$ AND $(H^+)_{Total}$

The apparent activity obtained using NBS (National Institute of Standards and Technology [NIST]) buffers is related to the total proton concentration by

$$a_H = f\ [H^+]_T, \qquad \text{(C-1)}$$

where the factor f includes the activity coefficient of the proton in the brine and a term related to the liquid junction potential, and the subscript T refers to total concentration. The factor f can be determined experimentally by titrating an artificial brine with HCl. The electrode emf can be fitted to the Nernst equation

$$E = E^* + \left(\frac{RT}{F}\right)\ln[H^+], \qquad \text{(C-2)}$$

where E* is the standard potential in the brine at a fixed ionic strength. This equation can be used to determine the $[H^+]$ before the addition of HCl. If the electrode has also been calibrated using an NBS (NIST) buffer, the emf obtained before the addition of the HCl can be used to determine the apparent activity and the resultant f factor for the electrode system. Unfortunately, the value of f can vary from electrode to electrode and must be determined for the system of interest.

The total proton concentration in a brine can also be determined by using a buffer such as TRIS to calibrate the electrode system (Millero, 1979, 1986, 1992; Millero and Schreiber, 1982; Millero and Thurmond, 1983; Millero and Byrne, 1984; Millero and Hawke, 1992; Millero et al., 1984, 1987). Because the Pitzer parameters are available in all the major brine salts, it is possible to determine the pK* of TRIS in any brine. A TRIS buffer made up in this brine can be used to determine the pH of an unknown brine. The pH is determined using the equation

$$pH(BRINE) = pK^*(TRIS) + \frac{E_{BRINE} + E_{TRIS}}{k}, \qquad \text{(C-3)}$$

where k = (RT/F)log10 = 55.16 mV at 25°C. Because the pK* values of TRIS in various brines are quite similar, this method can be used for brines of similar composition without serious errors. To obtain an estimate of the f factor in the WIPP brines, one of the Panel (FJM) experimentally determined the value in 5 and 6 M NaCl buffered with TRIS (Millero et al., 1987) using a glass and calomel electrode system. The results are given in Table C-1.

Table C-1. "f" Factors Determined In 5.0 and 6.0 M NaCl

Concentration	$-\log[H^+]$	$-\log[H^+]_{NBS}$	Difference Between the pH Scales
5.0 M	8.956	8.258	0.70
6.0	9.142	8.263	0.88

These results yield the following equation that can be used to estimate the "free" proton concentration in the WIPP brines:

$$pH_F = pH_{NBS} + (0.18\ I - 0.20), \qquad \text{(C-4)}$$

which is valid from ionic strength, I = 5 to 7 (the subscript F is used to denote the free proton). This equation has been used to estimate the values of pH_F for the brines in Table 4. The concentration of the total proton in a brine is related to the free value by

$$[H^+]_T = \frac{[H^+]_F}{(1 + K_{HSO_4^-}[SO_4^{2-}])}, \qquad \text{(C-5)}$$

where K_{HSO_4} is the stability constant for the formation of HSO_4^-. The values of K_{HSO_4} calculated from the Pitzer program have been used to estimate the difference between the two pH scales

$$pH_T = pH_F + \log(1 + K_{HSO_4^-}[SO_4^{2-}]). \qquad \text{(C-6)}$$

The values of pH_T can be used to estimate the concentration of various acidic anions at a given pH in the brine using the ionization constants provided in Table 6. The concentration of $B(OH)_4^- = B$ can be estimated from

$$[B(OH)_4^-] = [HB]_T \left[\frac{K_{HB}}{K_{HB} + [H^+]_T} \right] \qquad \text{(C-7)}$$

The values of $B(OH)_4^-$ (given in Table 4), as well as other acid anions, such as HCO_3^- and CO_3^{2-}, can be calculated in this same manner. The final composition of the brines, after adjusting for the concentration of $B(OH)_4^-$ and balancing the equivalents is given in Table 4.

APPENDIX D: ESTIMATION OF ACTINIDE SOLUBILITIES IN WIPP (UNPUBLISHED LETTER REPORT FROM G.R. CHOPPIN TO L.H. BRUSH)

Report

Estimation of Actinide Solubilities in WIPP

Gregory R. Choppin

Introduction

The purpose of this study was to provide estimates of the probable solubility of actinides in the WIPP repository based on stability (complexation formation) constants, β_i, and solubility products, K_{sp}. Upper and lower limits as well as the most probable values of the solubilities were requested for two solutions, the Castile and the ingranular Salado brines. These calculations required a review of the available literature data, estimates of β_i and K_{sp} values for the possible species at the ionic strength and pH values of these brines and use of these estimated values to predict the species in solution and the net solubilities. The uncertainties in redox conditions did not allow reasonable estimates of the relative concentrations of species of different oxidation states of the same element (e.g., plutonium).

The brine compositions were provided by L. Brush:

	Salado	Castile
B	151 mM	92 mM
Br	13 mM	6.4 mM
Ca	10 mM	8.7 mM
Cl	6.07 M	5.02 M
K	510 mM	74 mM
Mg	1.0 M	66 mM
Na	3.9 M	6.00 M
SO_4	160 mM	190 mM
Total $C(HCO_3)$	0.436 mM	5.6 mM
pH	6.1	7.06

From these data, the ionic strengths were calculated to be: 7.66 M for the Salado and 6.14 M for the Castile brines.

Literature Data

The brine composition indicated that complexation by Br^-, Cl^-, SO_4^{-2} and CO_3^{-2} and hydrolysis are the sources of the possible species of the actinides. However, since Br^- is a weaker complexor than Cl^- and the concentration is much less than that of Cl^-, complexation by Br^- was not considered. In addition to the inorganic anions in the brines, several organic ligands are present in the wastes. The possible complexation of the actinides by these ligands as the wastes are released to the brines must be considered in the speciation. The ligands and their estimated (L. Brush) concentrations in the brines are:

	Concentration		
	Minimum	Average	Maximum
Citrate	0.0964 mM	0.193 mM	0.481 mM
EDTA	3.13×10^{-4} mM	6.26×10^{-4} mM	1.56×10^{-3} mM
TTA	7.31×10^{-3} mM	0.0146 mM	0.0365 mM
8-OH Quinolinate	0.0338 mM	0.0676 mM	0.169 mM

A number of authors have compiled the stability constants available in the literature and these sources were reviewed for appropriate values. For the inorganic ligands, compilations by Phillips, et al. (1), IAEA (2), and Kim et al. (3) were useful. The data base for the Livermore Lab EQ 3/6 code was also checked. The values for the organic ligands were obtained from Martell and Smith (4) and an IAEA review in progress (5). Unfortunately, there were no experimental values for any of the stability constants of interest at the ionic strengths of the brines. For a few metal-ligand systems, data existed up to 2-3 M ionic strength, but for the majority of the metal-ligand pairs of interest, values of β_i and/or K_{sp} existed only for 1 M ionic strength or lower. In all systems, the values at different ionic strengths were reported by different research groups using a variety of techniques. The values were often contradictory, so the more valid value was frequently a matter of subjective judgment. Another problem which interfered with as reliable an estimation as desirable was that the experimental values of β are consistently limited to 1:1 (metal:ligand) or 1:2 complexes whereas the 1:3 and 1:4 complexes are frequently of greater interest.

Since the β_i values are limited to lower ionic strengths, it was necessary to estimate the values at 6.14 M and 7.66 M ionic strengths. The Radioactive Waste Management Committee of the Nuclear Energy Agency of the OECD has reviewed the theoretical and empirical methods of estimating stability constants at unknown ionic strengths. The order of preference for use in the NEA Thermochemical Data Base is:

1. the specific ion interaction method in the Guggenheim-Bronsted-Scatchard form;
2. the Davies equation.

The latter is useful for $I < 0.1$ M (e.g., for estimation of β_i at very low ionic strengths of many natural waters). The specific interaction models adopt equations of the form:

$$\log \beta_i = \log \beta_i^0 + \frac{\Delta Z^2 \ I^{1/2}}{1+B \ I^{1/2}} - \Delta\Sigma \cdot I \qquad (1)$$

where β_i^0 is the stability constant at infinite dilutions. ΔZ^2 is given by

$$\Delta Z^2 = (Z_{complex})^2 - (Z_M^2 + Z_{ligand}^2).$$

B is set at 1.5 for most systems. $\Delta\Sigma$ is the difference in the specific interaction parameters of the metal (M), ligand (L) and inert electrolyte (NX). For these brines, NX can be considered NaCl. Thus, $\Delta\Sigma$ is equal to:

$$\Delta\Sigma = \Sigma(ML_i, X) - i\Sigma(N,L) - \Sigma(M,X)$$

Compilations of Σ values are available (6,7) but these do not include most of the complex species of interest to this study. As a result, a modified approach was used.

Equation 1 can be rewritten to the same form as the "extended Davies" equation form:

$$\log \beta_i = \log \beta_i^0 + \frac{\Delta Z^2 \ I^{1/2}}{1+1.5 \ I^{1/2}} + bI \qquad (2)$$

in which b replaces $-\Delta\Sigma$. If β_i values are known at different ionic strengths, Eq. 2 can be used in the form:

$$A = \log \beta_i - \frac{\Delta Z^2 \ I^{1/2}}{1+1.5 \ I^{1/2}} = \log \beta_i^0 + bI \qquad (3)$$

Plots of A vs. I should be linear with a slope of b and intercept of $\log \beta_i^0$. This relationship has been used up to 3 M ionic strength (1) but is untested experimentally above this value.

Despite the uncertainty of the validity of equation 2 in the range of 6-8 M ionic strength, it was used in this study as no other approach was feasible. The plots of A vs. I had the advantage of testing the value of the literature data by calculating the correlation coefficient of the linear relation. Rarely were more than 3 or 4 values of β_i at different I available for any complex which further increases the uncertainty in the final values calculated for I = 6.14 M and 7.66 M.

To show the results of use of equation 3, the variation of log β_i as a function of I is shown in Figures 1-3. Figure 1 shows the data for formation of the monofluoride complexes of Am^{+3}, Th^{+4}, and UO_2^{+2}. The experimental values are labeled "e" on each curve. The dotted curve for AmF^{+2} is based on experimental values in ref. 2 (I = 1 M maximum) whereas the solid line includes an unpublished experimental value at I = 6.0 M from this laboratory. The difference in these two curves indicates the problem in using eq. (3) for data of I $\leq$ only. Figure 2 shows the parallel behavior of the calculated curves for ThF^{+3} and ThF_2^{+2} formation. Figure 3 shows this parallel behavior persists even for 1:4 complexation. Where no β_i (i > 1) values were available, this parallel behavior was used to obtain estimated values for the higher complexes.

Speciation Results

The values of log β_i obtained by these procedures are listed in Table I. Values of pK_w calculated by the same procedure are included as they were used in calculation of hydroxide concentration. The values of pK_a for $HCO_3^- \rightarrow CO_3^{2-} + H^+$ were calculated also and were 9.7 (6.14 M) and 0.9 (7.55 M).

The amount of each species relative to the aquated cation (e.g., $PuCl^{+2}/Pu^{+3}$) were calculated by the relation:

$$R = \frac{[MX]}{M} = \beta \cdot [X] \qquad (4)$$

where [X] is the concentration of the "free" ligand. For simplicity, the free ligand concentration was assumed to be the ligand concentration of the brine as listed previously. The calculated R values are listed in Table II. From those values, it is clear that the significant species are:

Oxidation State	Dominant Species
III	$M(OH)_n$
IV	$M(OH)_4$
V	MO_2Cl
VI	$MO_2(OH)_2$

No reliable values exist for formation of $M(OH)_2^{+1}$ and $M(OH)_3^0$. The values of the EQ 3/6 data base (I=0) allowed estimates of K_1/K_2 and K_1/K_3 ratios which should be relatively independent of $I(K_1 \equiv \beta_1,\ K_2 = \beta_2/\beta_1,\ K_3 = \beta_3\ \beta_2)$. Estimates from these data indicate that $M(OH)^{+2}$ would be in 50 fold excess over the higher order complexes. The estimated β_1 in Table 1 seems rather high so we conclude M(III) would exist in the brines as a mixture of mostly $M(OH)^{+2}$ and $M(OH)_2^{+}$.

Speciation by Organic Ligands

Estimation of the effect of the organic ligands on speciation is much more difficult.

For 8-hydroxyquinoline, no stability constants are available. However, at the pH values of the brines, this ligand would remain protonated at the nitrogen site, weakening complexation. Extraction with this ligand of Ln^{+3}, Pu^{+4}, and UO_2^{+2} into organic solvents is performed in the pH range of the brines, which reflects greater organic solubility and, by implication, less complexation in the aqueous phase. We conclude that complexation of actinides in the brines by 8-hydroxyquinoline is not a concern at the concentrations of ligand present although this conclusion cannot be confirmed by calculations.

Values of log β_1 are available at 0 and 0.1 M ionic strength for complexing of UO_2^{+2}, Th^{+4}, Pu^{+4}, and Nd^{+3} by acetylacetonate, AA (Nd^{+3} is a good analog for trivalent actinides). The values ranged from 5.4 to 9. This ligand is a β-diketonate with similar binding characteristics to those of thenoyltrifluoroacetone (TTA). Since the K_a of AA is 100 times larger than that of TTA, the log β values of TTA complexation would be at least 10 times smaller; i.e., log β_1 for TTA complexes is at least 1 unit less than that for AA complexes. We also found that the curves of log β_1 vs. I for actinide complexation (Fig. 4) by acetate indicated that log β_i at I ~ 6-7 M is comparable to log β_i at I = 0. From these considerations and the log β_i for AA complexation, values of log β_i of 4.5 (M^{+3}), 8 (M^{+4}), 6.5 (MO_2^{+2}) were used to estimate the speciation with TTA. These showed that at the maximum concentration of TTA, no significant effect of TTA complexation would be present.

Values of log β_i for citrate complexation of actinides are limited to I = 1 or less. This prevents use of eq. 2 for estimation of log β_i at I = 6-8 M. Moreover, the high concentration of Mg^{+2} in the Salado brine would result in formation of Mg-Cit complexes and reduce the free citrate to very low values. Assuming the citrate is all bound by Mg^{+2}, the "free" citrate can be estimated as:

$$[Cit]_f = [MgCit]/\beta_{MgCit} \cdot [Mg]$$
$$= (0.5x10^{-3})/10^2x(1) = 5x10^{-6}\ M.$$

For M^{+3}, the log β_1 at I = 0 is ca. 9, therefore

$$\frac{[MCit]}{[M]} = \beta \cdot [Cit] = 10^9(5x10^{-6}) = 5x10^3$$

Since $[M(OH)]/[M] \approx 2x10^6$, the MCit is a negligible contribution (< 1%). A similar estimation for the Castile brines indicates that the citrate complex of M^{+3} would have an equally small contribution (i.e., < 1%). The citrate would affect the M^{+3} more than the more extensively hydrolyzed M^{+4} and MO_2^{+2} ions so the effect on these latter would be << 0.1%. The estimates for the MO_2^+ cations is less certain as no log β values for NpO_2Cit^{-2} are listed. Assuming these values are the same as that for $CaCit^-$ formation (ca. 5), it is estimated that the effect of citrate complexing is ca. 1% of the NpO_2Cl formation in the Salado brine and 5-10% in the Castile brine - assuming the maximum citrate concentration. Using the 'probable' value of citrate, the effect for MO_2^+ can be ignored unless log β (MO_2Cit^{-2}) is > 5, which is unlikely.

The complexation of metal ions by ethylenediamminetetraacetate, EDTA, is very strong. We can assume strong complexation by Mg^{+2} so $[MgEDTA] \approx [EDTA]$. Thus,

$$[EDTA]_f = [MgEDTA]/[Mg] \cdot \beta_{MgEDTA}$$
$$= 1.6x10^{-15}\ M \text{ for Salado brine}$$
$$= 2x10^{-14}\ M \text{ for Castile brine.}$$

The experimental values for the actinide complexes are:

M^{+3}-EDTA, log β = 17.0 (0.1 M), 16.2 (0.5 M);

M^{+4}-EDTA, log β = 26 (0.1 M);

MO_2^{+}-EDTA, log β = 7.3 (0.1 M);

MO_2^{+2}-EDTA, log β = 10.4 (0.1 M).

Arbitrarily, one unit was added to the 0.1 M values to obtain the estimated log β for 6-8 M ionic strength. This results in values of R of:

Ion	R (Salado)	R (Castile)
M^{+3}	$1.6x10^{3}$	$2x10^{4}$
M^{+4}	$1.6x10^{11}$	$2x10^{12}$
MO_2^{+2}	$3.2x10^{-7}$	$4x10^{-6}$
MO_2^{+2}	$5x10^{-4}$	$6x10^{-3}$

When these R values are compared to those in Table II, it is obvious that the EDTA would have no significant effect on the speciation of any of the oxidation states, even at its highest concentration.

We conclude that the organic ligands in the wastes would not have significant effect on the speciation of the actinides with the possible exception of the MO_2^{+} in the Castile brines. Even in this case, the probable increase in solubility is < 5%.

Redox

Due to the uncertainties in the redox characteristics of the various areas of the repository, no redox speciation was attempted. Americium would be present as Am^{+3}, thorium as Th^{+4}, but the redox speciation of U, Np and Pu is uncertain.

Solubilities

The inability to perform redox speciation makes it impractical to predict elemental solubilities. However, the solubility for a particular oxidation state can, within the limitation of the available data, be estimated if we assume no perturbation by a lower solubility of another oxidation state of a particular element. Almost no data is given on the variation of K_{sp} values with ionic strength. To minimize this deficiency and, noting that the hydroxy species are dominant for the M^{+3}, M^{+4}, and MO_2^{+2} species, the K_{sp} values of the EQ 3/6 data base have been combined with the log β_i values (both at I = 0) of the neutral hydroxy species to obtain an equilibrium constant for the reaction:

$$M(OH)^0_{n(s)} = M(OH)_{n(aq)};\ \log Q = [M(OH)_{n(aq)}] \qquad (5)$$

The lack of charges in this equation should, in principle, make the log Q independent of ionic strength. In practice, it is not, but the present state of experimental data and of theory offer no attractive alternative to this approach.

For $Am(OH)_3$, this approach gives a solubility of $Am(OH)_3$ of 10^{-7} M. However, if this is valid, this must be multiplied by a factor to obtain $[Am(OH)^{+2}] + [Am(OH)_2^{+}]$, which are the dominant species. This result is a prediction of americium(III) of ca. 10^{-4} M Kim, et al. (8) report solubilities of 10^{-5} M (pH ~7) which reduces to 10^{-6} M at pH ~7.6 in 0.1 M $NaClO_4$ and 10^{-6} M at pH 6.7 in 5 M NaCl. So, a solubility of ca. 10^{-5} - 10^{-6} M is reasonable for the WIPP brines for the trivalent state of the actinides (assuming no effect of redox).

The calculations for thorium give a solubility of $\sim 10^{-6.5}$ M. However, Ryan and Rai have measured the solubility of $ThO_{2(am)}$ in 0.1 M $NaClO_4$ solution to be ca. 10^{-9} M above pH 6 (9). They give a value for the log K_{sp} of < 44.8. With this value, a new solubility of $10^{-8.5}$ M is obtained:

	log K
$ThO_{2(am)} + 2H_2O = Th^{+4} + 4OH^-$	-44.8
$Th^{+4} + 4OH^- = Th(OH)_{4(aq)}$	36.3
$ThO_{2(am)} = Th(OH)_{4(aq)}$	- 8.5

For Pu(IV), using the values of Rai (10), this procedure gives a solubility of $10^{-10.4}$ M. Such a value is consistent with the solubility studies of Kim (8).

The solubility of MO_2^+ is very difficult to estimate. Plutonium has been found to exist, at concentrations < 10^{-6} M, as PuO_2^+ in neutral, oxic solutions. However, the solubility is determined by the redox reaction which forms the insoluble $Pu(OH)_4$. In such systems, the solubility of PuO_2^+ is very dependent on the redox potential and on the pH. Based on the data for I = 0 in the EQ 3/6 data base, the solubility of NpO_2^+ (as NpO_2Cl) is estimated to be $5x10^{-9}$ M, which seems orders of magnitude too low.

For MO_2^{+2}, the data for uranyl can be used from the EQ 3/6 data base as a first estimate. For $UO_{3(am)}$ or $UO_2(OH)_{2(am)}$, if the equations are valid as written - e.g.,

$$UO_{3(am)} + 2H^+ = UO_2^{+2} + H_2O; \log K = ^-10.41$$

a solubility of UO_2^{+2} of ca. 10^{-4} M is estimated at pH 7. For $UO_2(OH)_{2(am)}$, the solubility of UO_2^{+2} would be $10^{-8.8}$ M. Since the $UO_2(OH)_2$ is the dominant species, the solubility of UO_2^{+2} must be multiplied by R ($10^{-8.8}$ x $10^{6.7}$) which gives $10^{-2.1}$ M as the net solubility. This is much too high and suggests that the log K above must be erroneous. The concentration of uranium in sea water is ca. 10^{-8} M, due mainly to the $UO_2(CO_3)_3^{-4}$ species. Therefore, at I = 0.7 M we assume the solubility of $UO_2(OH)_{2(aq)}$ to be less than 10^{-8} M. Estimating log β_2 at I = 0 for formation of $UO_2(OH)_2$ to be 16.6 (i.e., K_1/K_2 = 6.3), for the reaction of eq. 3 we obtain log K = -5.6, indicating a solubility of U(VI) (as $UO_2(OH)_2$) of $10^{-5.6}$ M.

Colloids

This report has ignored the possible effects of colloids which are common in neutral and basic solutions. Colloids provide a large net surface area which may have a high tendency to sorb actinide species, especially if these latter are hydrolyzed. Kim (3,8) has paid particular attention to this problem, but the data are too site-specific to allow use in modeling analysis. However, the presence of colloids in the brines could serve to increase the concentration of actinide ions (particularly in the III, IV, and VI states) in the solution phase. For brine moving through a packed structure, the colloids may be reduced but this is an effect which should be evaluated.

Summary

For the Castile and Salado brines, the actinides should exist as hydrolyzed species except in the pentavalent state when they would more likely be the mono and/or dichlorocomplex. M^{+3} is predominantly MOH^{+2} whereas M^{+4} and MO_2^{+2} are the neutral species, $M(OH)_4$ and $MO_2(OH)_2$, respectively. The organic contaminants in the waste would not perturb the speciation (or the solubility) except in the case of MO_2^+ where a < 5% effect could occur.

Solubilities are more difficult to calculate. The estimated solubilities are 10^{-5} to 10^{-6} M for Am(III), 10^{-10} - 10^{-11} M for Pu(IV), $10^{-8.5}$ M for Th(IV), ca. 10^{-8} M for NpO_2Cl, and ca. 10^{-6} M for U(VI). However, no solubility data could be found for higher ionic strengths so these estimates are based on I = 0 and must be considered as quite uncertain.

Measurements of the hydrolysis constants (β_1^*) at 6-8 M ionic strength are necessary to confirm these measurements. Stability constants for EDTA and citrate at these ionic strengths in the presence of Mg(II) are also necessary to ensure the absence of solubility increases by these chelators. Finally, the binding by sidereophores in these brines are necessary to learn if microbial byproducts could increase the solubility.

No data exists on the necessary K_{sp} data for the ionic strengths of these brines. These measurements on the hydrous oxides are necessary as the K_{sp} values used in this study are not reliable. Finally, solubilities of NpO_2Cl and NpO_2OH is necessary.

Finally, proper evaluation of the Np and Pu solubility is very dependent on the oxidation state present in the sealed repository. This should be of highest priority.

References

1. S. L. Phillips, C. A. Phillips, and J. Skeen, "Hydrolysis, Formation and Ionization Constants at 25°C and at High Temperature-High Ionic Strength", LBL-14996, Lawrence Berkeley Laboratory, 1985.

2. J. Fuger, I. L. Khodakovsky, V. A. Medvedev and J. D. Navratil, "The Actinide Aqueous Inorganic Complexes", Part 12, Intern. Atom. Ener. Agency, in press.

3. J.-I. Kim, "Basic Actinide and Fission Products Chemistry", RCM-02085, Tech. U. Munchen, 1985.

4. A. E. Martell and R. M. Smith, Critical Stability Constants, Vol. 1-4, Plenum Press.

5. P. A. Baisden, G. R. Choppin, B. Myasaedov, and J. C. Navratil, "The Actinide Aqueous Organic Complexes", Part 14, IAEA, in preparation.

6. L. Ciavatta, Ann. Chim. (Rome), 70, 551 (1980).

7. D. Ferri, I. Grenthe, and F. Salvatore, Inorg. Chem., 22, 3162 (1983).

8. J.-I. Kim, et al., RCM 00187, Tech. U. Munchen, 1987.

9. J. L. Ryan and D. Rai, Inorg. Chem., 26, 4140 (1987).

10. D. Rai, Radiochim. Acta, 35, 97 (1984).

Table I

Estimated Stability Constants (log β)

a. Castile Brine: I = 7.66 M; pK_w = 13.58

Species	M^{+3}	M^{+4}	MO_2^+	MO_2^{+2}
MCl	-0.15	0.43	1.0	-0.27
MSO_4	1.85	6.09(?)	0.76	1.80
MCO_3	6.73	12.5	0.76	7.86
MOH	12.8(?)	13.4	3.0	11.1
$M(OH)_2$	---	---	---	22.0(?)
$M(OH)_4$	---	48.0	---	---

b. Salado Brine: I = 7.66 M; pK_w = 13.55

Species	M^{+3}	M^{+4}	MO_2^+	MO_2^{+2}
MCl	0.13	0.60	1.0	-0.17
MSO_4	2.08	7.66	1.18	2.51
MCO_3	7.13	12.9	1.18	8.12
MOH	14.7(?)	13.8	3.0	12.2
$M(OH)_2$	---	---	---	24.0(?)
$M(OH)_4$	---	49.0	---	---

(?) indicates that, although this is the value obtained by the methods described in the text, it seems too large.

Table II

Calculated R Values

I(M)	R_{Cl}	R_{SO_4}	R_{CO_3}	R_{OH}	$R(OH)_n$
			a. M^{+3}		
6.14	3.6	13.5	60.2	$1.8x10^{6}$	
7.66	4.5	19.2	0.	$2.9x10^{7}$	
			b. M^{+4}		
6.14	neg.	neg.	neg.	$7.1x10^{6}$	$2.5x10^{27}$ *
7.66	24.0	52.0	480.0	$3.4x10^{6}$	$1.6x10^{28}$
			c. MO_2^{+}		
6.14	50.0	0.	neg.	neg.	
7.66	60.0	2.4	neg.	neg.	
			d. MO_2^{+2}		
6.14	2.5	neg.	8.0	$3.7x10^{4}$	$5.6x10^{6}$ ≠
7.66	4.1	neg.	neg.	$7.9x10^{4}$	$3.2x10^{9}$

* $n = 4$

≠ $n = 2$

FIGURE 1

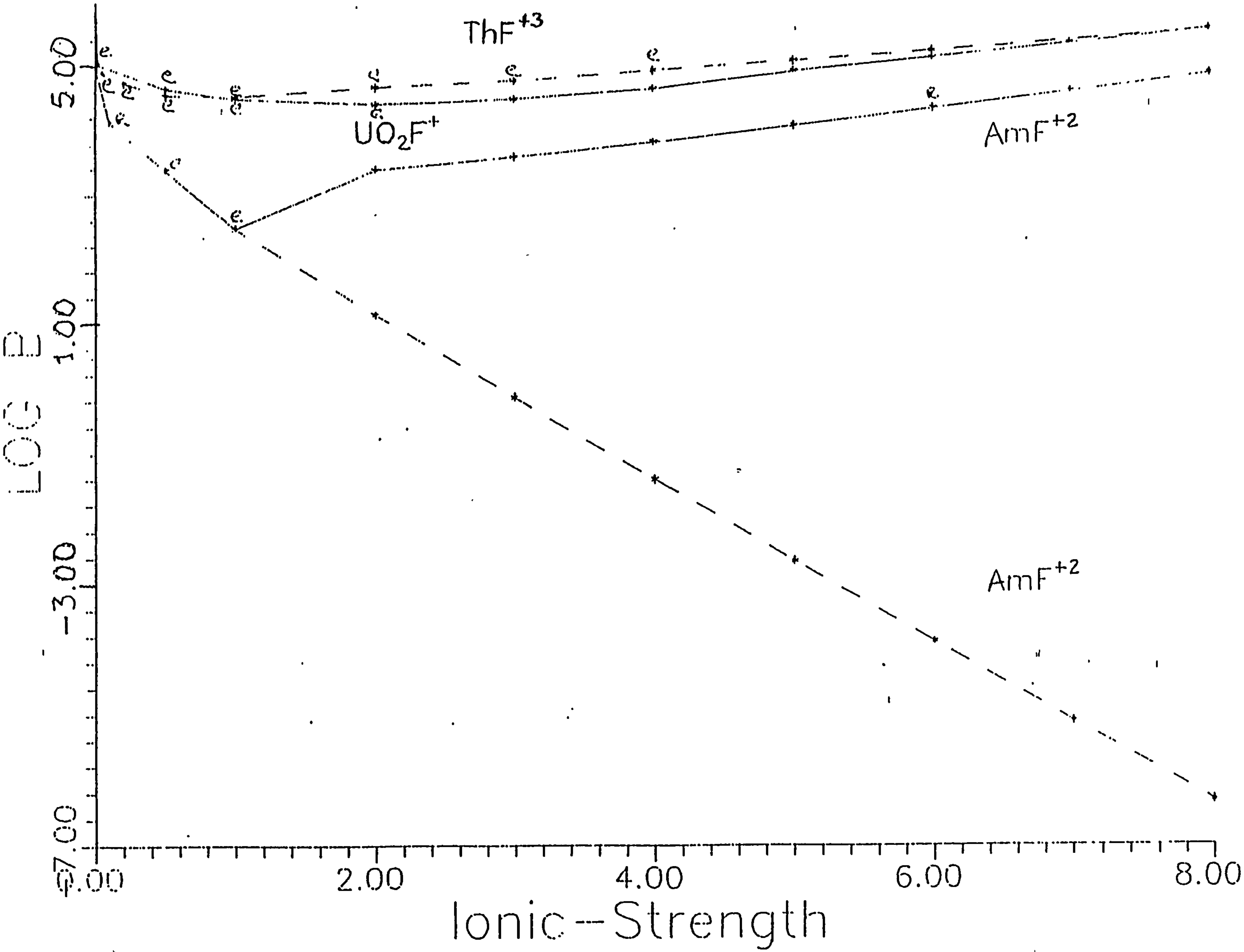

ThF+3
UO2F+
AmF+2
AmF+2
5.00
1.00
-3.00
-7.00
LOG B
0.00
2.00
4.00
6.00
8.00
Ionic--Strength

FIGURE 2

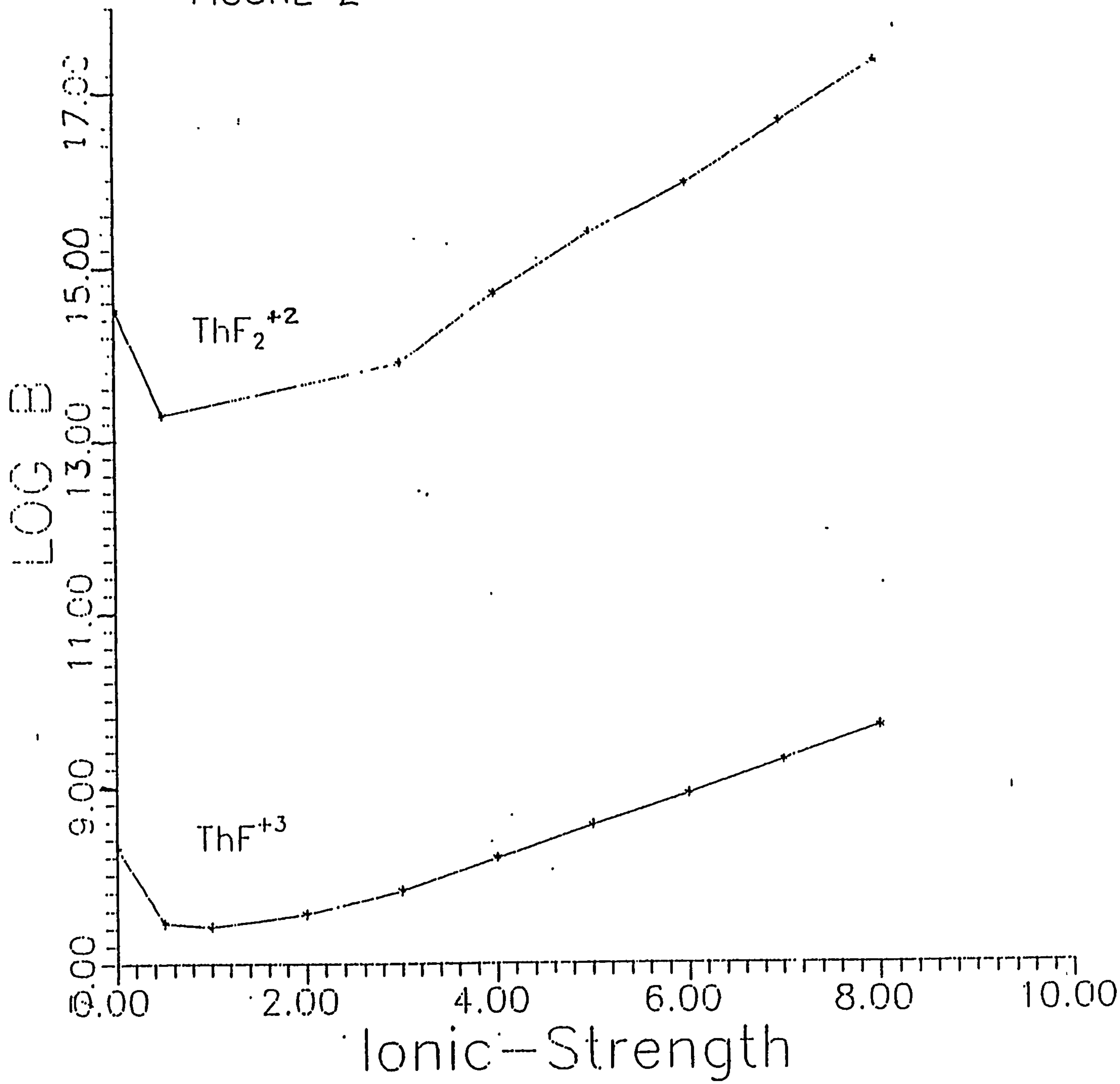

LOG B
17.00
15.00
13.00
11.00
9.00
0.00
ThF2+2
ThF+3
0.00
2.00
4.00
6.00
8.00
10.00
Ionic—Strength

FIGURE 3

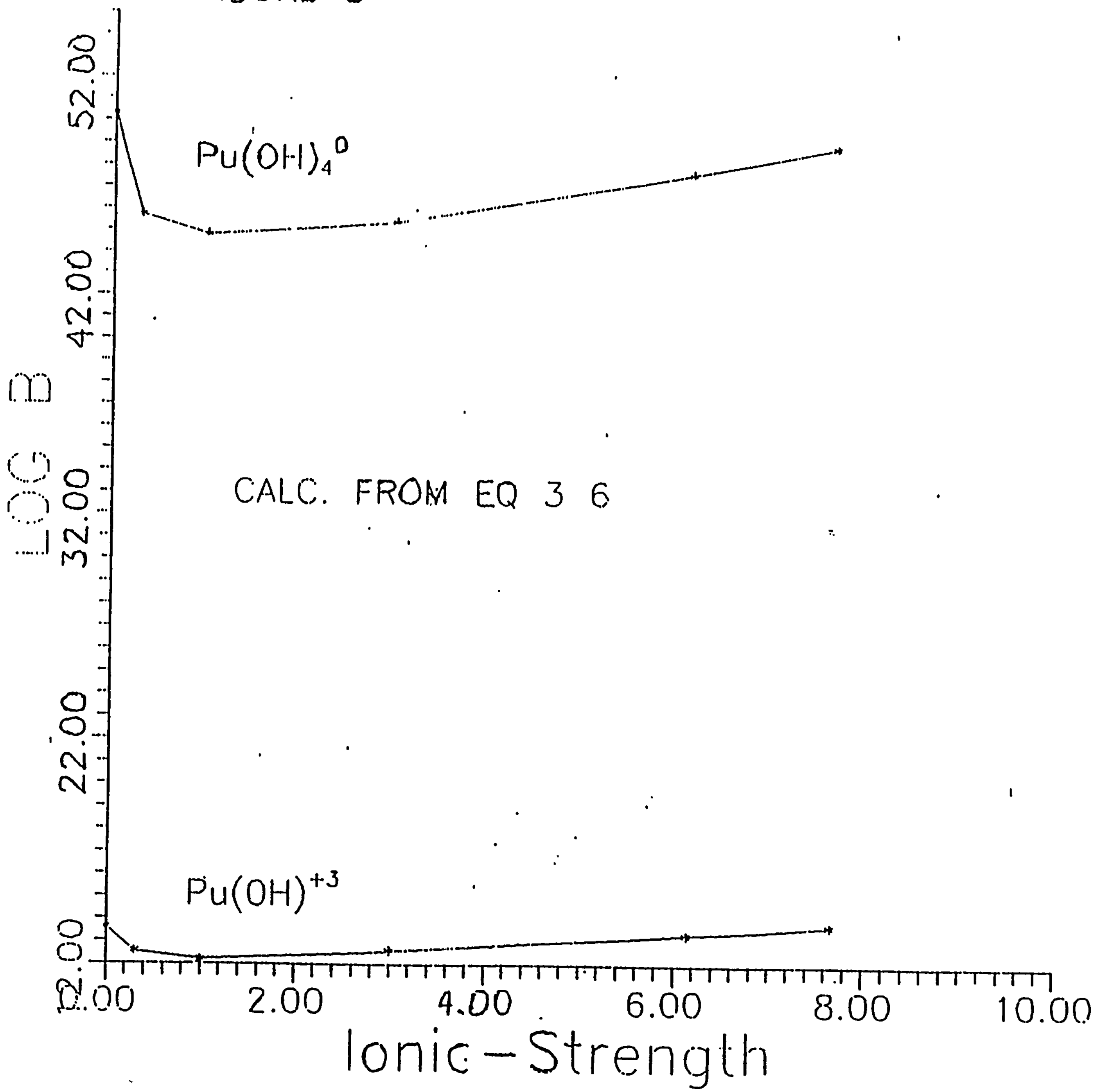

Pu(OH)4 0
CALC. FROM EQ 3 6
Pu(OH)+3
LOG B
52.00
42.00
32.00
22.00
2.00
0.00
2.00
4.00
6.00
8.00
10.00
Ionic-Strength

FIGURE 4

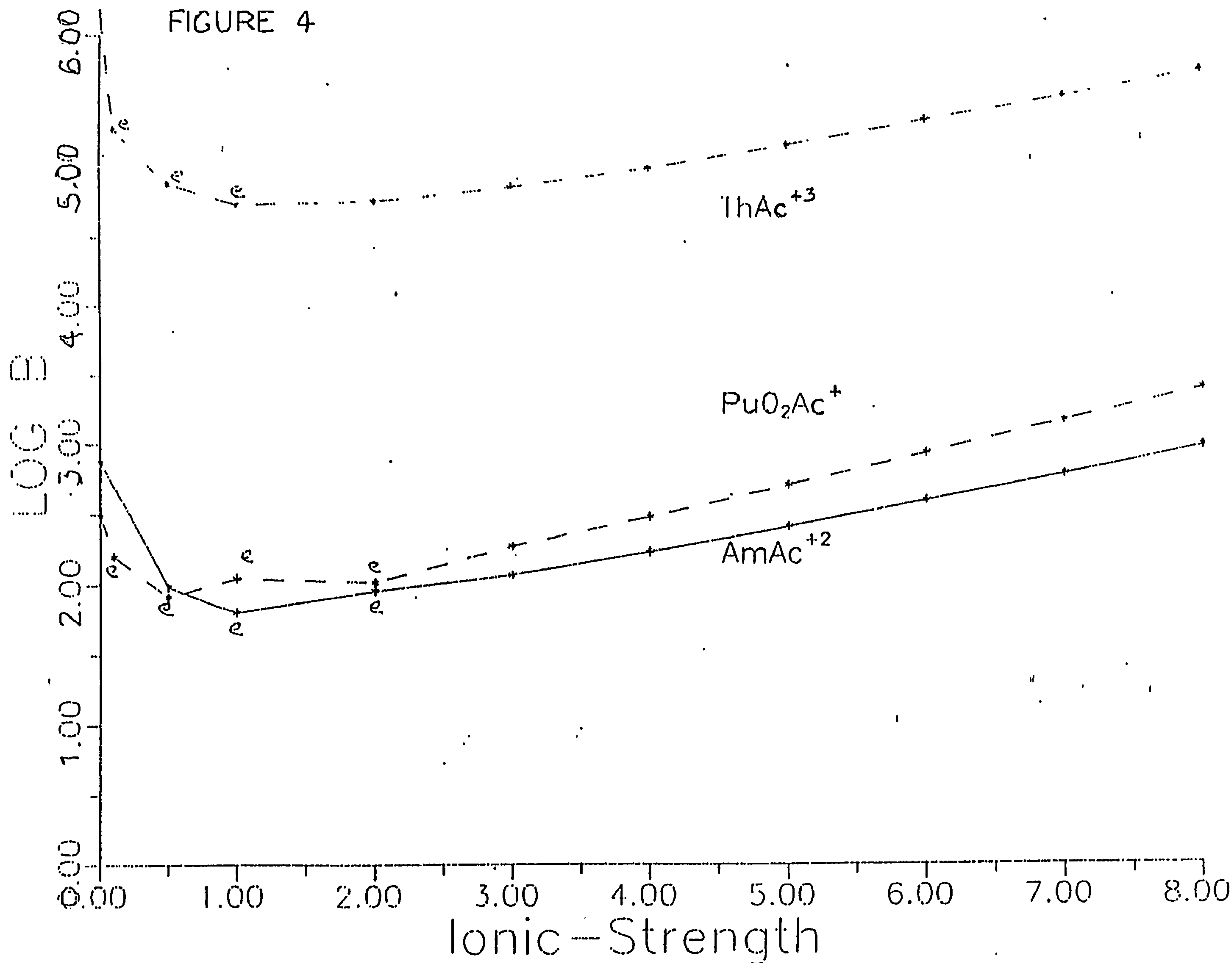
ThAc+3
PuO2Ac+
AmAc+2
LOG B
6.00
5.00
4.00
3.00
2.00
1.00
0.00
0.00
1.00
2.00
3.00
4.00
5.00
6.00
7.00
8.00
Ionic — Strength

APPENDIX E: ADDITIONAL INFORMATION ON BRINE LIGANDS

APPENDIX E: ADDITIONAL INFORMATION ON BRINE LIGANDS

The concentration of the carbonate ion in the brine can be determined from the total concentration of CO_2, $[CO_2]_T = 1$ M, by

$$[CO_3^{2-}]_T = [CO_2]_T\left(\frac{K_2}{K_2 + [H^+]}\right), \qquad \text{(E-1)}$$

where the subscript T refers to the total concentrations. The values estimated from this equation are given below and represent the maximum values one would expect in the brines if the choice of $[CO_2]_T$ is correct and is not greater than 1M. The concentration of carbonate in the brine will most likely be controlled by the Mg^{2+} ion concentration and the solubility of $MgCO_3$ in the brine. The equilibrium concentration of the CO_3^{2-} ion can be estimated from

$$[CO_3^{2-}]_T = \frac{Ksp^*}{[Mg^{2+}]_T}. \qquad \text{(E-2)}$$

The value of $Ksp^* = Ksp/\{\gamma_T(Mg)\ \gamma_T(CO_3)\}$ can be estimated from the infinite dilution value of pKsp = 7.6 to 8.1 (Mucci and Morse, 1990, Table 1) given in Table E-1 and the total activity coefficients given in Table 5. This yields what we call the minimum values of total carbonate in the brines (Table E-2). These estimates from the solubility of $MgCO_3$ are lower, but are probably more realistic. It would be useful to do a full analysis of the brines that would be expected using the Pitzer equations with the solid phases included. Other metal carbonates could also effect the carbonate levels in the brines. Certainly the input speciation calculations should be made at variable amounts of total carbonate. The total inorganic carbon dioxide of Brine A was 0.010 M. This value of $[CO_3]_T$ gives a value of $[CO_3^{2-}] = 6\times10^{-4}$M . It is close to the value estimated from the $MgCO_3$ and will be used in further calculations for Brine A.

The other inorganic ligand that is important in the brines is the $[OH^-]$ ion, the concentration of which can be estimated from the values of K_w in the brines (Table 6).

$$[OH^-] = \frac{K_W^*}{[H^+]} \qquad \text{(E-3)}$$

If the input proton concentration is made as the free value, then the values of K_w* should also be made on the free scale, $K_w^* = K_w \div [\gamma_F(H)\ \gamma_F(OH)]$. Because the formation of most hydroxide complexes are given as hydrolysis constants relative to $[H^+]_F$, the free scale is normally needed. It should be pointed out that the activity coefficients and resultant constants given in Table 5 include the interactions of Mg^{2+} with all the major anions in the brine (Cl^-, Br^-, SO_4^{2-}, OH^-, HCO_3^-, CO_3^{2-}, and $B(OH)_4^-$). Estimates of the free or uncomplexed ions in the brines can be approximated from the activity coefficients of Na^+, Cl^- and ClO_4^- solutions (subsequently documented in Millero, 1992, and in Millero and Hawke, 1992) given in Table **9**.

Table E-1. The Solubility Product of Divalent Metal Carbonates

Carbonate (Mineral)	pKsp
$MgCO_3$	7.59, 8.09
$CaCO_3$ (Aragonite)	8.31
$CaCO_3$ (Calcite)	8.48
$SrCO_3$	9.27
$BaCO_3$	8.55
$NiCO_3$	6.87
$CuCO_3$	9.63
$CoCO_3$	9.98
$ZnCO_3$	10.00
$MnCO_3$	10.59
$FeCO_3$	10.91
$CdCO_3$	11.31
$PbCO_3$	13.21

(Mucci and Morse, 1990, Table 1)

Table E-2. Maximum and Minimum Values of Total Carbonate in the Brines

		G-Seep	SB-3	Brine A	Brine B
pKsp*		5.04-5.54	4.92-5.42	4.64-5.14	5.83-6.33
$[CO_3^{2-}]_T$	Max	0.0070	0.0092	0.0594	0.0044
	Min	1×10^{-5}	1.2×10^{-5}	2×10^{-5}	2×10^{-4}

APPENDIX F: SUMMARY OF MASS ACTION EQUATIONS USED FOR CALCULATING CONCENTRATION VALUES FOR THE 0.1 AND 0.9 FRACTILES

Thorium

(s) = solid

Dominant aqueous species	Solubility limits imposed by solids
$Th(OH)_4(aq)$	upper limit - eq. w/ $Th(OH)_4(s)$ $\log a_i = -6.257$ lower limit - eq. w/ ThO_2 (thorianite) $\log a_i = -14.05 + 2 \log a_{H_2O}$

$Th(OH)_4(s) / Th(OH)_4^0$

$$Th(OH)_4(s) = Th(OH)_4^0 \qquad \log K = -6.257$$

$\boxed{\log a_{Th(OH)_4^0} = -6.257}$ in eq. w/ $Th(OH)_4$

$ThO_2(s) / Th(OH)_4^0$

$$ThO_2(s) + 2H_2O = Th(OH)_4(aq) \qquad 14.05$$

$\boxed{\log a_{Th(OH)_4^0} = -14.05 + 2 \log a_{H_2O}}$ in eq. w/thorianite

Uranium

Dominant aqueous species	Solubility limits imposed by solids
$U(OH)_4(aq)$	upper limit - eq. w/ $UO_2(am)$
	$\log a_i = -4.44 + 2 \log a_{H_2O}$
	lower limit - eq. w/ $UO_{2.6667}(\sim U_3O_8)$
	$\log a_i = -25.39 - 0.3333 \log f_{O_2(g)} + 2 \log a_{H_2O}$
$UO_2(CO_3)_2^{2-}$	upper limit - eq. w/ $UO_3 \cdot 2\,H_2O$
	$\log a_i = 1.14 + 2 \log a_{HCO_3^-} - 3 \log a_{H_2O}$
	lower limit - eq. w/ UO_2
	$\log a_i = 23.97 + 2 \log a_{HCO_3^-} + \frac{1}{2} \log f_{O_{2(g)}}$

Neptunium

Dominant aqueous species	Solubility limits imposed by solids
$NpO_2CO_3^-$	upper limit - eq. w/ $NpO_2(OH)(am)$
	$\log a_i = -1.49 + \log a_{HCO_3^-} - \log a_{H_2O}$
	lower limit - eq. w/ $NaNpO_2CO_3 \cdot 3.5H_2O$
	$\log a_i = -6.96 - \log a_{Na^+} - 3.5 \log a_{H_2O}$
$Np(OH)_5^-$	upper limit - eq. w/ $Np(OH)_4$
	$\log a_i = -13.49 + pH + \log a_{H_2O}$
	lower limit - eq. w/ NpO_2
	$\log a_i = -22.1 + pH + 3 \log a_{H_2O}$

$NpO_2 / Np(OH)_5^-$

$$Np^{4+} + 5H_2O = Np(OH)_5^- + 5H^+ \qquad -14.3$$

$$NpO_2 + 4H^+ = Np^{4+} + 2H_2O \qquad -7.8026$$

$$NpO_2 + 3H_2O = Np(OH)_5^- + H^+ \qquad -22.1$$

$$-22.1 = \log a_{Np(OH)_5^-} - pH - 3\log a_{H_2O}$$

$$\boxed{\log a_{Np(OH)_5^-} = -22.1 + pH + 3\log a_{H_2O}}$$

$Np(OH)_5^- / Np(OH)_4$

$$Np(OH)_5^- + 5H^+ = Np^{4+} + 5H_2O \qquad 14.3$$

$$Np^{4+} + 4H_2O = Np(OH)_4 + 4H^+ \qquad -0.8103$$

$$Np(OH)_5^- + H^+ = Np(OH)_4(s) + H_2O \qquad 13.4897$$

$$13.4897 = -\log a_{Np(OH)_5^-} + pH + \log a_{H_2O}$$

$$\boxed{\log a_{Np(OH)_5^-} = -13.4897 + pH + \log a_{H_2O}}$$

$NaNpO_2CO_3 \cdot 3.5H_2O / NpO_2CO_3^-$

$$NaNpO_2CO_3 \cdot 3.5H_2O = Na^+ + NpO_2^+ + CO_3^{2-} + 3.5H_2O \qquad -11.563$$

$$NpO_2^+ + CO_3^{2-} = NpO2CO_3^- \qquad 4.6$$

$$NaNpO_2CO_3 \cdot 3.5H_2O = Na^+ + NpO_2CO_3^- + 3.5H_2O \qquad -6.963$$

$$-6.963 = \log a_{Na^+} + \log a_{NpO_2CO_3^-} + 3.5\log a_{H_2O}$$

$$\boxed{\log a_{NpO_2CO_3^-} = -6.963 - \log a_{Na^+} - 3.5\log a_{H_2O}}$$

$NpO_2CO_3^- / NpO_2OH(am)$

$$\begin{array}{lr}
NpO_2^+ + CO_3^{2-} = NpO_2CO_3^- & 4.6 \\
H^+ + NpO_2OH \quad = NpO_2^+ + H_2O & 4.2364 \\
HCO_3^- = CO_3^{2-} + H^+ & -10.3288 \\
\hline
NpO_2(OH)(am) + HCO_3^- = NpO_2CO_3^- + H_2O & -1.4924
\end{array}$$

$$-1.4924 = \log a_{NpO_2CO_3^-} + \log a_{H_2O} - \log a_{HCO_3}$$

$$\boxed{\log a_{NpO_2CO_3^-} = -1.4924 + \log a_{HCO_3^-} - \log a_{H_2O}}$$

Plutonium

Dominant aqueous species	Solubility limits imposed by solids
PuO_2^+	upper limit - eq. w/ $Pu(OH)_4$
	$$\log a_i = 2.94 + \frac{1}{4}\log f_{O_2(g)} - pH - 2.5\log a_{H_2O}$$
	lower limit - eq. w/ PuO_2
	$$\log a_i = -5.19 + \frac{1}{4}\log f_{O_2(g)} - pH - \frac{1}{2}\log a_{H_2O}$$
Pu^{3+}	upper limit - eq. w/ $Pu(OH)_4$
	$$\log a_i = -3.02 - \frac{1}{4}\log f_{O_2(g)} - 3pH - 3.5\log a_{H_2O}$$
	lower limit - eq. w/ PuO_2
	$$\log a_i = -11.15 - \frac{1}{4}\log f_{O_2(g)} - 3pH - 1.5\log a_{H_2O}$$
$Pu(OH)_5^-$	upper limit - eq. w/ $Pu(OH)_4$
	$$\log a_i = -14.22 + pH + \log a_{H_2O}$$
	lower limit - eq. PuO_2
	$$\log a_i = -22.34 + pH + 3\log a_{H_2O}$$

$Pu(OH)_5^- / PuO_2$

$$
\begin{array}{lr}
Pu(OH)_5^- + 5H^+ = Pu^{4+} + 5H_2O & 14.9802 \\
Pu^{4+} + 2H_2O = PuO_2(s) + 4H^+ & 7.3646 \\
\hline
Pu(OH)_5^- + H^+ = PuO_2(s) + 3H_2O & 22.3448
\end{array}
$$

$$\log K = pH - \log a_{Pu(OH)_5^-} + 3\log a_{H_2O}$$

$$\boxed{\log a_{Pu(OH)_5^-} = -22.3448 + pH + 3\log a_{H_2O}} \quad \text{eq. w/ } PuO_2(s)$$

$Pu(OH)_5^- / Pu(OH)_4$

$$
\begin{array}{lr}
Pu(OH)_5^- + 5H^+ = Pu^{4+} + 5H_2O & 14.9802 \\
Pu^{4+} + 4H_2O = Pu(OH)_4(s) + 4H^+ & -0.7578 \\
\hline
Pu(OH)_5^- + H^+ = Pu(OH)_4(s) + H_2O & 14.2224
\end{array}
$$

$$\log K = pH - \log a_{Pu(OH)_5^-} + \log a_{H_2O}$$

$$\boxed{\log a_{Pu(OH)_5^-} = -14.2224 + pH + \log a_{H_2O}} \quad \text{eq. w/ } Pu(OH)_4(s)$$

Pu^{3+} / PuO_2

$$
\begin{array}{lr}
PuO_2 + 4H^+ = Pu^{4+} + 2H_2O & -7.3646 \\
\frac{1}{2}H_2O + Pu^{4+} = Pu^{3+} + \frac{1}{4}O_2(g) + H^+ & -3.7825 \\
\hline
PuO_2(s) + 3H^+ = Pu^{3+} + 1.5H_2O + \frac{1}{4}O_2(g) & -11.1471
\end{array}
$$

$$-11.1471 = \log a_{Pu^{3+}} + 1.5\log a_{H_2O} + \frac{1}{4}\log f_{O_2(g)} + 3pH$$

$$\boxed{\log a_{Pu^{3+}} = -11.1471 - 1.5\log a_{H_2O} - \frac{1}{4}\log f_{O_2(g)} - 3pH}$$

$Pu^{3+} / Pu(OH)_4$

$$Pu(OH)_4 + 4H^+ = 4H_2O + Pu^{4+} \qquad 0.7578$$

$$\tfrac{1}{2}H_2O + Pu^{4+} = Pu^{3+} + \tfrac{1}{4}O_2(g) + H^+ \qquad -3.7825$$

$$Pu(OH)_4(s) + 3H^+ = Pu^{3+} + 3.5H_2O + \tfrac{1}{4}O_2(g) \qquad -3.0247$$

$$-3.0247 = \log a_{Pu^{3+}} + 3.5\log a_{H_2O} + \tfrac{1}{4}\log f_{O_2(g)} + 3pH$$

$$\boxed{\log a_{Pu^{3+}} = -3.0247 - \tfrac{1}{4}\log f_{O_2(g)} - 3pH - 3.5\log a_{H_2O}}$$

PuO_2^+ / PuO_2

$$PuO_2(s) + 4H^+ = Pu^{4+} + 2H_2O \qquad -7.3646$$

$$\tfrac{1}{4}O_2 + Pu^{4+} + 1.5H_2O = PuO_2^+ + 3H^+ \qquad 2.1773$$

$$PuO_{2(s)} + H^+ + \tfrac{1}{4}O_2(g) = PuO_2^+ + \tfrac{1}{2}H_2O \qquad -5.1873$$

$$-5.1873 = \log a_{PuO_2^+} + \tfrac{1}{2}\log a_{H_2O} - \tfrac{1}{4}\log f_{O_2(g)} + pH$$

$$\boxed{\log a_{PuO_2^+} = -5.1873 + \tfrac{1}{4}\log f_{O_2(g)} - pH - \tfrac{1}{2}\log a_{H_2O}}$$

$PuO_2^+ / Pu(OH)_4$

$$Pu(OH)_4(s) + 4H^+ = Pu^{4+} + 4H_2O \qquad 0.7578$$

$$\tfrac{1}{4}O_2 + Pu^{4+} + 1.5H_2O = PuO_2^+ + 3H^+ \qquad 2.1773$$

$$Pu(OH)_4(s) + \tfrac{1}{4}O_2 + H^+ = PuO_2^+ + 2.5H_2O \qquad 2.9351$$

$$\boxed{\log a_{PuO_2^+} = 2.9351 - pH + \tfrac{1}{4}\log f_{O_2(g)} - 2.5\log a_{H_2O}}$$

Americium

(am) ≡ amorphous
(s) ≡ solid
(aq) ≡ aqueous

Dominant aqueous species

$AmCl_2^+$

Solubility limits imposed by solids

upper limit - eq. w/ Am(OH)3 (am)

$$\log a_i = 18.46 + 2\log a_{Cl^-} - 3pH - 3\log a_{H_2O}$$

lower limit - eq. w/ AmOHCO3

$$\log a_i = 3.29 - \log a_{HCO_3^-} - 2pH + 2\log a_{Cl^-} - \log a_{H_2O}$$

$AmOHCO_3 / AmCl_2^+(HCO_3^-)$

$AmOHCO_3$	$= Am^{3+} + CO_3^{2-} + OH^-$	-22.6
$CO_3^{2-} + H^+$	$= HCO_3^-$	10.3288
$OH^- + H^+$	$= H_2O$	14
$Am^{3+} + 2Cl^-$	$= AmCl_2^+$	1.5628
$AmOHCO_3 + 2Cl^- + 2H^+ = AmCl_2^+ + HCO_3^- + H_2O$		3.2916

$$3.2916 = \log a_{AmCl_2^+} + \log a_{HCO_3^-} + \log a_{H_2O} + 2pH - 2\log a_{Cl^-}$$

$$\boxed{\log a_{AmCl_2^+} = 3.2916 - \log a_{HCO_3^-} - 2pH + 2\log a_{Cl^-} - \log a_{H_2O}}$$

$\boxed{Am(OH)_3(am) / AmCl_2^+}$

$$\begin{array}{lr} Am(OH)_3(am) = Am^{3+} + 3\left(OH^-\right) & -25.1 \\ 3\left(OH^-\right) + 3H^+ \quad = 3H_2O & 42 \\ Am^{3+} + 2Cl^- \quad = AmCl_2^+ & 1.5628 \\ \hline Am(OH)_3(am) + 3H^+ + 2Cl^- = AmCl_2^+ + 3H_2O & 18.4628 \end{array}$$

$$18.4628 = \log a_{AmCl_2^+} + 3\log a_{H_2O} - 2\log a_{Cl^-} + 3pH$$

$$\boxed{\log a_{AmCl_2^+} = 18.4628 + 2\log a_{Cl^-} - 3pH - 3\log a_{H_2O}}$$

APPENDIX G: PITZER EQUATIONS

APPENDIX G: PITZER EQUATIONS

Pitzer (K.S. Pitzer, *Activity Coefficients in Electrolyte Solutions*, 2nd Edition, CRC Press, 1991, pp. 76-101) has shown that the partial molar (or molal) thermodynamic functions (chemical potential, Helmholtz free energy, etc.) of electrolytes in high-ionic-strength solutions are functions of the electrostatic interactions of the ion species. Thermodynamic functions can therefore be expressed in terms of the ion concentrations. The activity coefficient for a cation M in a solution where only binary cation-anion and ion-neutral interactions are considered, may be expressed as (Harvie, C.E., Møller, N., Weare, J.H. *Geochim. Cosmochim. Acta.* V. 48, pp. 723-751, 1984)

$$\ln \gamma_M = z_M^2 + \sum_{a=1}^{N_a} m_a (2B_{Ma} + ZC_{Ma}) + |z_M| \sum_{c=1}^{N_c} \sum_{a=1}^{N_a} m_c m_a C_{ca} + \sum_{n=1}^{N_n} m_n (2\lambda_{nM}) \qquad \text{(G-1)}$$

where γ_M is the activity coefficient of cation M, the subscripts a, c, and n refer to all anion, cation, and neutral species, respectively, z is the ionic charge, Z is the weighted sum of the solution charge, and λ represents the ion-ion or ion-neutral interaction. B_{MX} is a function that describes the chemical interactions between species M and species X and depends on the charge of the individual ions. For "2-2" electrolytes (e.g., $MgSO_4$), an expression for B_{MX} would be

$$B_{MX} = \beta_{MX}^{(0)} + \beta_{MX}^{(1)} \exp(-\alpha_1 I^{\frac{1}{2}}) + \beta_{MX}^{(2)} \exp(-\alpha_2 I^{\frac{1}{2}}) \qquad \text{(G-2)}$$

where I is the ionic strength and the coefficients α are characteristic of the electrolyte type (2-2, 2-1, etc.). The coefficients $\beta^{(0)}$, $\beta^{(1)}$, $\beta^{(2)}$ are "Pitzer parameters." The other Pitzer parameter is C^{ϕ} in the equation

$$C_{MX} = \frac{C^{\phi}}{2\sqrt{|z_M z_x|}} \qquad \text{(G-3)}$$

where C_{MX} is the coefficient C_{ca} in Equation (G-1).

WIPP
UC721 - DISTRIBUTION LIST

Federal Agencies

US Department of Energy (6)
Office of Civilian Radioactive Waste Management
Attn: Deputy Director, RW-2
Associate Director, RW-10/50
Office of Program and Resources Management
Office of Contract Business Management
Director, RW-22, Analysis and Verification Division
Associate Director, RW-30
Office of Systems and Compliance
Associate Director, RW-40
Office of Storage and Transportation
Director, RW-4/5
Office of Strategic Planning and International Programs
Office of External Relations
Forrestal Building
Washington, DC 20585

US Department of Energy
Albuquerque Operations Office
Attn: National Atomic Museum Library
PO Box 5400
Albuquerque, NM 87185-5400

US Department of Energy
Research & Waste Management Division
Attn: Director
PO Box E
Oak Ridge, TN 37831

US Department of Energy (6)
Carlsbad Area Office
Attn: G. Dials
D. Galbraith
M. McFadden
R. Lark
J.A. Mewhinney
R. Stroud
PO Box 3090
Carlsbad, NM 88221-3090

US Department of Energy
Office of Environmental Restoration and Waste Management
Attn: J. Lytle, EM-30
Forrestal Building
Washington, DC 20585-0002

US Department of Energy (3)
Office of Environmental Restoration and Waste Management
Attn: M. Frei, EM-34, Trevion II
Director, Waste Management Projects
Washington, DC 20585-0002

US Department of Energy
Office of Environmental Restoration and Waste Management
Attn: S. Schneider, EM-342, Trevion II
Washington, DC 20585-0002

US Department of Energy (2)
Office of Environment, Safety and Health
Attn: C. Borgstrom, EH-25
R. Pelletier, EH-231
Washington, DC 20585

US Department of Energy (2)
Idaho Operations Office
Fuel Processing & Waste Mgmt. Division
785 DOE Place
Idaho Falls, ID 83402

US Environmental Protection Agency (2)
Radiation Protection Programs
Attn: M. Oge
ANR-460
Washington, DC 20460

US Geological Survey
Attn: I-Ming Chou
Mail Stop 959, Room 4B-318
12201 Sunrise Valley Drive
Reston, VA 22092

Boards

Defense Nuclear Facilities Safety Board
Attn: D. Winters
625 Indiana Ave. NW, Suite 700
Washington, DC 20004

Nuclear Waste Technical Review Board (2)
Attn: Chairman
S. J. S. Parry
1100 Wilson Blvd., Suite 910
Arlington, VA 22209-2297

State Agencies

Attorney General of New Mexico
PO Drawer 1508
Santa Fe, NM 87504-1508

Environmental Evaluation Group (3)
Attn: Library
7007 Wyoming Blvd. NE, Suite F-2
Albuquerque, NM 87109

New Mexico Energy, Minerals, and Natural Resources Department
Attn: Library
2040 S. Pacheco
Santa Fe, NM 87505

NM Environment Department (3)
Secretary of the Environment
Attn: Mark Weidler
1190 St. Francis Drive
Santa Fe, NM 87503-0968

New Mexico Bureau of Mines and Mineral Resources
Socorro, NM 87801

New Mexico Environment Department
WIPP Project Site
Attn: P. McCasland
PO Box 3090
Carlsbad, NM 88221

Laboratories/Corporations

Battelle Pacific Northwest Laboratories
Attn: R.E. Westerman, MSIN P8-44
Battelle Blvd.
Richland, WA 99352

CTAC
Attn: L. Eriksson
PO Box 1270
Carlsbad, NM 88221

INTERA, Inc.
Attn: G.A. Freeze
1650 University Blvd. NE, Suite 300
Albuquerque, NM 87102

INTERA, Inc.
Attn: J.F. Pickens
6850 Austin Center Blvd., Suite 300
Austin, TX 78731

INTERA, Inc.
Attn: W. Stensrud
PO Box 2123
Carlsbad, NM 88221

Lawrence Livermore National Laboratory
Attn: C.J. Bruton
Earth Sciences Department, L-219
PO Box 808
Livermore, CA 94550

Lawrence Livermore National Laboratory
GTS-ITS
Attn: G.T. Seaborg, MS-L-396
PO Box 808
Livermore, CA 94551

Los Alamos National Laboratory
Attn: B. Erdal, INC-12
PO Box 1663
Los Alamos, NM 87544

RE/SPEC, Inc.
Attn: Angus Robb
4775 Indian School NE, Suite 300
Albuquerque, NM 87110-3927

RE/SPEC, Inc. - CTAC
Attn: D.E. Hobart
4775 Indian School NE, Suite 300
Albuquerque, NM 87110-3927

RE/SPEC, Inc.
Attn: J.L. Ratigan
PO Box 725
Rapid City, SD 57709

Southwest Research Institute (2)
Center for Nuclear Waste Regulatory Analysis
Attn: P.K. Nair
6220 Culebra Road
San Antonio, TX 78228-0510

Tech Reps, Inc. (4)
Attn: J. Chapman (1)
Loretta Robledo (2)
Faith Puffer (1)
5000 Marble NE, Suite 222
Albuquerque, NM 87110

Westinghouse Electric Corporation (5)
Attn: Library
J. Epstein
J. Lee
B.A. Howard
R. Kehrman
PO Box 2078
Carlsbad, NM 88221

S. Cohen & Associates
Attn: Bill Thurber
1355 Beverly Road
McLean, VA 22101

National Academy of Sciences, WIPP Panel

Howard Alder
Oxyrase, Incorporated
7327 Oak Ridge Highway
Knoxvill, TN 37931

Bob Andrews
Board of Radioactive Waste Management
GF456
2101 Constitution Ave.
Washington, DC 20418

Rodney C. Ewing
Department of Geology
University of New Mexico
Albuquerque, NM 87131

Charles Fairhurst
Dept. of Civil and Mineral Engineering
University of Minnesota
500 Pillsbury Dr. SE
Minneapolis, MN 55455-0220

B. John Garrick
PLG Incorporated
4590 MacArthur Blvd., Suite 400
Newport Beach, CA 92660-2027

Leonard F. Konikow
US Geological Survey
431 National Center
Reston, VA 22092

Carl A. Anderson, Director
Board of Radioactive Waste Management
National Research Council
HA 456
2101 Constitution Ave. NW
Washington, DC 20418

Christopher G. Whipple
ICF Kaiser Engineers
1800 Harrison St., 7th Floor
Oakland, CA 94612-3430

John O. Blomeke
720 Clubhouse Way
Knoxville, TN 37909

Sue B. Clark
University of Georgia
Savannah River Ecology Lab
PO Drawer E
Aiken, SC 29802

Konrad B. Krauskopf
Department of Geology
Stanford University
Stanford, CA 94305-2115

Della Roy
Pennsylvania State University
217 Materials Research Lab
Hastings Road
University Park, PA 16802

David A. Waite
CH_2 M Hill
PO Box 91500
Bellevue, WA 98009-2050

Thomas A. Zordan
Zordan Associates, Inc.
3807 Edinburg Drive
Murrysville, PA 15668

Universities

Rosenstiel School of Marine and Atmospheric Science
University of Miami
Attn: F.J. Millero
4600 Rickenbacker Causeway
Miami, FL 33149-1098

University of New Mexico
Geology Department
Attn: Library
141 Northrop Hall
Albuquerque, NM 87131

University of Washington
College of Ocean & Fishery Sciences
Attn: G.R. Heath
583 Henderson Hall, HN-15
Seattle, WA 98195

Libraries

Thomas Brannigan Library
Attn: D. Dresp
106 W. Hadley St.
Las Cruces, NM 88001

Government Publications Department
Zimmerman Library
University of New Mexico
Albuquerque, NM 87131

New Mexico Junior College
Pannell Library
Attn: R. Hill
Lovington Highway
Hobbs, NM 88240

New Mexico State Library
Attn: N. McCallan
325 Don Gaspar
Santa Fe, NM 87503

New Mexico Tech
Martin Speere Memorial Library
Campus Street
Socorro, NM 87810

WIPP Public Reading Room
Carlsbad Public Library
101 S. Halagueno St.
Carlsbad, NM 88220

Foreign Addresses

Studiecentrum Voor Kernenergie
Centre D'Energie Nucleaire
Attn: A. Bonne
SCK/CEN Boeretang 200
B-2400 Mol, BELGIUM

Atomic Energy of Canada, Ltd.
Whiteshell Laboratories
Attn: B. Goodwin
Pinawa, Manitoba, CANADA ROE 1L0

Francois Chenevier (2)
ANDRA
Route de Panorama Robert Schumann
B. P. 38
92266 Fontenay-aux-Roses, Cedex
FRANCE

Claude Sombret
Centre D'Etudes Nucleaires De La Vallee Rhone
CEN/VALRHO
S.D.H.A. B.P. 171
30205 Bagnols-Sur-Ceze, FRANCE

Commissariat a L'Energi Atomique
Attn: D. Alexndre
Centre d'Etudes de Cadarache
13108 Saint Paul Lez Durance Cedex
FRANCE

Bundesanstalt für Geowissenschaften und Rohstoffe
Attn: M. Langer
Postfach 510 153
D-30631 Hannover, GERMANY

Bundesministerium für Forschung und Technologie
Postfach 200 706
5300 Bonn 2, GERMANY

Institut für Tieflagerung
Attn: K. Kuhn
Theodor-Heuss-Strasse 4
D-3300 Braunschweig, GERMANY

Gesellschaft für Anlagen und Reaktorsicherheit (GRS) mbH
Attn: B. Baltes
Schwertnergasse 1
D-50667 Cologne, GERMANY

Physikalisch-Technische Bundesanstalt
Attn: P. Brenneke
Postfach 3345
D-3300 Braunschweig, GERMANY

Shingo Tashiro
Japan Atomic Energy Research Institute
Tokai-Mura, Ibaraki-Ken, 319-11
JAPAN

Netherlands Energy Research Foundation ECN
Attn: L.H. Vons
3 Westerduinweg
PO Box 1
1755 Zg Petten
THE NETHERLANDS

Svensk Kärnbränsleforsorjning AB
Attn: F. Karlsson
Project KBS (Karnbranslesakerhet)
Box 5864
S-102 48 Stockholm
SWEDEN

Nationale Genossenschaft für die Lagerung
Radioaktiver Abfälle (2)
Attn: S. Vomvoris
P. Zuidema
Hardstrasse 73
CH-5430 Wettingen
SWITZERLAND

AEA Technology
Attn: J.H. Rees
D5W/29 Culham Laboratory
Abington, Oxfordshire OX14 3DB
UNITED KINGDOM

AEA Technology
Attn: W.R. Rodwell
O44/A31 Winfrith Technical Centre
Dorchester
Dorset DT2 8DH
UNITED KINGDOM

AEA Technology
Attn: J.E. Tinson
B4244 Harwell Laboratory
Didcot, Oxfordshire OX11 ORA
UNITED KINGDOM

D.R. Knowles
British Nuclear Fuels, plc
Risley, Warrington, Cheshire WA3 6AS, 1002607
UNITED KINGDOM

Internal

MS	Org.	
1324	6115	P.B. Davies
1320	6719	E.J. Nowak
1322	6121	J.R. Tillerson
1328	6749	D.R. Anderson
1328	6741	H.N. Jow
1335	6705	M. Chu
1341	6811	A.L. Stevens
1341	6748	J.T. Holmes
1341	6748	L.M. Brush
1341	6748	C.F. Novak
1343	6751	R.E. Thompson
1343	6751	K.M. Trauth
1343	6751	R.F. Weiner
1395	6700	P. Brewer
1395	6800	L. Shephard
1395	6707	M. Marietta
1395	6841	V.H. Slaboszewicz
1330	6752	C.B. Michaels (2)
1330	6752	NWM Library (20)
9018	8523-2	Central Technical Files
0899	4414	Technical Library (5)
0619	12615	Print Media
0100	7613-2	Document Processing (2) for DOE/OSTI